HOLOCENE EARTHQUAKE HISTORY OF THE NORTHERN WEBER SEGMENT OF THE WASATCH FAULT ZONE, UTAH

by
Alan R. Nelson, Mike Lowe, Stephen Personius, Lee-Ann Bradley, Steven L. Forman, Robert Klauk, and John Garr

MISCELLANEOUS PUBLICATION 05-8
UTAH GEOLOGICAL SURVEY
a division of
Utah Department of Natural Resources
2006

HOLOCENE EARTHQUAKE HISTORY OF THE NORTHERN WEBER SEGMENT OF THE WASATCH FAULT ZONE, UTAH

by

Alan R. Nelson[1], Mike Lowe[2], Stephen Personius[1], Lee-Ann Bradley[1], Steven L. Forman[3], Robert Klauk[4], and Jon Garr[5]

[1]U.S. Geological Survey, Golden, Colorado
[2]Utah Geological Survey
[3]University of Illinois at Chicago, Department of Earth and Environmental Sciences, Chicago, Illinois
[4]Wisconsin Department of Commerce, Division of Environmental and Regulatory Services, Oskosh, Wisconsin
[5]Montgomery Watson, Salt Lake City, Utah

Cover photos:
Top photo shows Garner Canyon; bottom photos show trench 2 in eastern Ogden City. Photos by Alan R. Nelson.

ISBN 1-55791-741-8

MISCELLANEOUS PUBLICATION 05-8
UTAH GEOLOGICAL SURVEY
a division of
Utah Department of Natural Resources
2006

STATE OF UTAH

Jon Huntsman, Jr., Governor

DEPARTMENT OF NATURAL RESOURCES

Michael Styler, Executive Director

UTAH GEOLOGICAL SURVEY

Richard G. Allis, Director

PUBLICATIONS
contact
Natural Resources Map/Bookstore
1594 W. North Temple
telephone: 801-537-3320
toll-free: 1-888-UTAH MAP
website: http://mapstore.utah.gov
email: geostore@utah.gov

THE UTAH GEOLOGICAL SURVEY
contact
1594 W. North Temple, Suite 3110
Salt Lake City, UT 84116
telephone: 801-537-3300
fax: 801-537-3400
web: http://geology.utah.gov

TAKE Pride IN UTAH

Printed on recycled paper

1/05

FOREWORD

This Utah Geological Survey Special Study, *Holocene Earthquake History of the Northern Weber Segment of the Wasatch Fault Zone, Utah,* is the thirteenth report in the Paleoseismology of Utah series. This series makes the results of paleoseismic investigations in Utah available to geoscientists, engineers, planners, public officials, and the general public. These studies provide critical information regarding paleoearthquake parameters such as earthquake timing, recurrence, displacement, slip rate, and fault geometry, which can be used to characterize potential seismic sources and evaluate the long-term seismic hazard presented by Utah's Quaternary faults.

This report presents the results of a cooperative investigation between the U.S. Geological Survey and the Utah Geological Survey of the earthquake history recorded at two sites on the northern part of the 61-km-long Weber segment of the Wasatch fault zone. This study was completed between 1985 and 1990. Early published reports on this study were preliminary. This UGS Miscellaneous Publication presents the investigation results in more detail than previously available. This report also includes a comprehensive evaluation of all paleoseismic information for the Weber segment, and synthesizes that information to give a clearer understanding of the segment's recent earthquake history.

This study shows that (1) four surface-faulting earthquakes occurred on the Weber segment in the middle to late Holocene, (2) comparison of earthquake histories at all trench sites on the Weber segment indicates that surface-faulting earthquakes of different size ruptured different lengths of the segment, (3) earthquakes that produce different rupture lengths and displacements complicate recurrence-interval calculations, (4) surface displacements measured across fault scarps along the segment point to differences in rupture extent and hence earthquake magnitude, (5) Holocene slip rates calculated from scarp profiles are inconsistent with much lower slip rates determined from trench-derived displacement data, and (6) additional investigations are required to answer critical questions along the rapidly urbanizing Weber segment.

William R. Lund, Editor
Paleoseismology of Utah Series

CONTENTS

FIGURES

TABLES

PLATES

HOLOCENE EARTHQUAKE HISTORY OF THE NORTHERN WEBER SEGMENT OF THE WASATCH FAULT ZONE, UTAH

by

Alan R. Nelson, Mike Lowe, Stephen Personius, Lee-Ann Bradley, Steven L. Forman, Robert Klauk, and Jon Garr

ABSTRACT

Analysis of stratigraphy and thermoluminescence, charcoal ^{14}C, and apparent mean residence ^{14}C ages on buried A horizons in five trenches across parallel fault scarps, which cut middle and late Holocene alluvial fans at the East Ogden site, yield a history of three large surface-faulting earthquakes and a smaller, most recent, surface-faulting earthquake. An exposure of the main trace of the Weber segment at Garner Canyon, 5 km north of East Ogden, shows a similar record of at least three and probably four surface-faulting earthquakes, three of which correlate with the three large earthquakes at East Ogden. Fault displacements at Garner Canyon during each earthquake are less than half the displacements at East Ogden. Best estimates of the times of the four earthquakes at East Ogden and Garner Canyon are: earthquake A about 4.0 ka (range 4.8-2.8 ka), earthquake B about 2.5 ka (range 2.8-2.4 ka), earthquake C about 0.9 ka (range 1.0-0.5 ka), and earthquake D about 0.5 ka (range 0.6-0.2 ka).

Comparison of the recently revised earthquake history at Kaysville, 25 km south of East Ogden, with the composite history for the East Ogden and Garner Canyon sites supports a correlation of earthquakes B and C among all three sites yielding minimum surface rupture extents of 35 km, and probably at least three-fourths of the 61-km-long Weber segment. Although earthquake A is unrecorded at Kaysville, its large displacements farther north are inconsistent with a rupture extent confined to the northern half of the segment. Earthquake D is not recorded at Garner Canyon or Kaysville, and so its rupture was probably small (<0.5 m) and may not have reached either site.

Earthquakes with ruptures of different size and length complicate recurrence interval calculations. The two intervals between earthquakes A, B, and C at the East Ogden and Garner Canyon sites give an average recurrence of about 1.5 kyr, but the average may only apply to large earthquakes on the northern Weber segment. Because surface displacement during earthquake D was significantly smaller than displacements during earlier dated earthquakes, earthquake D's rupture was probably significantly shorter than the ruptures of the earlier earthquakes. For this reason, the shorter average recurrence interval obtained by averaging the earthquake C/D interval with earlier intervals gives an interval that probably does not accurately reflect the history of the entire segment.

Surface displacements measured across scarps along the Weber segment decrease dramatically within 10 km of segment boundaries—for scarps on deposits of all ages at the northern end, and for latest Pleistocene through middle Holocene deposits at the southern end. The decrease is consistent with ruptures terminating near either end of the segment, and/or with a lower frequency of surface faulting near the ends of the segment. Displacements in latest Pleistocene through middle Holocene deposits are significantly smaller south of Farmington, suggesting that ruptures have either been smaller or less frequent along the southern third of the segment.

With the exception of latest Pleistocene fault slip rates, slip rates derived from surface displacements along the segment are inconsistent with the much lower rates calculated from displacement data at two of the three exposure sites. To reconcile both types of rates we suggest that many Holocene surfaces along the Weber segment are 20-100% older than inferred by Nelson and Personius (1993), and that displacements measured for earthquakes A and B at East Ogden are about 1.5 m too high due to unrecognized antithetic faulting. The age and displacement adjustments yield rates for the segment of about 1-2 mm/yr, with the highest rates between Kaysville and Ogden.

Estimates of the magnitudes of the four most recent surface-faulting earthquakes along the Weber segment,

derived from adjusted displacement data at the three exposure sites, are: earthquake A, 6.9-7.4M; earthquake B, 7.0-7.4M; earthquake C, 6.9-7.4M; and earthquake D, 6.5-6.7M.

INTRODUCTION

This report summarizes, in more detail than has been previously published, a cooperative investigation between the Utah Geological Survey and the U.S. Geological Survey of the earthquake history at two sites on the northern part of the Weber segment of the Wasatch fault zone, largely completed between 1985 and 1990. Early reports on the investigation were preliminary (Nelson and others, 1987; Nelson, 1988; Machette and others, 1987), did not discuss all available data (Forman and others, 1991; Nelson and Personius, 1993; McCalpin, 1998, p. 145), or failed to fully integrate results of the studies of exposures of the fault with mapping of fault scarps along the Weber segment (Forman and others, 1991; Nelson and Personius, 1993; Machette and others, 1992). Here we describe with detailed logs of exposures and accompanying data how we developed earthquake histories for the East Ogden and Garner Canyon exposure sites (figure 1; plates 1 and 2). We take a more conservative, less precise approach in assessing errors on ages used to estimate the times of earthquakes than many previous paleoseismology studies in Utah (e.g., Machette and others, 1992; McCalpin and Nishenko, 1996). In our history at Garner Canyon, we incorporate 10 radiocarbon ages and seven thermoluminescence ages—collected and analyzed long after our study of the site by McCalpin and Forman (1989) and Stafford and Forman (1993)—published only in a textbook figure (McCalpin, 1998, p. 145). We compare our earthquake histories with the history developed more recently for the Kaysville site by McCalpin and others (1994; figure 1). We also discuss surface displacements measured from topographic profiles across fault scarps, and calculation of slip rates from them for the Weber segment, in greater detail than Nelson and Personius (1993) to evaluate fault displacement histories from the three fault exposure sites with detailed information along the segment.

Although data discussed here have aged at least a decade, evaluation of all paleoseismic data for the Weber segment leads to a clearer understanding of the complexity of its recent earthquake history. The evaluation also spotlights the need for additional investigations designed to answer critical questions about earthquake hazard along the rapidly urbanizing Weber segment, as outlined in the compilation of Lund (2005). For discussion of earlier work on the Weber segment, the Wasatch fault zone's tectonic context in the Rocky Mountain region, and the importance of paleoseismic studies in assessing Utah's earthquake hazard, we rely on the many earlier reports about the Wasatch fault (e.g., Lund and others, 1991; Machette and others, 1992; McCalpin and Nishenko, 1996; Lund and Black, 1998) cited in Lund (2005).

DATING FAULTED DEPOSITS

Radiocarbon (^{14}C) and thermoluminescence (TL) ages, used here to infer approximate times of sediment deposition and related surface-faulting earthquakes, include those previously reported by Machette and others (1992, appendix) and Forman and others (1991), and more recent ages briefly summarized in a textbook figure by McCalpin (1998, p. 145; McCalpin and Forman, 1989; Stafford and Forman, 1993). Two types of organic materials were dated by two different ^{14}C methods: charcoal fragments and organic-matter concentrates from soil A horizons (organic-rich surface horizons) by radiometric (gas-proportional counters) and accelerator mass spectrometer (AMS) methods (table 1). Interpretation of the A-horizon ages, termed apparent mean residence time (AMRT) ages, is complex and uncertain and the potential age range of carbon in AMRT samples is large (Mathews, 1980; Machette and others, 1992; Paul and others, 1997). TL ages were determined on the silt fraction of fine-grained sediments in A horizons developed on colluvial deposits adjacent to fault scarps. Although TL ages determined by three different methods of analysis were consistent, the errors on TL ages may be as large as those on many AMRT ages because the values of several parameters used to calculate TL ages at these sites are not well known (Forman and others, 1991).

Because errors on ages discussed in this report are hundreds of years, we list ages in thousands of years before AD 1950 (ka) and round them to the nearest century. We also use a time-interval format (e.g., 3.9-3.1 ka) similar to that used for calibrated ^{14}C ages (e.g., Stuiver and Kra, 1986). The format emphasizes that the age distribution of dated material in a sample is unknown; that is, true sample ages are not necessarily more likely to be near the midpoints of age intervals than near their ends. Note that we do not calibrate A-horizon AMRT ^{14}C ages as has been done in many previous fault-trench studies in Utah (discussed below).

Charcoal ^{14}C Ages

The three charcoal ^{14}C ages are calibrated using standard methods (Bronk Ramsey, 1995, 2001; Stuiver and others, 1998) and reported as time intervals at 2σ (table 1). For ^{14}C ages from the 1980s, questions persist about whether or not all interlaboratory and analytical uncertainty is included in age errors reported by dating laboratories (Scott and others, 1990, 1998; Taylor and others, 1996). Because the reported errors on our three charcoal ages are large (±70-180 ^{14}C yr BP), we do not arbitrarily double report age errors before calibration as did Forman and others (1991) and Machette and others (1992). Al-

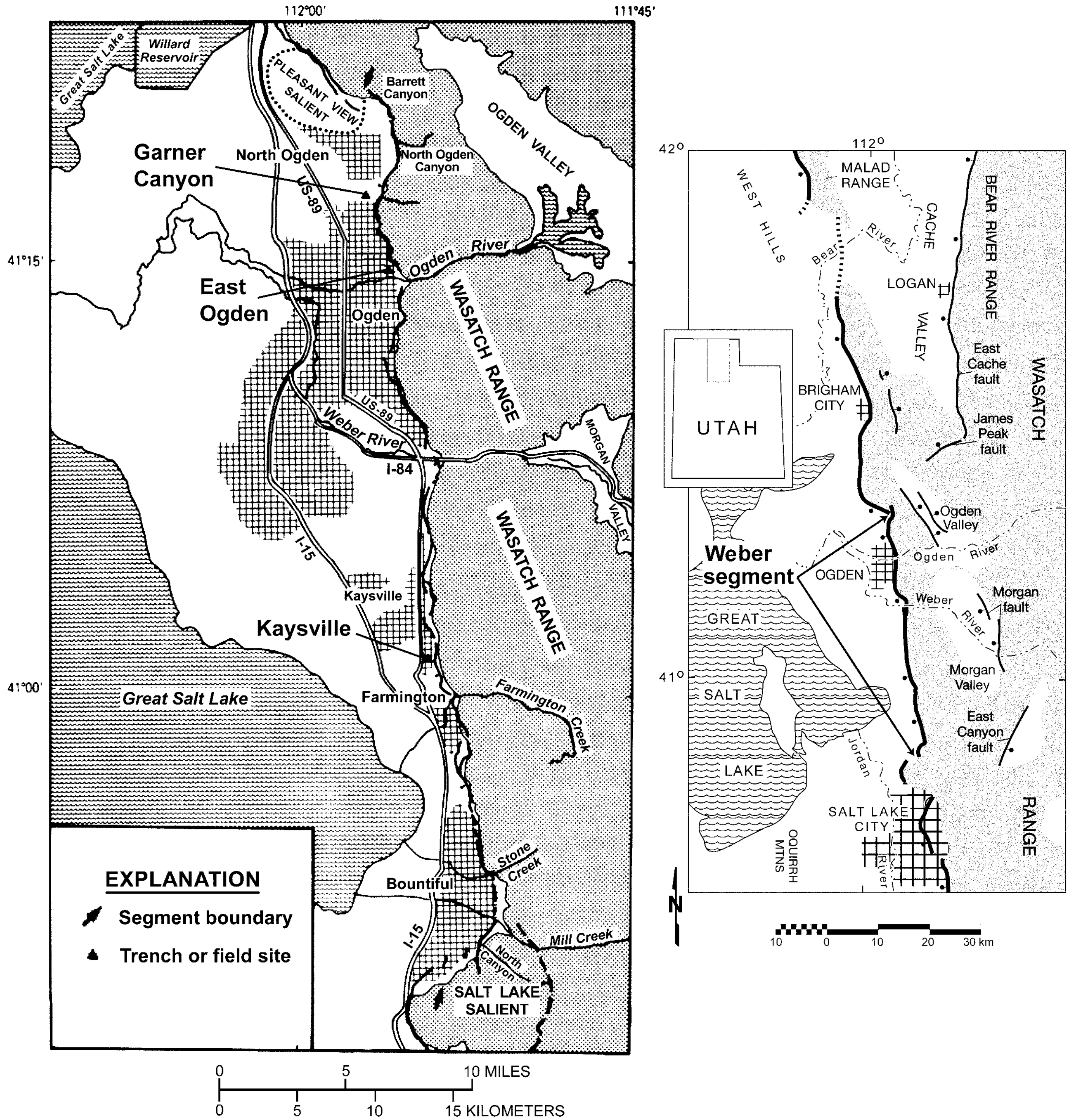

Figure 1. *Location of the Weber segment of the Wasatch fault zone in north central Utah, between the Brigham City segment on the north and the Salt Lake City segment on the south. Bold fault on smaller map is the Wasatch fault. On both maps arrows mark the north and south ends of the Weber segment. The location of the East Ogden and Kaysville trench sites and the Garner Canyon exposure are shown on the larger map. The Pleasant View and Salt Lake salients bound the Weber segment on its north and south ends, respectively. Nelson and Personius (1993) show fault traces and Quaternary deposits along the Weber segment at a scale of 1:50,000 and selected areas at a scale of 1:10,000.*

Table 1. *Radiocarbon data for samples from the East Ogden and Garner Canyon sites and estimated times of A-horizon burial.*

Sample no.	Unit no.	Location (h;v)[1]	Sample type[2]	Sample depth[3]	Thickness of sampled zone[4]	Sample weight (g)[5]	Organic matter (%)[6]	Sample weight (g)[6]	Lab-reported age (^{14}C yr BP)[7]	Radiocarbon lab no.[8]	Comment or correction[9]	Mean age of carbon (ka)[10]	Time of A horizon burial (ka)[11]
East Ogden – trench 1													
11	1cA	20.6,6.5	S	0.12	0.05	59.7	3.9	59.7	285±30	PITT-100	—	0.4-0.1	modern soil
12	3bA	19.2,6.3	D	0.72	0.15	75.1	2.8	75.1	1365±40	PITT-098	—	1.5-1.2	1.4-0.7
East Ogden – trench 2													
21	1dA	17.9,6.8	S	0.45	0.10	48.3	2.8	48.3	122% of modern	PITT-097	burrowed		
22	1cA	17.9,6.4	S	0.05	0.05	31.3	3.4	31.3	122% of modern	PITT-106	burrowed		modern soil
23	3aA	17.8,7.7	D	1.29	0.15	75.7	3.3	75.7	1065±30	PITT-096	—	1.2-0.9	1.1-0.4
24	5aA	19.1,9.6	D	2.65	0.10	67.2	1.0	67.2	3295±130	PITT-104	+200	3.8-3.2	3.9-2.7
25	5aA	19.2,9.6	C	2.67	0.10	0.0084	—	0.0084	4780±100	AA-2270	calibrated ->	5.73-5.30	reworked
26	7A	20.8,10.4	C	2.35	0.15	1.6	—	1.6	4100±180	USGS-2499	calibrated ->	5.35-3.95	<5.35-3.95
27	7A	20.9,10.4	F	2.35	0.15	124.0	1.8	124.0	4505±65	PITT-094	+500	5.2-4.8	5.1-4.3
East Ogden – trench 3													
31	6aA	8.5,0.9	F	0.60	0.08	65.2		65.2	290±60	PITT-101	—	0.5-0.1	0.4-0
32	9bA	8.5,1.4	D	0.95	0.12	48.7	1.9	48.7	1340±95	PITT-095	—	1.5-1.2	1.4-0.7
33	10aA	8.1,2.1	F	1.65	0.10	93.6	1.2	93.6	2820±65	PITT-107	—	3.0-2.7	2.9-2.2
34	5aA	16.2,4.6	F	0.80	0.08	32.3	3.7	32.3	112% of modern	PITT-105	burrowed		
35	9a	16.4,4.7	C	0.80	1	0.0189	—	0.0189	580±70	AA-2269	calibrated ->	0.67-0.50	<0.67-0.50
East Ogden – trench 4													
41	2aA	7.3,1.1	D	0.38	0.03	32.5	4.4	32.5	460±65	PITT-103	—	0.6-0.3	0.5-0
42	4aA	7.3,1.3	S	0.68	0.05	41.6	2.6	41.6	105±55	PITT-102	burrowed		
East Ogden – trench 5													
51	1aA	10.3,3.5	S	0.05	0.04	37.1	3.8	37.1	815±45	PITT-108	reworked	1.0-0.7	
52	1bA	10.7,3.9	S	0.30	0.03	76.2	5.7	76.2	390±25	PITT-099	—	0.6-0.2	0.5-0
53	3aA	10.2,4.4	F	1.20	0.15	49.2	3.0	49.2	1040±75	PITT-109	—	1.2-0.9	1.1-0.4
Garner Canyon exposure													
01	1aA	6.0,2.6	S	0.08	0.10	—	12.5	—	modern	NSRL-527	—	—	modern soil
02	1aA	6.0,2.5	S	0.19	0.10	—	3.1	—	70±70	NSRL-528	—	0.2-0	modern soil
03	1bA	5.1,3.0	S	0.25	0.20	218	20.0	218	150±70	DIC-3298	—	0.2-0	modern soil
04	1bA	6.0,2.3	S	0.34	0.10	—	2.6	—	370±70	NSRL-529	—	0.5-0.2	0.4-0
05	3aA	5.5,2.2	S	0.71	0.10	—	1.3	—	990±80	NSRL-523	—	1.1-0.8	1.0-0.3
06	3aA	5.4,2.0	S	0.82	0.10	—	1.4	—	1290±70	NSRL-524	—	1.4-1.1	1.3-0.6
07	3aA	5.4,1.9	S	1.00	0.10	—	1.4	—	1360±80	NSRL-525	—	1.5-1.2	1.4-0.7
08	3aA	5.3,1.7	S	1.16	0.10	—	1.4	—	1390±90	NSRL-526	—	1.6-1.2	1.5-0.7
09	3aA	4.0,2.3	S	1.20	0.20	245	15.7	245	1300±80	DIC-3297	—	1.5-1.1	1.4-0.6
10	5A	5.4,1.2	S	1.67	0.10	—	1.3	—	2930±60	NSRL-520	—	3.1-2.8	3.0-2.3
11	5A	5.4,1.0	S	1.77	0.10	—	1.4	—	2550±60	NSRL-521	—	2.7-2.4	2.6-1.9
12	5A	4.0,1.5	S	1.90	0.15	234	9.8	234	2110±100	DIC-3237	—	2.3-1.9	2.2-1.4
13	5A	5.4,0.9	S	1.94	0.10	—	1.1	—	2730±90	NSRL-522	—	2.9-2.6	2.8-2.1

[1] *Location (horizontal, vertical) on meter reference grid used to map walls of exposures. Superscripts on sample ages shown in figures and plates are digits of field sample numbers (first column). NSRL ages at Garner Canyon from Stafford and Forman (1993) and McCalpin (1998, p. 145). Two ages reported by Stafford and Forman (1993) are not listed because the samples were from debris-facies colluvium rather than A-horizon sediment, which makes the source of the dated carbon difficult to interpret.*

[2] *S, A-horizon sediment deposited mostly by surface wash on scarp slope; D, A-horizon sediment developed on colluvial debris wedge; F, A-horizon sediment developed on fluvial deposits; C, detrital charcoal, possibly reworked.*

[3] *Vertical depth below the surface of center of sampled zone in meters.*

[4] *Thickness of zone of stratigraphic unit that was sampled in meters.*

[5] *The fine organic-rich fraction was concentrated from A-horizon samples by sedimentation and centrifugation using methods of Kihl (1975). This is the weight of the organic-rich clay-silt fraction submitted to radiocarbon laboratory. NSRL sample concentrates (<63 u fraction), dated by AMS methods, weighed 2-10 g. Charcoal was picked directly from sediment collected from the trench wall, dried, and cleaned of rootlets before submittal to radiocarbon laboratory.*

[6] *Percent by weight of organic matter in organic-rich clay-silt fraction (<125 u) of A-horizon samples using method of Walkley-Black (1934); the method of (Storer, 1984) was used for three Garner Canyon samples with sample weights.*

[7] *Age in radiocarbon years before present (AD 1950) and 1σ error reported by radiocarbon laboratory. A-horizon concentrate samples from East Ogden and three DIC samples from Garner Canyon were thoroughly pretreated with HCl and NaOH before gas-proportional radiometric ^{14}C analyses. NSRL A-horizon samples from Garner Canyon were decalcified with HCl and analyzed by AMS methods (Stafford and Forman, 1993). Ages for A-horizon samples are AMRT ages as discussed in text. Charcoal samples were pretreated using standard methods (HCl and NaOH).*

[8] *Laboratories are: AA, University of Arizona-NSF Accelerator Facility for Radioisotope Analysis; PITT, University of Pittsburg, Applied Research Center Radiocarbon Laboratory; USGS, U.S. Geological Survey, Menlo Park, California, Radiocarbon Laboratory; DIC, Dicarb Radioisotope Co., Norman, Oklahoma; NSRL, Stafford Research Laboratories, Inc., Boulder, Colorado. NSRL samples were run on the accelerator at Lawrence Livermore National Laboratory, Livermore, California.*

[9] *Comment on quality of dated sample, whether laboratory-reported ages were calibrated, and the correction added for two old samples where the difference between radiocarbon years and solar (calibrated) years is >150 yr.*

[10] *Mean age of dated sample carbon in thousands of radiocarbon years (ka), listed as time intervals at 2σ and rounded to nearest hundred years. Rounding makes the difference between radiocarbon years and solar (calibrated) years insignificant, except for the two corrected ages (note 9). Errors for laboratory-reported ages from the 1980s are increased to ±80 ^{14}C yr, if reported errors are less than that value, as recommended by Taylor and others (1996). The three charcoal calibrated ages are expressed as time intervals of >95% probability distribution at 2σ. These three ages are in solar years calculated using OxCal (version 3.4; Bronk Ramsey, 1995, 2001; probability method) with the INTCAL98 dataset of Stuiver and others (1998). Ages shown on figures and plates are midpoints of these time intervals rounded to nearest hundred years.*

[11] *Estimated time of A-horizon burial or additional comment. For most samples, the time of A-horizon burial is inferred to coincide with surface faulting. For AMRT samples, an AMRT effect of 100-500 yr is assumed and this range in age uncertainty is subtracted from the time interval in the column to the left (see text). Detrital charcoal ages provide maximum times for surface faulting. Times expressed as intervals rounded to the nearest hundred years.*

though we lack $^{13}C/^{14}C$ values with which to correct the three ages for isotopic fractionation, any such corrections on wood charcoal ages would be much smaller than the laboratory reported errors.

Any unreported additional interlaboratory or analytical errors are insignificant compared with the uncertainties of geologic interpretation of ages on detrital charcoal samples due to sample context errors (Waterbolk, 1983; Taylor, 1987; McCalpin and Nelson, 1998). The greatest uncertainty is the length of time between the death of the woody plant that burned to yield charcoal (at Weber segment sites, burned sagebrush that probably grew over a period of less than 30 years) and its incorporation in the sampled sediment. In many fault trenches, detrital soil charcoal is hundreds to thousands of years older than host sediment, whereas in others, charcoal in burrow infillings or root casts may be hundreds of years younger than the time the burrowed or root-bound sediment was originally deposited (McCalpin and Nelson, 1998; Nelson and others, 2003).

AMRT Ages

Difficulties in interpreting ^{14}C ages on organic matter in bulk samples of A-horizon sediment in the 1970s (e.g., Scharpenseel and Schiffmann, 1977) made paleoseismologists involved in the first trenching studies in Utah (e.g., Swan and others, 1980) hesitant to date surface-faulting earthquakes by this method. But the ubiquity of buried A horizons adjacent to faults and the lack of charcoal stratigraphically associated with faulting in later trenches, coupled with increasingly detailed ^{14}C dating studies of A horizons in northwest Europe, soon led to reliance on A-horizon AMRT ages for estimating times of faulting at many Wasatch fault sites (e.g., Lund and others, 1991; Machette and others, 1992; Stafford and Forman, 1993; Black and others, 1996; McCalpin and Nishenko, 1996; Black and others, 2000; McCalpin and Forman, 2002). The AMRT ages set useful limits on times of faulting at Wasatch sites primarily because the 1-2 kyr intervals between large surface-faulting earthquakes along the fault's central segments insures that A horizons sampled adjacent to faults are young (no older than the previous surface-faulting earthquake) relative to soil A horizons dated in most other geomorphic settings (e.g., Machette and others, 1992; Scharpenseel and others, 1996).

Unfortunately, the need to distinguish frequent surface-faulting earthquakes of different age within and among fault segments led to overinterpretation of the precision of many AMRT ages from Wasatch fault trench studies. For example, Machette and others (1992) used AMRT ages to estimate ages for the upper and lower contacts of A horizons to within 50 years at seven sites including two discussed in this report. McCalpin and Nishenko (1996, their table 2; McCalpin, 1998, p. 144) followed a similar procedure in applying very limited information on rates of A-horizon colluvial sedimentation at a few sites to many sites along the Wasatch fault. Although McCalpin and Nishenko (1996) wisely limited ages used to those collected within 5 m of faults, differences in slope position, vegetation, and animal burrowing among sites make application of the colluvial rates to many sites questionable. Recent studies (e.g., Lund and Black, 1998; Black and others, 2000; McCalpin and Forman, 2002) continue to assume a precision on AMRT ages that is unsupported by any systematic studies on the age distribution of carbon in buried A horizons in the region. For example, although Stafford and Forman's (1993) AMRT ages from one of the sites discussed in this report (Garner Canyon, figure 1, plate 2) generally increase with sample depth in successively buried A horizons, AMS ^{14}C ages on different organic fractions within the same samples differ by as much as 60% or 1000 ^{14}C yr. Although all investigators acknowledge the lack of A-horizon carbon distribution studies, assumed errors on AMRT ages vary widely (e.g., compare Black and others, 2000, with McCalpin and Forman, 2002).

A horizons are complex sedimentologic-biologic systems and many factors complicate the interpretation of AMRT ages on soil organic matter (e.g., Mathews, 1985; Wang and others, 1996; Kristiansen and others, 2003). The gradual accumulation of organic matter at the top of the soil horizon, the removal of organic matter through decay and oxidation throughout the horizon, the penetration of plant roots into the horizon, the mixing of organic material within the horizon by animals (insects, worms, rodents) or woody roots (sagebrush, oak brush), and the continual translocation of insoluble as well as soluble organic compounds from higher to lower parts of the horizon results in a diverse mixture of carbon of different ages throughout the horizon. All these processes of carbon cycling (accumulation, transport, and removal) are highly dependent on the topographic setting of the soil (slope, aspect, and drainage), the type and rate of biologic activity in the soil, the inorganic sedimentation rate, the type of vegetation (for example, grassland versus forest), the geomorphic history of the site, and climate (Machette and others, 1992; Scharpenseen and Becker-Heidman, 1992; Paul and others, 1997; Rumpel and others, 2003).

A further problem in interpreting AMRT ages is that sample pretreatment procedures before ^{14}C analysis vary with the objectives of each study. A number of different procedures have been used to isolate different components of soil organic matter that yield very different ^{14}C ages (e.g., Stuckenrath and others, 1979; Mathews, 1985; Scharpenseen and Becker-Heidman, 1992; Trumbore and Zheng, 1996; Tsao and Bartha, 1999). No single procedure is optimal, but consistent pretreatment of all samples from a site is mandatory for meaningful interpretation of AMRT ages. For the samples from the East Ogden site and our original three samples from Garner Canyon (table 1), we followed many previous studies in using physical methods to isolate the fine organic fraction of the A-horizon sediment (Kihl, 1975), and then we asked our three dating laboratories to centrifuge this fraction during HCl and NaOH treatments (table 1). The remaining dated fine fraction consisted mostly of humins, which commonly yield the oldest and most consistent ages from organic-rich soils (e.g., Wang and others, 1996; Pessenda and others, 2001; Kristiansen and others, 2003).

For the more recent A-horizon AMRT samples from Garner Canyon, Stafford and Forman (1993) used similar methods to prepare the humin fraction and also dated the decalcified soil (HCl treatment only) and humic acid (KOH soluble) fractions of the same samples. In contrast to most studies of different A-horizon fractions, the humin fraction of Stafford and Forman's (1993) samples gave ages as much as 37% younger than the ages from the decalcified soil fractions (McCalpin, 1998, p. 145). Stafford and Forman (1993) offered no explanation for the unusual age relations among the paired decalcified-fraction and humin-fraction ages. In this report, we use the ages on the decalcified fractions because they have been previously published (McCalpin, 1998, p. 145), because the ages on both humin and decalcified fractions overlap our estimated times of A-horizon burial (table 1), and because the preparation of the decalcified samples was similar to the preparation of most other AMRT samples from Wasatch fault paleoseismology sites.

As implied by the term "apparent mean residence time," A-horizon AMRT ages are older than the time of A-horizon burial by the amount of time represented by the "mean residence time" of the type of carbon dated in the buried A horizon (Mathews, 1980). The distribution of AMRT ages with mean sample depth in modern surface A horizons (<0.5 m depth) at central Utah trench sites shows that apparent residence times range from hundreds to thousands of years (figure 2). Even samples from the upper 0.1 m of A horizons have ages that range from 100 to 1400 years. Ages increase only slightly with depth and the weak relation between age and depth (r^2=0.35 for all samples from <0.5 m depth, r^2=0.29 for data from faults with <2 kyr recurrence, figure 2) suggests that many factors besides depth have affected the dated carbon in different ways at different sites. Discounting samples that may have been extensively mixed with younger carbon by burrowing or that may contain much older reworked carbon, the steeper regression line of figure 2 suggests that ages from mean depths of <0.2 m in A horizons on scarp slopes of faults with recurrence intervals of <2 kyr are typically 0.1-0.5 ka (although the 95% confidence interval on the regression line suggests ages as great as 1.8 ka), whereas ages from the same depths adjacent to faults with longer recurrence intervals are typically greater, perhaps about 0.5-1.2 ka. McCalpin and Nishenko (1996; McCalpin, 1998, p. 144) report an unpublished study of one A horizon buried in response to surface faulting on the Rock Creek fault in Wyoming with an age-depth gradient of 4.1 yr/mm. This gradient is significantly less steep than those of figure 2 and may or may not apply to Wasatch fault sites. For example, mixing by burrowing rodents or tree roots, as occurs in A horizons at Weber segment

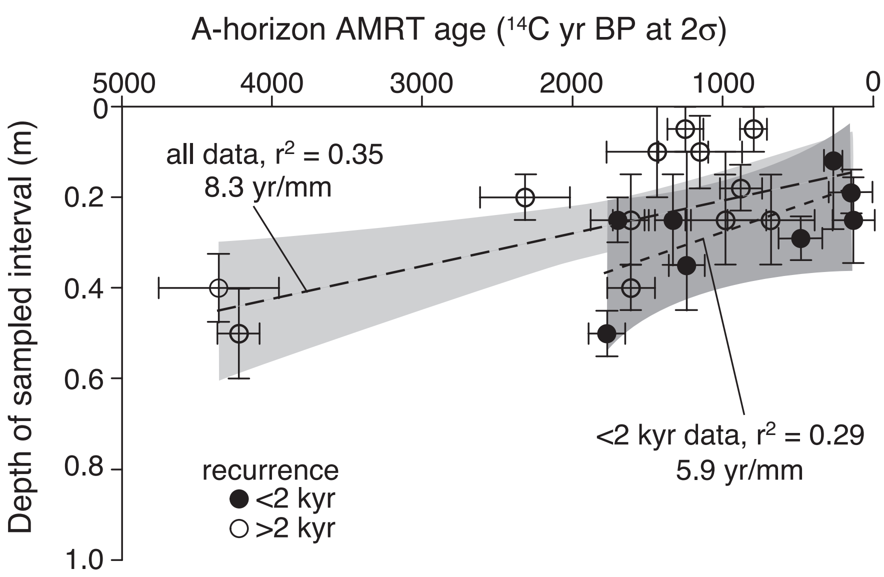

Figure 2. Sample depth versus apparent mean residence time (AMRT) ^{14}C ages on concentrates of organic matter from the A horizons of modern soils at fault trench sites in central Utah. Error bars on ages are twice laboratory reported errors (2σ); total age errors are much greater. Four hundred years has been added to the two oldest ages as an approximate correction for the difference between ^{14}C years and solar years for ages in this age range (e.g., Stuiver and others, 1998). For younger ages these differences are <150 years and no correction is made. Error bars on depths show interval of sediment sampled. Ages from samples whose mean depths are >0.5 m, or those probably influenced by ^{14}C produced by thermonuclear explosions in the 1960s, are not shown. Symbols distinguish ages from trench sites where surface-fault recurrence is thought to be <2 kyr (solid dots) and >2 kyr (circles). Linear regression lines thru all data, and <2-kyr data, are dashed; shading shows 95% confidence intervals about regression lines. Ages compiled from Nelson and VanArsdale (1986), Foley and others (1986), West (1989, 1994), Personius (1991), Machette and others (1992), McCalpin (1998, p. 145), Black and others (2000), and McCalpin and Forman (2002).

trench sites, would substantially increase A-horizon age gradients and decrease apparent residence times.

Samples from the East Ogden site illustrate another problem in using AMRT ages on modern A horizons to estimate apparent mean residence times for buried A horizons. Some AMRT ages from East Ogden (from depths as great as 0.8 m) have greater than modern ^{14}C activity, which shows that burrowing has mixed significant amounts of "bomb" carbon produced by above-ground nuclear testing in the early 1960s into the lower parts of some sandy surface A horizons. It is difficult to estimate how much of the carbon in the modern A horizons is bomb carbon, which horizons have been burrowed and which have not, and whether organic-rich sediment from older A horizons farther up the slope has been reworked into modern horizons. For these reasons, even a very extensive program of radiocarbon dating of modern A horizons might not significantly improve estimates of the AMRT effect in modern A horizons at sites along the Weber segment. Buried A horizons at Weber segment sites are unaffected by bomb carbon because the sampled parts of the horizons near faults lie below the burrowing depth of most rodents and translocated modern carbon in ground water was removed during chemical pretreatment of AMRT samples (Machette and others, 1992).

Comparison of paired samples from the same stratigraphic units in central Utah trenches dated by different methods suggests a range of hundreds of years for the apparent mean residence times of carbon in AMRT samples. On average, AMRT ages are 100 to 700 yr older than TL ages or AMS ^{14}C ages on charcoal from the same units (figure 3). But some AMRT ages are younger than their paired TL or AMS ages and others are older by as much as 1200 yr. Furthermore, like AMRT ages, TL ages and AMS ages are maximum ages for the burial times of the sampled A horizons: thermoluminescence analysis dates scarp-slope sediment that accumulated gradually and was mixed within A horizons prior to burial, and dated charcoal is detrital and so older than its host sediment by an unknown number of years. Considering the many uncertainties suggested by figures 2 and 3, we assume a range of apparent residence times for dated carbon in AMRT ages from Weber segment sites of 100-500 yr and include that additional uncertainty in estimating the times of A horizon burial (table 1). Although wider than the range assumed for many other Wasatch fault trench studies, the range includes the AMRT values used in previous studies (e.g., Lund and Black, 1998; Lund and others, 1991; Machette and others, 1992; Black and others, 1996; McCalpin and Forman, 2002).

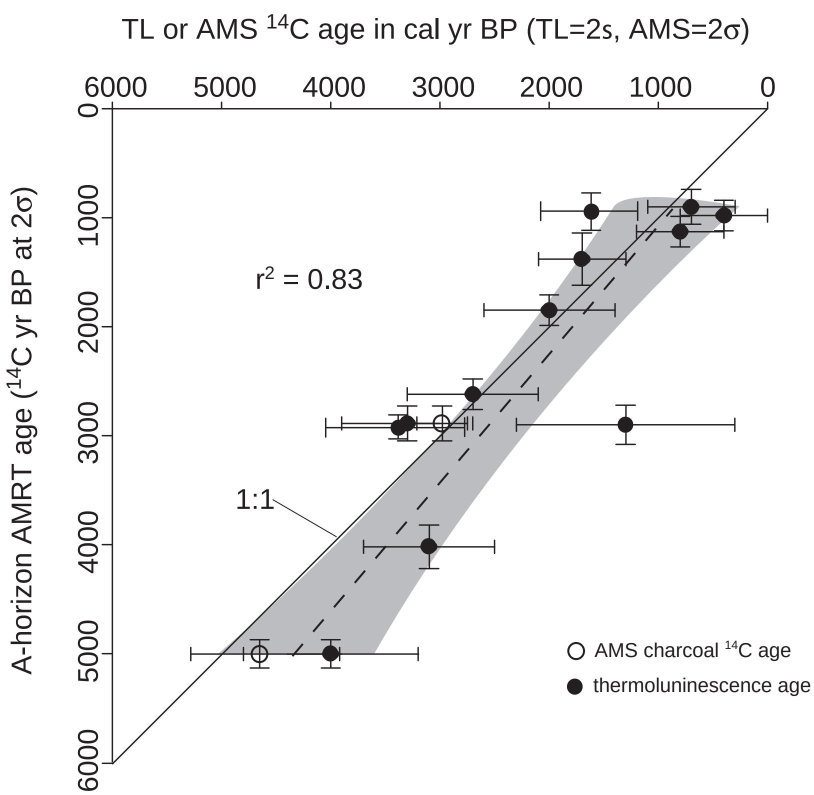

Figure 3. *Comparison of apparent mean residence time (AMRT) ^{14}C ages on concentrates of A-horizon organic matter with AMS ages on detrital charcoal (circles) or thermoluminescence ages on sediment (solid dots) from the same stratigraphic units in central Utah fault trenches. Error bars on AMRT ages are twice laboratory reported errors (2σ); total age errors are much greater. Error bars on charcoal ages show 2σ interval on calibrated ages (methods of Bronk Ramsey 1995, 2001, and Stuiver and others, 1998). Error bars on thermoluminescence ages (table 2) are shown at 2σ. Only paired ages <5 ka are shown. We make approximate corrections to AMRT ages for the difference between ^{14}C years and solar years only for ages where the difference is >150 years (corrections of 200 to 700 years made to seven ages). Linear regression line thru data points is dashed; shading shows 95% confidence interval about regression line. Ages compiled from Foley and others (1986), Forman and others (1989), Forman and others (1991), Lund and others (1991), Jackson (1991), Machette and others (1992), McCalpin and others (1994), and McCalpin (1998, p. 145).*

We use the AMRT ages from Weber segment sites, along with TL and charcoal AMS ages, to estimate times of A-horizon burial inferred to coincide with surface faulting (table 1; e.g., McCalpin, 1998). We increase errors for laboratory reported AMRT ages to ±80 yr, if reported errors are less than this value, as recommended by Taylor and others (1996). To the 2σ estimate of the mean age of the carbon in each dated sample we then subtract an assumed AMRT with a range of 100-500 yr from each AMRT age to estimate the time of A-horizon burial (table 1). For example, for a sample whose carbon has a mean age (2σ) of 1.5-1.2 ka, we subtract a minimum AMRT of 0.1 kyr from the older end of the mean age interval and a maximum AMRT of 0.5 kyr from the younger end of the mean age interval to yield a range in the time of burial of 1.4-0.7 ka. Although ages on thin A-horizon samples (<0.1 m) are likely to have lower AMRTs than thick (>0.2 m) horizons (e.g., McCalpin and Nishenko, 1996), present Utah data are insufficient to support previously proposed corrections for sample thickness or mean depth (e.g., Machette and others, 1992; McCalpin and Forman, 2002). Unlike most previous Utah trench studies (e.g., Lund and others, 1991; Machette and others, 1992; McCalpin and Nishenko, 1996; Lund and Black, 1998), we do not calibrate most AMRT ages to account for fluctuations in the rate of ^{14}C production in the upper atmosphere (Taylor and others, 1996; Stuiver and others, 1998). Calibration procedures were not designed for ages on samples with carbon age distributions as broad and uncertain as those of AMRT samples from Utah trench sites. Our only adjustment for fluctuations in the rate of ^{14}C production is to add +200 or +500 years to two ages that fall within parts of the calibration curve that deviate by more than a 150 years from solar (calendar) years (table 1). Much smaller uncertainties in AMRT ages, such as corrections for isotopic fractionation, are assumed to be incorporated within the large error ranges that we apply to AMRT ages. Although these procedures result in less precise estimates of the times of Wasatch fault earthquakes than many previous studies, our uncertainties are comparable to those recently recommended by Lund (2005).

Thermoluminescence Analyses

TL dating of fine-grained sediment from Wasatch fault exposure sites, including East Ogden and Garner Canyon, was an early, particularly successful application of this dating method (Forman and others, 1989a, 1989b, 1991, 2000). The TL technique directly dates silicate mineral grains in sediment, grain ages reflecting the time since the sediment was last exposed to sunlight (bleached). For samples from East Ogden and Garner Canyon, the analyzed fraction consisted of silt (4-11 microns) from eolian-enriched A horizons developed on fine-grained colluvium adjacent to faults (McCalpin and Forman, 1989; Forman and others, 1991; Nelson, 1992; Stafford and Forman, 1993; e.g., McCalpin and Berry, 1996). A moisture content of 10±3% was assumed for all samples. Because ages for the same samples determined by two or three different TL methods (total bleach, partial bleach, and regeneration methods) overlap at 1σ, the samples were apparently well light bleached prior to deposition. For simplicity, we use the ages by the total bleach method (table 2), with the residual level defined by a ≥12-hour exposure to sunlight, in interpreting the history of faulting at the two sites (Forman and others, 1991; Stafford and Forman, 1993). Ages are reported in ±1σ format, following Forman and others (1991; table 2).

TL ages from buried A horizons along the Wasatch fault are maximum ages—commonly inferred to be close maxima—for the times of A-horizon burial in response to surface faulting. Although A horizons accumulate gradually, mostly through surface-wash processes, mixing by plants and animals is particularly thorough in the uppermost parts of the horizons that were sampled for dating. Some of the analyzed silt may also have been infiltrated from the surface into the upper parts of horizons. For these reasons, the TL ages are approximate average ages for the silt throughout the sampled thickness of the horizon. Ages from the surface-wash dominated A horizons at East Ogden probably predate burial of the horizons by at least tens of years and perhaps a century or two. Ages from distal A-horizon sediment in colluvial wedges overlying buried A horizons are minimum ages for the times of burial.

Stafford and Forman (1993) reported TL ages from the Garner Canyon exposure that were mostly much older than stratigraphically equivalent AMRT ages (table 2; plate 2) indicating that much of the dated silt in the samples was derived from older sediment in the fault scarp free-face and inadequately bleached before deposition. Age differences among AMRT and TL samples were less for samples near the tops of buried A horizons (McCalpin (1998, p. 146), probably because mixing by woody roots and rodents at Garner Canyon is thorough and frequent in the uppermost parts of A horizons. Such mixing brings A-horizon sediment to the surface where it is exposed to sunlight.

EAST OGDEN TRENCH SITE

Overview and Methods

The faulted alluvial fans at the base of the mountain front on the east edge of the City of Ogden interested Gilbert (1928, his plates 15A and 18A) as much as they do us (Nelson, 1988). Four parallel, linear scarps—the two highest with 5 m and 8 m of surface displacement, respectively—and many small secondary scarps cut alluvial fans of two relative ages below the 17-to-16-ka Provo shoreline of Lake Bonneville (map on plate 1; Oviatt and others, 1992; Oviatt, 1997; Lund, 2005, p. 16). The degree of argillic soil horizon development on the older fans (soil profile 1 on log of trench 1, plate 1; table 3) and their geomorphic position relative to the lower fans (of late Holocene age) show that the older fans are some of the oldest Holocene alluvial deposits along the Weber segment (Nelson and Personius, 1993). Equivalent-aged fans at the mouths of most other canyons along the fault have been eroded or buried. Gilbert (1928, his plate 15A) thought that the sharper crested, 8-m scarp was younger than the 5-m scarp. Below, we conclude that he was right.

We measured topographic profiles perpendicular to scarps to measure the amount of surface displacement across scarps using two methods. Eleven surface displacements along seven profiles were measured with a stadia rod and Abney level (methods of Bucknam and Anderson, 1979, and Machette, 1989; plates 1 and 2) and an additional 31 displacements were measured from profiles constructed using air photographs and a computer–assisted photogrammetric plotter (method discussed by Nelson and Personius, 1993, and in section V). The map on plate 1 shows all surface displacements for the East Ogden site, including those measured on scarps visible on 1952 air photography where the scarps no longer exist.

To date the faulted alluvial fans and reconstruct the earthquake history of the East Ogden site, we excavated five trenches across the three highest scarps: trench 1 and trench 5 across the 5-m scarp, trench 2 and trench 3 across the 8-m scarp, and trench 4 across a 2-m-displacement scarp antithetic to the 8-m scarp (map on plate 1). The fourth parallel scarp, and other small scarps west of it, were modified or removed during housing construction in the 1970s and could not be trenched. The vertical walls of trenches 4 and 5 and the end-most thirds of the longer trenches were supported with hydraulic aluminum shores. The middle thirds of the longer trenches were unsupported, but their unmapped walls were sloped for safe egress. Trenches were logged with standard methods (McCalpin, 1998, p. 56-70). The lowest 1.5 m of the central parts of trenches 1 and 2 were only exposed for 15 minutes just prior to backfilling the trenches.

Interpretation of Trench Stratigraphy

Sequence of Faulting and Deposition in Trench 1

We excavated trench 1 in fan sediment across the 5-m scarp at the East Ogden site, between two wide, late Holocene alluvial fans (map on plate 1). Measured displacement of the surface near the trench along the scarp-per-

Table 2. *Thermoluminescence ages for samples from the East Ogden and Garner Canyon sites.*

TL Lab No.	Unit No.	Location (h,v)[1]	Sample type[2]	Sample depth[3]	Equivalent dose (Gy)[5]	Lab-reported age (ka)[6]	Interval age (ka)[7]
East Ogden – trench 1							
ITL-113	3bA	26,7.9	W	0.26	10.99±1.18	1.2±0.1	1.4-1.0
ITL-47	3bA	26,8.2	W	0.45	8.87±1.10	1.2±0.2	1.6-0.8
ITL-112	3bA	26,8.3	W	0.69	15.73±1.67	2.0±0.2	2.4-1.6
ITL-75	3bA	26,8.6	W	0.88	25.31±2.56	2.5±0.3	3.1-1.9
ITL-72	3bA	26,8.9	W	1.26	24.49±2.20	3.1±0.3	3.7-2.5
ITL-24	3bA	26,9.5	W	1.76	31.52±3.64	2.7±0.3	3.3-2.1
ITL-138	7aA	26,9.7	F	1.92	35.78±3.45	4.6±0.4	5.4-3.8
East Ogden – trench 2							
ITL-115	3aA	22,9.2	W	0.75	13.98±1.31	1.5±0.2	1.7-1.3
ITL-114	3aA	22,9.5	W	1.03	16.00±1.32	1.8±0.2	2.2-1.4
ITL-74	5aA	22,9.8	W	1.27	29.30±2.54	3.2±0.3	3.8-2.6
ITL-80	7A	21.2,10.5	F	2.21	37.74±3.56	4.0±0.4	4.8-3.2
Garner Canyon exposure							
OTL-329	1bA	6.1,2.6	W	0.12	4.39±0.90	1.1±0.3	1.7-0.5
OTL-332	1bA	6,1,2.5	W	0.26	12.68±2.55	3.2±0.5	
OTL-334	1bA	6.2,2.2	W	0.40	16.92±3.11	3.4±0.6	
OTL-335	3aA	6.1,2.0	W	0.75	6.29±0.68	1.6±0.2	2.0-1.2
OTL-341	3aA	6.1,1.6	W	1.10	17.64±0.91	5.3±0.4	
OTL-342	4a	6.1,1.4	D	1.25	48.99±5.91	14.0±3.0	
OTL-330	5A	6.7,1.2	W	1.75	20.31±2.90	3.4±0.3	4.0-2.8

[1] *Location (horizontal, vertical) on meter reference grid used to map wall of exposures. Superscripts on sample ages shown in figures and plates are the digits of sample numbers (first column).*

[2] *W, A-horizon sediment deposited mostly by surface wash on scarp slope; F, sediment in A-horizon developed on fan surface prior to faulting; D, colluvial debris facies derived from alluvial deposits exposed in scarp face.*

[3] *Vertical depth below the surface of center of sampled zone in meters. Samples were about 0.12 m thick.*

[5] *Equivalent dose at 1σ. Measurements by the total bleach method as explained in Forman and others (1991). Samples were preheated to 150º for 16 hours prior to analysis and exposed to 16 hours of natural sunlight in Boulder, Colorado, to define residual level. Equivalent dose calculated using temperature range of 250-350ºC for East Ogden samples and 300-400°C for Garner Canyon samples.*

[6] *Laboratory reported thermoluminescence (total bleach) age in thousands of years before present (ka). Errors listed at 1σ, calculated by averaging errors across the temperature range.*

[7] *Ages for samples from modern A horizons or those buried by colluvial sediment produced in response to surface faulting. Ages (from column 7) are expressed as time intervals at 2σ rounded to the nearest hundred years. Because errors on the ages are large, some age intervals probably include the times when A horizons were buried in response to surface faulting.*

Table 3. *Properties of soils on Holocene alluvial-fan sediments at the East Ogden site.*

Horizon[1]	Average depth (cm)	Parent material[2]	Munsell dry color[3]	Volume percent[4]			Percent by weight[5]			Percent[6] carbonate	Percent[7] organic matter	Structure[1]	Clay films[1]
				Pebbles (0.2-8 cm)	Cobbles (8-25 cm)	Boulders (>25 cm)	Sand (2-0.5 mm)	Silt (50-2 um)	Clay (<2 um)				
Soil profile 1 – East Ogden trench 1, m 4.4													
A1	0-5	S (1aA)	7.5YR 4/3	0	0	0	81	13	6	0.3	2.4	vw,f,sb-pl	—
A2	5-15	S (1aA)	7.5YR 5/3	0	0	0	82	11	7	0.2	0.9	vw,f,gr	—
A3	15-31	S (1bA)	7.5YR 5/3	0	0	0	80	12	8	0.3	0.7	w,f,sb	—
A4	31-43	S (7aA)	7.5YR 5/3	0	0	0	79	12	9	0.3	0.5	vw,f,gr	—
AB	43-59	S (7aA)	7.5YR 5/4	15	15	0	78	12	10	0.3	0.5	sg	1co
2B1t	59-78	F (7cBt)	7.5YR 6/5	30	20	10	80	10	10	0.3	0.3	vw,m,ab	2co,0fbr
2B2t	78-142	F (7cBt)	7.5YR 6/5	30	20	10	79	11	10	0.3	0.3	wm,m-c,ab	3co,2dbr,0fpo
2CB	142-182+	F (7d)	7.5YR 7/3	40	20	8	86	8	6	0.3	0.2	vw,m,ab	2co,0fbr
Soil profile 2 – East Ogden trench 5, m 3.2													
A1	0-14	S (1aA)	7.5YR 5/3	10	5	0	68	20	12	0.3	1.0	wm,m,sb-pl	—
A2	14-32	S (3aA)	7.5YR 5/4	10	10	0	71	14	15	0.3	0.6	vw,m,sb	—
Bt	32-72	S (3bBt)	7.5YR 6/4	8	15	0	80	10	10	0.3	0.4	vw,f,ab	1co
2Bt	72-114	F (4bBt)	7.5YR 7/4	35	5	3	85	8	7	2.2	0.5	sg-vw,f,ab	3co,0fbr,si
3C	114-165+	C (5b)	10YR 7/3	40	5	3	92	5	3	3.9	0.1	sg	si,ca

[1]Horizon nomenclature, field properties, and terminology of Soil Survey Staff (1975) and Birkeland (1984, 1999). Structure – vw, very weak; w, weak; wm, weak to moderate; m, moderate; f, fine; m, medium; c, coarse; sg, single grain; sb, subangular blocky; pl, platy; gr, granular; ab, angular blocky; dash indicates a range in property. Clay Films – 0, very few; 1, few; 2, common; 3, many; f, faint; d, distinct; co, colloid coats grains; br, bridging grains; po, in pores; si, silt coatings on clasts; ca, carbonate coatings on clasts. Profiles described by Alan Nelson, September 1986.

[2]C, stream (channel) deposit; F, debris-flow deposit; S, surface wash colluvium with minor amounts of loess. Unit labels from plates 1 and 2 in parentheses.

[3]Dominant dry color of unit; Munsell color of Oyama and Takehara (1970).

[4]Particle size distribution of <2 mm fraction using sieve-pipette methods (Singer and Janitzky, 1986) with removal of carbonates and organic matter (Jackson, 1956).

[6]Percent carbonate by method of Dreimanis (1962).

[7]Percent organic matter by method of Walkley and Black (1934).

pendicular profile line is 5.0 m. Stratigraphic displacement of the unit 7aA/7cBt contact across fault F1 is 6.3±0.5 m. The stratigraphic displacement exceeds the surface displacement because of backtilting of the footwall. For trench 1 and other trenches, we calculated stratigraphic displacement errors (method of Machette, 1989) from reasonable minimum and maximum slopes of contacts measured from trench logs on plates 1 and 2. Three distinct colluvial wedges in trench 1 (units 1 through 6, plate 1) formed in response to three surface-faulting earthquakes (labeled A, B, and C in red) following development of a clay-rich soil on middle Holocene debris-flow deposits (unit 7). The wedge deposited following the earliest earthquake (A) is similar to the earthquake-A wedge in trench 2 in that coarse, bouldery debris-facies colluvium overlies sandy debris facies within the wedge (facies terminology of Nelson, 1992). The thick, fine-grained A horizons that developed on colluvial wedges following earthquakes B and C consist mostly of surface-wash sediment transported from the slope above the scarp. A similar A horizon on the earthquake-A wedge (unit 6) has been eroded and incorporated into the overlying wedge.

Based on the lithologies, stratigraphic relations, and ages from units in trench 1, we infer the following sequence of events:

(1) Lake Bonneville shoreface sand and gravel (unit 12) were deposited on mountainfront slopes, probably during the transgression to the Bonneville shoreline about 22-17 ka (Oviatt and others, 1992; Oviatt, 1997; Lund, 2005, p. 16). The sand and gravel were eroded during the subsequent regression from the Provo shoreline about 17-16 ka.

(2) A series of debris-flow and stream deposits (units 11 through 7bE) spread over the shoreface units during the early and middle Holocene. Here and there, the streams and flows eroded into the shoreface units and earlier flow and stream deposits, filling the channel cuts with younger alluvial sediment. A TL age from the A horizon on a debris flow (unit 7) near m 26 suggests that the flow was deposited prior to 5.4-3.8 ka (table 2; plate 1; figure 4).

(3) A thin mantle of colluvium consisting of surface-wash sediment and loess (units 7aA and 7bE) slowly accumulated on unit 7 and was mixed with younger sediment as soil development proceeded forming an argillic Bt horizon (unit 7cBt; table 3) and a discontinuous E horizon (unit 7bE; eluvial, light-colored soil horizon leached of clay, silt, and organic material).

(4) A surface-faulting earthquake (earthquake A) on fault F1 displaced unit 7 vertically about 2.4 m. This displacement value is the remaining displacement after subtracting displacements during later earthquakes from the stratigraphic displacement of the unit 7aA/7cBt contact (table 4; because such displacements are based on maximum wedge thicknesses, we do not estimate errors on inferred displacements). During or shortly after earthquake A, coarse, cobbly, sandy gravel derived (partly by slumping) from shoreface units was deposited in an open fissure (unit 6e and perhaps 6c) at the base of the scarp produced by an inferred antithetic fault near m 22. A thick wedge of similar lower debris-facies colluvium (units 6a and 6b; plate 1) was deposited over the sediment filling the graben. No ages constrain the time of earthquake A in trench 1.

(5) Sandy, gravelly, lower wash-facies colluvium was then deposited more gradually on the west-facing slope of the wedge (unit 6f). Later deformation, erosion, and mixing of this unit with overlying unit (4) obscured the contact between these two units. Irregular patches of silty sediment in unit 6f may be chunks of an eroded Bw horizon that developed on the unit-6 debris-facies wedge before earthquake B. A TL age of 3.3-2.1 ka at m 26 on sediment in the lower part of unit 3bA shows that a few tenths of meters of distal A-horizon sediment accumulated on unit 7aA following earthquake A (table 2; plate 1; figure 4). We infer that this A horizon developed on the distal part of the colluvial wedge (unit 6f) several meters to the east and was later incorporated into younger unit 4.

(6) A second surface-faulting earthquake (earthquake B) on the same fault displaced units 6 through 12 vertically down-to-the-west about 2.9 m (table 4). Unit 6a was backtilted during this earthquake and a pre-existing fissure widened or a new fissure formed in unit 7d at the west edge of unit 6a (unit 6d). The fissure rapidly filled with slumped sediment from the overlying debris wedge (units 6a and 6f). The entire unit-6 wedge was deformed through stretching along fault F1 during this earthquake. The clast-supported, open-work structure (little matrix sediment) of unit 6c suggests that it might have formed by filling of a small fissure during earthquake B rather than by filling of the graben during earthquake A. Immediately following earthquake B, a wedge of scarp-derived, lower debris-facies sediment (unit 5b) was deposited against the scarp above the unit-6 wedge. Unit 5b has the characteristic cross section of a lower debris-facies wedge deposited in response to normal faulting (plate 1; Schwartz and Coppersmith, 1984; Nelson, 1992).

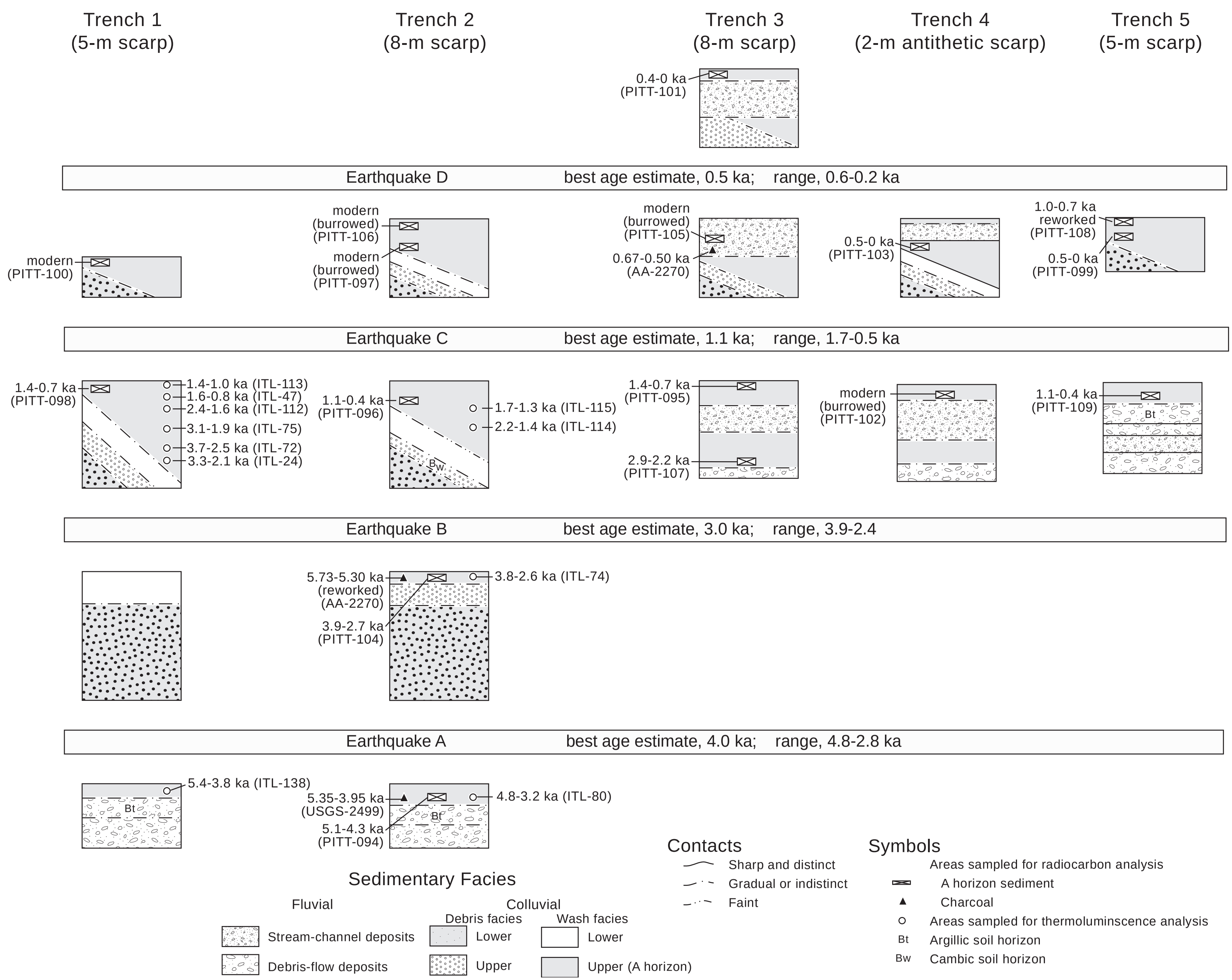

Figure 4. *Schematic diagram showing the position of dated samples and correlation of debris-flow and colluvial units in trenches at the East Ogden site. Original age data shown on tables 1 and 2. Best age estimates for the times of four surface-faulting earthquakes and the age ranges during which the earthquakes probably occurred are listed between units deposited prior to or in response to each earthquake.*

Table 4. Vertical component of fault slip inferred from exposures along the northern Weber segment

Surface displacement and surface-faulting earthquake(s)[1]	Maximum colluvial wedge thickness (m)[3]	Vertical displacement (m) from[2]			Cumulative vertical displacement (m)[7]
		Stratigraphic displacement (m)[4]	Fault slip per event (m)[5]	Surface displacement per event (m)[6]	
East Ogden site					
Trench 1 – 5.0 m					
earthquake C	0.7	–	1.0	0.9	5.0
earthquake B	1.8	–	2.9	2.2	4.1
Post-unit-7 faulting, earthquake A	<1.5	6.3 (5.8-6.8)	2.4	1.9	1.9
Trench 2 – 7.8 m					
earthquake D?	0.3?	–	<0.5?		
earthquake C	1.2	1.2+0.3+0.2	1.7 **2.3**	2.3	7.8
earthquake B	1.9	–	2.8 **2.6**	2.6	5.5
Post-unit-8 faulting, earthquake A	2.3	7.8 (7.3-9.5)	3.3 **2.9**	2.9	2.9
Trench 3 – 2.3 m					
earthquake D	0.8-0.9	–	0.8	0.8	2.3
Post-unit-9 faulting, earthquake C	0.4 + 0.8	2.2 (2.1-2.4)	1.4	1.5	1.6
Post-unit-10 faulting	–	2.5 (2.3-2.7)	–	–	–
Trench 4 – 0.7 m					
Post-unit-5 faulting, earthquake C	1.0	1.2 (1.1-1.5)	1.2	0.4	0.7
Post-unit-6 faulting, earthquake B?	–	2.2 (1.9-2.3)	1.0	0.3	0.3
Trench 5 – 1.2 m					
Post-unit-4 faulting, earthquake C	0.8	1.8 (1.8-2.0)	1.2	1.2	1.2
Garner Canyon site					
Exposure – 4.4 m					
earthquake C	1.0	–	>1.0	1.3	4.4
earthquake B	0.8	–	>0.8	1.0	3.4
earthquake A	0.9	–	>0.9	1.1	2.3
earlier earthquake?	>0.8?	–	>0.8	1.0	1.3

Notes: *Because fault dips below base of exposures are difficult to estimate, we tabulate only vertical displacement during surface-faulting earthquakes as measured or inferred from stratigraphic relations in trenches and surface displacements across scarps. Dash indicates no data.*

[1] *Earthquakes listed from youngest to oldest. Question mark indicates uncertainty in occurrence of earthquake. Presence of earthquake D in trench 2 and earthquake B in trench 4 is uncertain as explained in text. Numbers following exposure name are surface displacement at exposure site as measured from scarp-perpendicular profiles (plates 1 and 2).*

[2] *Vertical component of displacement from faulting and folding, including back tilting, and antithetic faulting, projected into vertical plane of trench wall. Trenches are perpendicular to scarps.*

[3] *Maximum thickness of debris and wash facies near main fault deposited in response to surface-faulting earthquakes. Earthquake A wedge thickness in trench 1 is greater than original thickness of wedge because wedge was stretched out along fault plane during later earthquakes. For earthquake C in trench 3, we sum the thickness of two wedges deposited adjacent to two separate faults (F1 and F3).*

[4] *Vertical component of fault slip estimated from displacement of the same contact on either side of fault zone. Reasonable range of uncertainty in listed values in parentheses. For earthquake C in trench 2, stratigraphic displacement during slip on three fault strands (F2, F3, F4) totals 1.7 m. Although post-unit-10 displacement in trench 3 is 0.3 m greater than post-unit-9 displacement, the apparent difference in displacement is too small to attribute to surface faulting during a major earthquake.*

[5] *Vertical component of slip during each earthquake estimated by apportioning stratigraphic displacement based on the ratio of maximum colluvial-wedge thicknesses for each earthquake to total maximum thickness of all wedges. In trench 2, because colluvial wedges become thinner with successive earthquakes on large scarps, we infer a similar vertical component of slip during earthquakes A, B, and C (values in bold) in contrast to slip indicated by colluvial-wedge thicknesses. Vertical slip during earthquake B? in trench 4 is estimated by subtracting vertical slip in earthquake C from total post unit-6 displacement.*

[6] *Vertical component of slip during each earthquake estimated by apportioning displacement across scarp profile near exposure site based on the ratio of maximum colluvial wedge thicknesses for each earthquake to total maximum thickness of all wedges.*

[7] *Cumulative vertical displacement across trenched scarps using surface displacement per event estimates (column 5).*

(7) Over the next few tens to hundreds of years following the deposition of unit 5b, more distal colluvial wedges were deposited as three units (5a, 4, and 3d) over the earlier debris-facies wedges (units 6 and 5b). Unit relations are obscure in this part of the trench, but it is clear that unit 5a is the finer grained facies of the debris wedge deposited by gravity and surface-wash processes following earthquake B. Overlying units 3d and 4 consist mostly of wash facies (surface-wash sediment), and the development of both A and E horizons in these units as they gradually accumulated obscured their contacts with adjacent units. Both units may have been slightly deformed by antithetic faulting during earthquake C. The abundant boulders in unit 4 probably rolled from higher shoreline slopes. Unit 4's fine-grained lithology and footslope position probably attracted burrowing animals. We interpret unit 4 as a burrowed mixture of (1) wash-facies colluvium from the adjacent colluvial wedge, and (2) post-earthquake-B, gravity-deposited and wash-deposited colluvium transported from higher on the scarp. The upper part of unit 4 is probably the downslope facies equivalent of unit 5a. Unit 3d is less burrowed and its light color suggests the gradual development of an indistinct E horizon as overlying units accumulated.

(8) As colluvial deposition slowed and the scarp slope gradually stabilized, an organic-rich, wash-facies colluvium accumulated over units 3d and 4 (units 3cA and 3bA). We interpret an AMRT age from the upper east end of unit 3cA to indicate that the unit accumulated until about 1.4-0.7 ka (table 1; plate 1). Stratigraphic relations and TL ages (samples 24, 72, 75, 112, 47, and 113, table 2; figure 4) suggest that unit 3bA is a fine-grained facies equivalent of unit 3cA, deposited between one and three thousand years ago. At m 26 in trench 1, the rate of deposition was greatest immediately following earthquake B, and deposition then slowed exponentially until about the time of earthquake C (Forman and others, 1991). A slight fining-upward lithologic change across an indistinct, gradational contact between units 3bA and 3aA west of m 26 may be the result of a gradual decline in the slope of the scarp hundreds of years after earthquake B.

(9) A third surface-faulting earthquake (earthquake C) displaced units 3 through 12 and buried the east end of unit 3cA with debris facies after 1.4-0.7 ka (tables 1 and 2; plate 1; figure 4). Based on stratigraphic displacement of unit 7 and colluvial wedge thickness, vertical slip during this earthquake was about a meter (table 4). The fault contact between units 5 and 10 was sheared during this earthquake as indicated by the halves of a bisected, weathered, schist pebble (note n6, plate 1) displaced 0.15 m. Unit 2, the lower debris-facies wedge deposited following earthquake C, is small and discontinuous, reflecting the small surface displacement during the earthquake. The three small, stacked, debris-facies wedges of unit 2 are probably the result of slumping of the free face several times soon after faulting.

(10) During the following few hundreds of years, surface wash gradually deposited a long wash-facies wedge of organic-rich A-horizon sediment (unit 1eA) over units 2, 3cA, and 3bA. We could not identify any lithologic discontinuity within units 3bA and 1eA near the base of the scarp that would correspond with the time of earthquake C; the contact between the units is inferred based on the two youngest TL ages at m 26. Mixing of the cumulic A horizon has probably destroyed any prior discontinuity between the units. The upper part of unit 3bA grades almost imperceptibly into slightly finer grained unit 3aA in the western part of the trench. Although such a contact might record a change in scarp slope sedimentation following a surface-faulting earthquake, TL ages indicate that the contact is considerably older than the time of earthquake C.

(11) The modern A horizon (unit 1cA) developed through surface wash and mixing of organic material and previously deposited sediment by roots and animals over the past few hundred years.

Sequence of Faulting and Deposition in Trench 2

We excavated trench 2 across the 8-m scarp on the scarp-perpendicular profile line of trench 1 (map on plate 1). Measured displacement of the surface across the scarp is 7.8 m; stratigraphic displacement of the unit 8aE/8bBt contact across this scarp is 7.8±0.5 m (table 4). As in trench 1, three colluvial wedges (units 1 through 6) formed in response to three surface-faulting earthquakes following soil development on middle Holocene debris-flow deposits (unit 8). Each wedge consists of coarse, lower debris-facies colluvium overlain by finer grained upper debris facies and wash facies. In the oldest wedge, deposited in response to earthquake A, bouldery lower debris facies (unit 6a) derived from debris-flow deposits overlie clean, sandy debris facies (unit 6b) derived from Lake Bonneville nearshore sand (unit 13).

Based on the lithologies, stratigraphic relations, and ages from units in trench 2, we infer the following sequence of events:

(1) Lake Bonneville shoreface sand and gravel (unit 13) were deposited on mountainfront slopes, probably during the transgression to the Bonneville shoreline about 22-17 ka (Oviatt and others, 1992; Oviatt, 1997; Lund, 2005, p. 16). The sand and gravel were eroded during the subsequent regression from the Provo shoreline about 17-16 ka.

(2) A series of debris-flow and stream deposits (units 12 through 8) spread over the shoreface units during the early and middle Holocene. Here and there, the streams and flows eroded into the shoreface units and earlier flow and stream deposits, filling the channel cuts with younger alluvial sediment. Two ^{14}C ages and a TL age from the lower part of an A horizon on a debris flow (unit 7A) suggest a broad age range for the A horizon (tables 1 and 2); the dated detrital charcoal is probably reworked. The youngest of the ages, the TL age, suggests the flow was deposited prior to 4.8-3.2 ka (table 2; plate 1; figure 4).

(3) A mantle of colluvium consisting of surface-wash sediment and loess (unit 7A) slowly accumulated on unit 8 and was mixed with younger sediment as soil development on the debris-flow deposits proceeded. Prior to the first surface-faulting earthquake (earthquake A), a weak, discontinuous, argillic horizon (unit 8bBt) and a weak transitional eluvial horizon (unit 8aE) developed on the debris-flow deposit. We attribute the apparent cross-cutting relations of the lower contact of unit 7A with underlying units 8aE and 8bBt to the discontinuous character of these soil horizons and to backtilting of units 7 and 8 during earthquake A. The ranges in the ages from unit 7A and the age for the inferred overlying unit 5aA suggest that unit 7A developed over hundreds to as much as 2700 years (plate 1; figure 4) both before and after earthquake A.

(4) A surface-faulting earthquake (earthquake A) on a fault, about in the position of faults F2 and F3, displaced units 7 and 8 vertically about 2.9 m down to the west. Because colluvial wedges become thinner with successive faulting events on large scarps, we infer a similar vertical component of slip during earthquakes A, B, and C (values in bold on table 4) in contrast to slip indicated by colluvial-wedge thicknesses. Coarse, lower debris-facies colluvium (unit 6), derived from units 7, 8, and 9, was eroded from the upper scarp and deposited against a free face following earthquake A. The thickness and rectangular cross section of unit 6 indicate that the lower parts of unit 6 filled a graben that formed at the base of the scarp during earthquake A. Evidence of the antithetic fault that probably bounded the graben on the west following earthquake A was apparently destroyed during later earthquakes. The upper part of unit 6 probably formed a wedge of coarse debris draped over the graben. Because unit 6b is sandier and less bouldery than unit 6a, we infer that unit 6b was derived mostly from sandy unit 9. Stratigraphic displacement on the main fault during earthquake A was greater than 2.9 m by the unknown amount of displacement on the inferred antithetic fault.

(5) Following earthquake A, coarse, sandy colluvium (unit 5) was gradually deposited on the west-facing slope of unit 6. We mapped small, thin (0.1- to 0.15-m-thick) remnants of a sandy A horizon (unit 5aA) developed on unit 5 near m 19. A TL age of 3.8-2.6 ka from sediment immediately overlying unit 7A (m 22) overlaps an AMRT age of 3.9-2.7 ka from the remnants of unit 5aA suggesting that the unit-5 A horizon once extended eastward across the graben and up the slope of a former unit-5 wedge (tables 1 and 2; figure 4).

The unit-5aA A horizon is thin, probably because a small but steep scarp formed quickly, mostly by slumping of units 8 and 9, and (or) because there was insufficient time for a thick soil to form before the next surface-faulting earthquake on faults F2 and F3. Charcoal in the unit-5aA remnant, which is much older than the AMRT age (table 1), may have been reworked from an older A horizon on the debris-flow deposit (unit 8) and deposited in unit 5aA when the soil was exposed in the scarp free face following earthquake A.

(6) A second surface-faulting earthquake (earthquake B) on the same inferred fault (about in the position of faults F3 and F2) displaced units 5 through 13 down-to-the-west about 2.6 m (table 4). Opening of another graben between m 19-21 severely deformed the western part of units 5 and 6. Immediately following earthquake B, bouldery debris derived from the slumping of units 10 and 11 filled the graben and built a wedge of overlying coarse debris (unit 4). Boulders and cobbles that fell from the remaining free face in units 8 and 9 rolled down the wedge. Organic-rich zones of sandy sediment (unit 4bA) in the graben-fill facies (units 4bA and 4c), and within the debris wedge at 19.8 (note n1), show that blocks of A-horizon sediment eroded from a scarp free face also rolled down the colluvial wedge and were deposited in the graben. The diffuse irregular contacts of many of these zones is due

to later decay of organic material and burrowing of the graben deposits by rodents. Erosion and slumping of the free face in units 10 and 11 moved the face eastward and deposited debris-facies colluvium (unit 4a) over undeformed (at that time) units 12 and 13. Most of the eastward backtilting of unit 8 between m 20 and m 23 may have occurred during earthquake B.

(7) As the exposed free face was eroded away, surface-wash sediment from it and above the scarp spread a sandy wedge of wash and debris colluvium (unit 3) over unit 4. The soil on unit 3 developed slowly enough for a thick, organic-rich A horizon to form (unit 3aA), and for silt and clay to be eluviated into unit 3cBw to form a weak B horizon. Rates of soil development in this region (Sullivan and others, 1988) suggest that this process must have taken at least a few hundred years. TL ages of 2.2-1.4 ka and 1.7-1.3 ka from the western distal part of unit 3aA suggest that it began accumulating before 2.0 ka and was still accumulating after 1.7 ka (plate 1, figure 4). Because contacts in the fine-grained wash sediment are so indistinct, we infer the position of the lateral facies change between units 3aA and 1hA from the TL ages. An AMRT age from the most organic-rich sediment in unit 3aA (m 18) suggests burial of unit 3aA about 1.1-0.4 ka (table 1).

(8) The upper contact of unit 3aA is a distinct marker recording deformation during earthquake C. Displacement of this contact on F3 was about 0.35 m and on F2 about 0.15 m during earthquake C. There may also have been less than a fraction of a meter of antithetic faulting on F1, but unit 3aA contacts are too indistinct to identify a displacement of that unit's upper contact. Because F4 is a new fault produced during earthquake C, we measure its displacement from the upper contact of unit 13 (1.2 m). Lower debris-facies colluvium (unit 2b) derived from units 10 and 11 was deposited immediately after earthquake C followed by more gradual accumulation of a long, thin wedge of less coarse, upper debris-facies colluvium (unit 2a). The fine grain-size distribution of the uppermost part of unit 2a suggests deposition by wash processes, and most of the upper half of the unit is intensively burrowed.

(9) With the possible exception of unit 1eA discussed below, unit 1 consists primarily of colluvium deposited by wash processes following deposition of debris facies after earthquake C. Recent burrowing has mixed these units and was particularly intense in unit 1dA. The deeper of two post-modern AMRT ages at m 18 shows the depth to which modern burrowing occurs. The TL age of 1.7-1.3 ka at m 22 suggests that unit 1hA west of m 23 accumulated gradually, both before and after earthquake C.

(10) Analysis of stratigraphic relations in trench 3 (plate 2; discussed below) shows that a small (<0.5 m), most-recent, surface-faulting earthquake (earthquake D) occurred on the 8-m scarp about 75 m northwest of trench 2 (map on plate 1), but trench-2 stratigraphy yields no clear sign of earthquake D. The most likely place in the trench wall for a small, recent faulting event is near m 20: unit 1eA has the characteristic cross section of a small lower debris-facies wedge and the deformed and burrowed contacts of units 3 and 4 between m 20 and m 21 hinder identification of displacement with a vertical component of <0.5 m. The high clast percentages with little matrix sediment and footslope location of unit 1eA show at least its upper half to be a sorted-debris wedge formed by the accumulation of pebbles and cobbles at the foot of the scarp. Perhaps its lower half is a debris wedge deposited against a small unrecognized scarp between m 20 and m 21. Less than 0.5 m of vertical displacement might also be concealed on faults F2, F3, and F4, particularly if each slipped a little during earthquake D. In the latter scenario, rounded clasts exposed in a small, newly formed free face(s) would surely have accumulated near the base of the scarp following earthquake D. And the shallow depth of unit 1eA suggests that it was deposited more recently than earthquake C.

(11) The modern A horizon (units 1aA and 1cA) accumulated over the last few hundreds of years.

Sequence of Faulting and Deposition in Trench 3

Trench 3 was excavated across the 8-m scarp on a late Holocene alluvial surface about 28 m southeast of a scarp-perpendicular profile line (map on plate 1). Measured displacement of the surface near the scarp is 2.3 m; stratigraphic displacement across the fault zone is 2.5±0.2 m, as measured from the upper contact of unit 10 (table 4). Unlike the stratigraphy in trenches 1 and 2, distinct, tapering colluvial wedges deposited in response to surface-faulting earthquakes were more difficult to identify. Reconstruction of the earthquake history was further complicated by deposition of thin fluvial deposits over a preexisting scarp, and by a 2-m-long boulder, which prevented excavation of the lower part of a graben in the fault zone (m 15, plate 2).

Based on the lithologies, stratigraphic relations, and ages from units in trench 3, we infer the following sequence of events:

(1) A series of debris-flow and stream deposits (units 12 through 10bBw) spread over older debris-flow and stream units (some of the same units exposed in trenches 1 and 2) during the middle and late Holocene. Some units fill channels cut during high-flow events on the alluvial fan. An AMRT age from the base of the unit 10 A horizon (unit 10aA) suggests that unit 10 was deposited before 2.9-2.2 ka (table 1). Changed hydraulics near the site of trench 3 following the rise of the scarps during earthquake A may have influenced the deposition of unit 10.

(2) A mantle of colluvium consisting of surface-wash sediment and loess (unit 10aA) gradually accumulated as a soil developed on unit 10. The degree of development of the Bw horizon in the upper part of unit 10 (unit 10bBw) suggests that the soil developed for at least a few hundred years before being buried by unit 9. Extensive burrowing in unit 10aA after it was buried suggests that the ^{14}C–dated sample from unit 10aA may have included some organic material much younger than unit 10aA. If so, the AMRT age of 2.9-2.2 ka could be a few hundred years younger than the time of unit 10 deposition. The age could not, however, be so much younger as to make unit 10 a correlative of the debris-flow units (7 and 8) in trenches 1 and 2; such a correlation would require an unreasonably high percentage (>25%) of modern carbon in the dated sample (Taylor, 1987, his table 5.3). Another reason why unit 10 in trench 3 is probably younger than earthquake A is that its displacement across the 8-m scarp is much smaller (2.5 m) than the displacement of unit 8 in trench 2 (7.8 m), only 75 m to the southeast (table 4; map on plate 1). For these reasons, the ^{14}C age from unit 10aA is probably not significantly affected by younger carbon and the soil developed on unit 10 probably postdates earthquake A.

We are unable to determine if unit 10 in trench 3 predates or postdates earthquake B. The AMRT age from unit 10's A horizon encompasses the younger third of the age range for earthquake B (table 1; figure 4). The difference between the displacements of the upper contacts of units 9 and 10 in trench 3 (0.3 m, table 4) may not be significant because it is of similar size to the errors in displacement measurements. Because the displacement during earthquake B in trench 2 on the same scarp was so much larger (2.6 m), we infer that unit 10 postdates earthquake B (see, however, an alternative presented in discussion of trench 4 below).

(3) Unit 9 was probably deposited by small streams, rill wash, sheetwash, and perhaps the wind—after 2.9-2.2 ka, based on the ^{14}C age from unit 10aA (table 1; m 8, plate 2). The lithologic heterogeneity and variable organic content of unit 9bA shows that it accumulated intermittently as a series of thin alluvial beds with interbedded, thin, lenticular A horizons. Burrowing is extensive in parts of unit 9 near faults F2 and F3. The AMRT age from the top of unit 9bA suggests burial of this unit about 1.4-0.7 ka (table 1; m 8.5, plate 2).

Because unit 9 is about 0.6 m thicker on the hanging wall than on the footwall of the F2-F3 fault zone, we infer that unit 9 was deposited against a scarp at least this high created during earthquake B. Debris facies produced by slumping and erosion of a small scarp soon after the earthquake could have been eroded by small streams flowing along the scarp; even uneroded parts of a debris wedge might be difficult to distinguish from the other facies of unit 9 in the fault zone.

(4) About or before the time that unit 9 was buried by units 5 and 6 (1.4-0.7 ka, table 1, and m 8.5, plate 2), a surface-faulting earthquake (probably earthquake C) on fault F3 displaced unit 9 and older units about 2.2+0.2/-0.1 m (table 4). Small, west-dipping, fault F1 near the west end of the trench also slipped during this earthquake, adding an additional 0.3 m of stratigraphic displacement across the scarp. Although labeled as separate faults on plate 2, faults F2 and F3 probably merge just below the boulder filling the graben at m 15. Cobbly wedges of sandy gravel (units 7 and 8) record earthquake C on faults F1 and F3, but the <0.8 m thickness of these debris-facies wedges suggests that the displacement across each fault was probably <1 m (table 4). The coarse lower debris facies adjacent to fault F3 only fill the small graben at m 13. Unit 7aA is a remnant of a weakly developed, burrowed A horizon (wash facies) on the unit-7c upper debris-facies wedge deposited following earthquake C. Unfortunately, we judged the organic matter content of this horizon to be too low for radiocarbon analysis. We map unit 8, adjacent to fault F1, as a debris-facies wedge, but the low percentage of clasts in its upper half indicate much sediment was deposited by wash processes.

(5) Because we were unable to confidently identify and correlate young units (2 through 5) in trench 3 deposited both before and after the latest surface-faulting earthquake (D), we use different labels for units on the footwall and

hanging wall. For example, we could not identify a contact that could be used to subdivide unit 5. Units 2, 3, and 6 were deposited above and across the scarp, whereas at least the lower part of unit 5 was apparently deposited along the scarp, primarily by small streams and rill wash. These units are sandier and contain more stream-deposited sediment than unit 9, but they also accumulated intermittently and probably contain much sheetwash sediment. The footslope as well as the crest of the scarp was probably eroded during deposition of these units. Based on their stratigraphic position, lithology, and inferred genesis we infer that the lower half of unit 5 is probably the age equivalent of unit 6 and, as explained below, both predate earthquake D. The upper half of unit 5 and all of unit 4 are probably the age equivalents of units 2 and 3 and postdate earthquake D.

Three ^{14}C ages show that units 5 and 6 were deposited recently. A 12-mm-diameter, angular, wood charcoal fragment from the lower part of unit 5b near fault F2 gave an age of 0.67-0.50 ka (table 1; m 16.5, plate 2). Because the fragment was within a bed of parallel-bedded coarse sand undisturbed by burrowing or deformation, the bed could have been deposited after this age but not prior to it. A discontinuous lens of coarse sand 0.08 m above the charcoal fragment yielded an AMRT age of 112% modern. Whether or not this lens is part of unit 5 or the lowest part of unit 4, the modern age indicates that burrowing has mixed substantial amounts of carbon dating from the past few decades into the lens. An AMRT age from the thin A horizon on unit 6 in the footwall (m 8.5, plate 2; table 1) suggests that soil development on this unit continued until at least 0.4 ka.

(6) The latest surface-faulting earthquake (earthquake D) on faults F2 and F3 displaced units 5 through 10. The block of units 7 and 9 between faults F2 and F3 slipped farther westward along F3 during earthquake D, displacing the unit 7c debris wedge and forming two zones of loose gravel with an open-work structure in the small graben at m 13 (note 6, plate 2). Tectonic extension across the F2-F3 fault zone is also reflected in about 0.2 m of backtilting on a small block of units 5 and 9 at m 16. The block is only displaced on its east edge; its west edge is a tight fold with no apparent displacement (note 4, plate 2).

No coarse debris wedge formed in response to earthquake D, suggesting that surface faulting was not expressed by a steep free face. Unit 7b may include debris facies derived from a free face <0.5 m high following earthquake D. More likely, modest slip along fault F3 slid the footwall up to the east at an angle similar to that of the eroded scarp face creating a gently sloping free face that did not produce abundant coarse debris. The thickness of debris facies deposited following faulting (0.8-0.9 m, table 4; unit 4, plate 2; discussed below), and our reconstruction of the scarp's profile before and after earthquake D, suggest about 0.8 m of vertical slip across the fault zone during earthquake D.

Earthquake D clearly postdates deformation of the block of unit 5b containing the charcoal fragment dated at 0.67-0.50 ka (table 1; m 16.5, plate 2). It probably predates unit 3, dated by an AMRT age on the underlying A horizon of 0.4-0 ka (table 1; m 8.5, plate 2).

(7) Following earthquake D, wash and debris facies (unit 4) accumulated against the lower part of the scarp, filling the shallow depression created between m 12 and m 16. Sheetwash, rill wash, and eolian transport of sediment from above the scarp probably all contributed sediment to unit 4. Units 2 and 3 were probably deposited over the scarp about this time. If so, unit 4 includes stream-deposited sediment equivalent with that in these units; erosion of the scarp crest contributed sediment to unit 4 as well. Some high-flow events on the alluvial fan would have also directed streams parallel with the scarp, eroding and redepositing sediment from units 4 and 5 near the scarp footslope (the facies boundary between the upper part of unit 5 and unit 4c is indistinct and arbitrary; note 2, plate 2). Burrowing of unit 4 is extensive; some burrowing was probably concurrent with gradual deposition of the upper part of unit 4.

(8) As footslope deposition slowed over the past few hundred years and the scarp slope gradually stablized, the modern A horizon developed on wash facies colluvium (units 1aA and 1bA). The thin, irregular thickness of the A horizon suggests that during peak flow events on the alluvial fan, thin beds of pebbly coarse sand continue to be deposited across the scarp.

Sequence of Faulting and Deposition in Trench 4

We excavated trench 4 across a small scarp antithetic to the 8-m scarp about 60 m west of trench 2 (map on plate 1). On the middle Holocene fan surface along the scarp-perpendicular profile line that runs near trenches 1 and 2, surface displacement across this scarp is about 1.9 m (plate 1). But at the location of trench 4, on the late Holocene alluvial-fan surface, the scarp's displacement is only 0.7 m. Measured stratigraphic displacement of the unit 5A/6aBw contact across the scarp is 2.2+0.1/-0.3 m (table 4), but because we cannot be certain of the amount of backtilting of the contact in a trench with such limited exposure of the contact the displacement is probably a maximum value. The trench was too short for us to be confident of the slopes of contacts; the displacement of the fan surface over tens of meters perpendicular to the scarp at trench 4 may be significantly less than 2.2 m. Sediments exposed in the trench are similar to those in trench 3.

Based on the lithologies, stratigraphic relations, and ages from units in trench 4, we infer the following sequence of events:

(1) Debris-flow and stream deposits (units 6 and 7) spread over older debris-flow and stream units (exposed in trenches 1, 2, and 3) during the late Holocene. Based on our stratigraphic and lithologic correlation of units 4, 5, and 6 in trench 4 with units 6, 9, and 10 in trench 3, respectively, unit 6 was probably deposited before 2.9-2.2 ka (table 1; figure 4). Changed hydraulics near the site of trench 3 following the rise of the scarps during earthquake A may have influenced the deposition of unit 6 near trench 4.

As with unit 10 in trench 3, it is unclear if unit 6 predates or postdates earthquake B. No ages are available for units 5 and 6 in trench 4. A strong argument for the displacement of unit 6 during earthquake B is the significant difference between the 2.2-m displacement of unit 6 in trench 4 and the following 1.2-m displacement of unit 5 (table 4). But this conclusion conflicts with our inference that the correlative unit in trench 3 (unit 10) was not displaced during earthquake B. Thus, either unit 10 in trench 3 is younger than unit 6 in trench 4, or unit 6 postdates earthquake B and the apparent greater displacement of unit 6 than unit 5 in trench 4 is due to highly localized antithetic faulting that is untypical of displacement elsewhere along the scarp. For either alternative, if we apportion stratigraphic displacements using the total surface displacement across the trench-4 scarp, the resulting displacements are small (0.3-0.4 m, table 4).

(2) A thick mantle of fine-grained colluvium (unit 5A) consisting of surface-wash sediment, loess, and lesser amounts of stream and rill wash sediment slowly accumulated on unit 6 as soil development proceeded. The thick Bw horizon developed in the upper part of unit 6 (unit 6aBw) suggests that soil development continued for at least a few hundred years. Unit 5A thickens by about 0.4 m toward the fault (F1) in trench 4, suggesting the presence of a small scarp about in the position of the fault when most of the unit was deposited. If our correlation of unit 5A with unit 9 in trench 3 is correct, as in trench 3, debris facies produced by slumping and erosion of a small scarp soon after earthquake B could have been eroded by small streams flowing along the scarp. Thus, based on difference in thickness of unit 5A across the fault, at least 0.4 m of vertical slip occurred on fault F1 in trench 4 during earthquake B.

(3) Streams and sheetwash deposited units 3 and 4 on the alluvial-fan surface near trench 4. We mapped unit 3 separately from unit 4 because unit 3 is thinner than unit 4 and lacks a distinct A horizon separate from the modern A horizon. Nevertheless, unit 3 is lithologically identical to unit 4 and is almost certainly the same unit. Deposition over a small preexisting scarp probably accounts for the thickening of unit 4c near the fault.

(4) The largest surface-faulting earthquake in trench 4 (earthquake C) on fault F1 vertically displaced the contacts between units 3, 4, and 5 1.2+0.3/-0.1 m (table 4). A small graben at the base of the scarp was partly filled with lower debris facies consisting of blocks of units 4aA and 4c (unit 4b), loose sediment from unit 4 (unit 2e), and cobbly gravel derived from unit 6 exposed in the scarp free face (unit 2d). A sandy, pebbly wedge of upper debris facies (unit 2c), derived from erosion of sandy unit 3 at the top of the scarp, then covered the lower debris facies. Distinct lenses of fine pebbly gravel (unit 2d) within the wedge record deposition following slumping of blocks in the free face or storms washing sediment from the crest of the scarp. As deposition of the upper debris-facies wedge slowed, gravelly sand (unit 2b) was deposited on the surface of the wedge, mostly by wash processes, and a thin A horizon (unit 2aA) began forming on the wedge.

(5) About 0.6-0.3 ka is a minimum age for earthquake C in trench 4. This is the apparent age of the carbon in an AMRT sample from the A horizon developed on the wedge deposited following the earthquake (table 1; unit 2aA; m 7, plate 2). However, a modern AMRT age from another sample in a lower stratigraphic position (unit 4aA) suggests that incorporation of modern carbon through burrowing has contaminated both AMRT ages. Such contamination might be anticipated from the shallow depth of the samples and the loose structure and irregular shape of the organic-rich zones of sediment near the samples, which suggest

intense burrowing.

(6) Following earthquake C, sheetwash and stream sediment (unit 1b) were deposited along the scarp, but flow velocities and water depths were apparently insufficient to deposit stream or sheetwash sediment on the footwall. The modern A horizon (unit 1aA) developed above and below the scarp. Unit 1aA may be thicker above the scarp than below the scarp because it developed during the entire period of time since earthquake C and was never buried by unit 1b.

Sequence of Faulting and Deposition in Trench 5

We excavated trench 5 across the 5-m scarp on a late Holocene alluvial fan deposited from the drainage to the south of the fan where the other trenches were sited, about 200 m southeast of trench 1 (map on plate 1). Measured displacement of the surface across the scarp is 1.2 m; stratigraphic displacement of the unit 3bBt/4bBt contact across the fault is 1.8+0.2/-0.0 m (table 4).

Based on the lithologies, stratigraphic relations, and ages from units in trench 5, we infer the following sequence of events:

(1) Small braided streams and debris flows successively deposited units 3 through 10 on a late Holocene alluvial fan; there may be unrecognized unconformities between some of the units.

(2) A thin mantle of colluvium consisting of surface-wash sediment and loess (unit 3aA) slowly accumulated on unit 3 as soil development proceeded within units 3 and 4. The argillic Bt horizon developed in units 3bBt and 4bBt (units are numbered differently because unit 4 contains much more gravel than unit 3) suggests at least a thousand and perhaps several thousand years of soil development. The lower Bt horizon of this soil (unit 4bBt) has about 3% more clay and more reddish color (7.5YR 7/4) than the underlying parent material (soil profile 2 in trench 5, plate 2; table 3).

(3) A surface-faulting earthquake (earthquake C) near m 10 displaced the alluvial-fan units down to the west (vertical slip about 1.8 m) along fault F5. During earthquake C, a block consisting of units 6 and 7 was faulted down about 0.5 m along F5. Down-to-the-east antithetic faulting near m 11 (faults F1 and F2), with backtilting of blocks of units 3-5 between F2 and F5, probably occurred simultaneously, forming a small graben parallel with the main scarp. As the edge of the easternmost backtilted block impacted the unit 6-7 block, the upper edge of the easternmost block was forced up and to the west forming reverse faults F3 and F4. The sandy gravel in units 4bBt and 7a in the lower parts of these blocks was severely deformed by the impact of the blocks and shearing in the fault zone. Colluvial debris (unit 2) derived from the free face, including blocks of A-horizon sediment from the crest of the scarp (note n4, trench 5, plate 2), rapidly filled the graben following faulting. The AMRT age from unit 3aA in the center of the graben indicates that faulting occurred after 1.1-0.4 ka (table 1).

(4) As deposition on the debris wedge deposited in response to earthquake C slowed, siltier, less cobbly colluvium accumulated on the wedge, mostly by sheetwash and rill wash (unit 1cA). Organic matter began accumulating within this wash sediment to form a cumulic A horizon, but some of the organic-rich wash sediment was derived from erosion of the surface A horizon above the scarp. More organic matter accumulated in small depressions on the wedge (unit 1bA) than on most of its surface; material from an organic-rich lens in one of the depressions indicates burial 0.5-0 ka (table 1; m 10.5, plate 2). Because the bedding of the matted organic material parallels adjacent unit contacts, probably little of the carbon in this sample was reworked from older soils, and so this age is a minimum age for earthquake C in trench 5.

(5) Erosion of the scarp crest and the surface A horizon above it continued over the past few hundred years. Sediment in the modern A horizon (unit 1aA) is primarily sheetwash sediment and loess. Unit 1aA is more than twice as thick on the hanging wall as on the footwall. An AMRT age of 1.0-0.7 ka from a depth of 5 cm in unit 1aA (table 1) suggests that much of the organic material in the modern A horizon, at least on the hanging wall, is reworked from unit 3aA above the scarp.

Correlation and Relative Size of Surface-Faulting Earthquakes

We correlate surface-faulting earthquakes among the five trenches at the East Ogden site based on the position of trenches on the same or different scarps, the amount of stratigraphic displacement of the same debris-flow and stream-channel deposits in adjacent trenches, the relative amount of slip during surface faulting suggested by colluvial wedge thicknesses, and our interpretation of ^{14}C and TL ages, which place minimum- and maximum-age constraints on the times of earthquakes. Errors on ages are far too great to directly demonstrate correlation of surface-faulting earthquakes among trenches, but in several cases, ages rule out possible correlations of earthquakes among trenches based solely on the position of faulted stratigraphic units within trench sequences.

Earthquake A

Earthquake A was only identified in the two largest trenches (1 and 2), which exposed debris-flow deposits of middle Holocene age. Correlation of earthquake A between the trenches relies on very similar faulted sequences of debris-flow deposits capped by A horizons of similar age in the two trenches, which are only 35 m apart on the same alluvial fan.

TL and ^{14}C ages from A horizons developed on the debris-flow deposits faulted during earthquake A gave ages of about 5-3 ka, with the youngest age 4.8-3.2 ka (table 2; figure 4). No ages are available from the colluvial wedge deposited in response to earthquake A in trench 1, but closely concordant ^{14}C and TL ages from an A horizon on the wedge in trench 2 give minimum ages for earthquake A of 3.8-2.6 ka and 3.9-2.7 ka. Although these ages only limit the time of earthquake A to 4.8-2.6 ka, the ages from the A horizon buried during earthquake A are probably much closer to the time of the earthquake than the ages from the top of the overlying colluvial wedge (e.g., McCalpin and Nishenko, 1996), which probably took at least two centuries to develop. Thus, our best estimate of the time of earthquake A is about 4.0 ka, with a range of 4.8-2.8 ka (figure 4).

By apportioning the stratigraphic displacement of the debris-flow deposits in each trench using the relative proportions of colluvial-wedge thicknesses, we estimate 3.3 m of vertical slip on the 8-m scarp and 2.4 m on the 5-m scarp during earthquake A (table 4). Such estimates do not consider the contributions of folding and antithetic faulting to total displacement across the trenched scarps. Furthermore, the wedge thicknesses are uncertain because the geometry of the colluvial wedges produced during earthquake A in both trenches is difficult to map accurately due to erosion and deformation during later earthquakes. Another factor to consider in using wedge thicknesses is that colluvial wedges produced in response to successive surface-faulting earthquakes of the same size on the same scarp become progressively longer and thinner as the scarp rises (Ostenaa, 1984; Machette and others, 1992; McCalpin, 1998). For this reason, we infer that vertical fault slip during each of the three earthquakes in trench 2 was more similar than suggested by the relative wedge thicknesses (table 4, note 5). Apportioning our vertical-slip estimates within the surface displacements measured across each of the scarps suggests about 2.9 m of displacement on the 8-m scarp and 1.9 m on the 5-m scarp during earthquake A.

Below we reduce the amount of surface displacement on the 8-m scarp during earthquakes B and C by 0.3-0.4 m, as estimated from stratigraphy and surface displacement across the scarp in trench 4, which exposes a fault antithetic to the 8-m scarp. Although trench 4 did not expose deposits as old as earthquake A, we infer that some slip probably occurred on the antithetic, trench-4 fault during earthquake A. If so, the 2.9 m of surface displacement across the 8-m scarp is a maximum for earthquake A; net displacement across the scarp was probably about 2.6 m. Combining values from the 5-m and 8-m scarps yields a total of 4.5 m of vertical displacement across the trenched scarps during earthquake A.

The presence of unstudied scarps southwest of the trenched scarps on the late Holocene fans at the East Ogden site (map on plate 1) raises questions about the total displacement across the entire 450-m-wide fault zone during individual earthquakes, as well as for deposits of different age. Displacement measurements on the most continuous of these scarps, about 25 m southwest of the trench-4 scarp, range from 1.2 to 2.8 m. However, much of the down-to-the-southwest displacement on this scarp is matched by down-to-the-northeast displacement on scarps 80-150 m west of it. Other small, discontinuous scarps with localized displacements of as much as 2.4 m are found on the western part of the fans. Even on predevelopment air photography these scarps are too discontinuous and distant from the higher scarps on the upper parts of the fans for us to determine how their formation may be related to the surface displacements that produced the 5-m and 8-m scarps. Several of the higher northeast-facing scarps may partly reflect landsliding of underlying Lake Bonneville deposits; others at the distal edge of the fans might record surface faulting older than that identified in the trenches.

Even though we do not include any displacement from the untrenched scarp west of the trench 4 scarp, our displacement of 4.5 m across the 5-m, 8-m, and nearby antithetic scarps may be a maximum value for the vertical displacement across the entire fault zone at East Ogden during earthquake A. Net sums of available displacements on both northeast- and southwest-facing scarps along lines running down the axes of the fans suggest that if our displacements for this and other earthquakes on table 4 are maximums, they are only small maxima—by no more than 0.2-0.4 m for each earthquake. To account for this additional uncertainty, we reduce our total displacement for earthquake A at the East Ogden site to 4.2 m (table 5).

Earthquake B

Earthquake B was also only positively identified in trenches 1 and 2. Correlation is based on the similarity of the sequence of debris and wash wedges deposited in response to earthquakes A and B in trenches 1 and 2, and on the concordance of AMRT and TL ages from A-horizon sediment on the earthquake-B wedge in these trenches (figure 4). We suggest that surface faulting during earthquake B is the best explanation for the difference in stratigraphic displacement between units 5 and 6 in trench 4 (table 4). Correlation of this earliest earthquake in trench 4 with earthquake B is based on our inference that unit 6 in trench 4 is probably only a little older than unit 10 in trench 3 (discussed above), and on our interpretation that

Table 5. Displacements and slip rates at exposure sites along the Weber segment[1].

Site	Displacements (m)[2] pP	mH	A	B	C	D	post-Provo[3]	post-middle Holocene[4]	A to B interval[5]	B to C interval[5]	C to D interval[5]
Garner Canyon	—	4.4	1.1	1.0 (2.1)	1.3	—		1.1	0.7 (1.4)	0.8	—
East Ogden	23.7	11.7	4.2 (2.7)	4.2 (2.7)	2.6	0.5	1.5	2.9 (2.1)	2.8 (1.8)	1.6	1.3
Kaysville	10.5	6.1	—	2.9	1.8	—	0.7	1.0	0.9	1.1	—

[1]Rates in mm/yr or m/yr calculated using age of 16 ka for Provo shoreline and best-estimate ages for earthquakes as explained in text (table 6), assuming correlations to Kaysville of figure 8. Age ranges for earthquakes (figure 4 and text) are so large that slip-rate ranges calculated with age ranges are not meaningful.

[2]Best estimate of total displacement at each site for post-Provo (pP) and middle Holocene (mH) to present time intervals, and during each of four earthquakes (A, B, C, and D), as explained in text. In this table we assume four earthquakes are recorded at Garner Canyon; if we use a larger displacement for earthquake B (2.1 m) obtained by assuming a record of only three earthquakes at Garner Canyon, the A-B slip rate increases to 1.4 mm/yr. At East Ogden, if total displacement is 1.5 m less for earthquakes A and B than the listed values (discussed in text), then post-middle Holocene and A to B slip rates would decrease to 2.1 and 1.8 mm/y, respectively. Data for Kaysville from McCalpin and others (1994).

[3]Displacement of Provo shoreline divided by age of 16 ka.

[4]Displacement of middle Holocene alluvial-fan deposits divided by the best estimate of their age (age of 4.0 ka from East Ogden, figure 4, also assumed for Garner Canyon; best estimate of 5.9 ka for Kaysville from McCalpin and others (1994).

[5]Displacement during later earthquake divided by interval of time since previous earthquake.

the second faulting event in trench 4 occurred during earthquake C.

The concordant ^{14}C and TL ages from the A horizon on the earthquake-A colluvial wedge in trench 2 provide a maximum age for earthquake B of 3.9-2.6 ka (figure 4). The oldest of nine ages (six TL, three AMRT) from A-horizon sediment of the wash wedge deposited in response to earthquake B provide minimum estimates of 3.3-2.1 ka and 3.7-2.5 ka (table 2; figure 4). In addition, an AMRT age of 2.9-2.2 ka from the A horizon at the top of unit-10 alluvium in trench 3 may provide an additional minimum age for earthquake B. Stratigraphic displacement of the A horizon on unit 10 in trench 3 is only about 2.5 m (table 4), a displacement too small to account for all post-earthquake-A displacement across the 8-m scarp (4.9 m), as measured in trench 2. By this reasoning, the faulting of the A horizon probably postdates earthquake B. Because the maximum ages on earthquake B in the buried A horizon in trench 2 are probably closer in time to the earthquake than the minimum ages, our best estimate of the time of earthquake B is about 3.0 ka with a range of 3.9-2.4 ka (figure 4).

We estimate vertical slip during earthquake B in trenches 1 and 2 from wedge thicknesses and surface displacements in the same way as for earthquake A. We estimate about 2.6 m on the 8-m scarp and 2.2 m on the 5-m scarp (table 4). As the fault in trench 4 is antithetic to the fault zone exposed in trench 2 on the 8-m scarp, we subtract the probable displacement of 0.3 m during earthquake B in trench 4 from the displacement in trench 2 (2.6 m) to yield a vertical displacement of 2.3 m during earthquake B on the 8-m scarp. Thus, the vertical displacement across the trenched scarps at East Ogden during earthquake B was about 4.5 m (2.2 + 2.3 m). As for earthquake A, we subtract an additional 0.3 m from this value to account for possible additional antithetic slip on faults marked by small, discontinous scarps near the distal edge of the fans at the East Ogden site for a total site displacement of 4.2 m during earthquake B (table 5). As discussed above, the small (0.3 m) apparent difference in stratigraphic displacement in trench 3 between units 9 and 10, which is well within typical uncertainties in measuring displacements, is too small for us to infer that the difference reflects displacement of unit 10 during earthquake B.

Earthquake C

Earthquake C is the only earthquake identified in all five trenches. Correlation is based on the similarity of the sequence of debris and wash wedges deposited in response to earthquakes A and B in trenches 1 and 2 and on the concordance of AMRT and TL ages from A-horizon sediment on the earthquake-B wedge in trenches 1 and 2, which were buried following earthquake C. We correlate faulted units in trenches 3 and 4 with earthquake C based on the AMRT age from the A horizon on faulted unit 9 in trench 3 and our correlation of unit 5 in trench 4 with unit 9 in trench 3. The single AMRT age on the A horizon buried by the most-recent-earthquake debris wedge in trench 5 dates the wedge to the time of earthquake C (figure 4).

The six concordant ^{14}C and TL ages from A horizons buried by the colluvial wedges produced in response to earthquake C in trenches 1, 2, and 5 provide a range of maximum ages for earthquake B of 1.7-0.4 ka (tables 1 and 2; figure 4). The AMRT age from the A horizon on unit 9, which was faulted during earthquake C, falls within this range. Ages from the earthquake-C colluvial wedge and modern soil are mostly modern due to burrowing and incorporation of bomb carbon, but two AMRT ages suggest that the wedge is older than 0.5-0 ka. The age on the piece of charcoal from fluvial sediment younger than earthquake C in trench 3 provides the most reliable minimum age for earthquake C: the earthquake cannot be younger than the 0.67-0.5-ka charcoal age. Because the maximum ages in the buried A horizons are probably closer in time to earthquake C than the minimum ages, our best estimate of the time of earthquake C is about 1.1 ka with a range of 1.7-0.5 ka (figure 4).

We estimated vertical slip during earthquake C in trenches 1 and 2 from wedge thicknesses and surface displacements in the same way as for earthquakes A and B (table 4). The estimated earthquake C displacement in trench 2 on the 8-m scarp by these methods yields the same 2.3-m value as the sum of the vertical components of slip along three strands of the fault measured from the sharp upper contact of unit 3aA in trench 2 (plate 1). As the fault in trench 4 is antithetic to the faults exposed in trench 2 on the 8-m scarp, we subtract the stratigraphic displacement of 0.4 m during earthquake C in trench 4 from the displacement in trench 2 (2.3 m) to yield an displacement of 1.9 m during earthquake C on the 8-m scarp (table 4). This value compares favorably with the 1.5 m of displacement estimated during earthquake C in trench 3, 75 m to the northwest. Similarly, on the 5-m scarp the estimated displacement of 0.9 m in trench 1 during earthquake C is close to the estimate of 1.2 m from trench 5, 200 m to the southeast (map on plate 1). Averaging the values from all trenches gives a vertical displacement across the trenched scarps during earthquake C of about 2.8 m. Subtracting an additional 0.2 m from this value to account for possible antithetic displacement along scarps near the distal edge of the fans yields a total displacement for the East Ogden site during earthquake C of 2.6 m (table 5).

Earthquake D

Earthquake D was only positively identified in trench 3 on the 8-m scarp based on the shearing and backtilting of deposits clearly younger than earthquake C. Based on the thickness of these deposits in trench 3, stratigraphic displacement during earthquake C was about 0.8 m (table 4). Although not identified in trench 2 on the same scarp, a small displacement of about 0.5 m would help explain the presence of unit 1eA in trench 2 (discussed above). We found no evidence of stratigraphic or surface displacement on the 5-m scarp younger than earthquake C. Perhaps the steeper angle of the slope of the 8-m scarp compared with the 5-m scarp reflects surface faulting on only the 8-m scarp during earthquake D (profiles on plate 1). Gilbert (1928, his plate 15A) interpreted the sharper crest of the 8-m scarp as evidence that the 8-m scarp was younger than the 5-m scarp.

Earthquake D postdates deformation of the block of unit 5b in trench 3 containing the piece of charcoal dated at 0.67-0.50 ka (table 1; m 16.5, plate 2). It may also postdate burial of unit 3 in trench 3 dated by an AMRT age on the underlying A horizon of 0.4-0 ka (table 1; m 8.5, plate 2). But a surface-faulting earthquake of the size of earthquake D clearly predates historical settlement of Utah beginning early in the 19th century. From these data we estimate the age of earthquake D at 0.5 ka, with a range of 0.6-0.2 ka (figure 4).

GARNER CANYON FAULT EXPOSURE

Overview

An artificial exposure cut into the 4-m-displacement scarp marking the main trace of the Weber segment 3 km north of the East Ogden site provides additional insight into the late Holocene history of the fault (map on plate 2; Nelson and Personius, 1993; McCalpin, 1998, p. 145). The exposure was cut in 1984 to make room for the cement foundation of an antique car storage garage. The 5-m-high, vertical, north wall of the cut was oriented at an angle of about 65° to the main trace of the fault (plate 2). Four cobbly colluvial wedges, juxtaposed by the fault against stream and debris-flow deposits, probably record four surface-faulting earthquakes on the fault (Machette and others, 1992; Nelson, 1992). Excellent exposures of the fault plane and the three younger wedges were also mapped in the 4-m-high, south wall of the cut.

Two topographic scarp profiles perpendicular to scarps on late Holocene fans, one a few tens of meters north of the Garner Canyon exposure and another on the fan 250 m to the south (methods of Machette, 1989), showed 4.4 m and 2.9 m of surface displacement, respectively (map on plate 2). We measured an additional six surface displacements in Holocene and Provo shoreline deposits along the scarp from profiles constructed using air photographs and a computer-assisted photogrammetric plotter (Nelson and Personius, 1993).

Sequence of Faulting and Deposition

Based on the lithologies, stratigraphic relations, and ages from units in the Garner Canyon exposure, we infer the following sequence of events:

(1) A series of debris-flow and stream deposits (units 13 through 8) were deposited on the alluvial fan during the late and possibly middle Holocene. Here and there, the streams and flows eroded into earlier flow and stream deposits, filling the channel cuts with younger alluvial sediment. The fan deposits at Garner Canyon are undated.

(2) A probable earliest surface-faulting earthquake (first earthquake at Garner Canyon, labeled “U” on plate 2 for “undated”) on the fault (F1, plate 2) displaced alluvial-fan deposits down

to the west below the base of the exposure. An oval-shaped unit (7c) of organic-rich sediment within unit 7b may be a clast of an A-horizon eroded from the scarp, or possibly a burrow filling. Although unit 7aA? has lost much organic material through decay, its light-gray color, silty texture, stratigraphic position, and into-the-fault dip suggest that it is a buried A horizon developed on debris facies of a colluvial wedge (units 7b, 7c, and 7d) deposited in response to surface faulting during the first earthquake. As unit 7aA? is the primary evidence we use to define the colluvial wedge deposited following this earthquake, if this unit is not a buried A horizon, then all of units 6 and 7 must be debris facies from a large debris wedge deposited in response to a younger, but larger surface-faulting earthquake. Because the colluvial-wedge evidence for the first earthquake is less distinct than for later earthquakes, we may have misinterpreted unit 7aA? and the exposure may record only three earthquakes rather than four. Based on the thickness of units 7aA?, 7b, 7c, and 7d, the vertical component of fault slip during the first earthquake was at least 0.8 m (table 4). We were unable to measure stratigraphic displacement in the Garner Canyon exposure because none of the units displaced by faulting are found in both the hanging wall and footwall.

(3) A second surface-faulting earthquake (probably earthquake A at East Ogden site; see discussion in section V) displaced units 7aA? through 7d vertically down-to-the-west. Assuming that unit 7aA? is correctly interpreted as a buried A horizon, unit 7aA? was backtilted during the second earthquake and then rapidly buried by lower debris facies (units 6a and 6b) eroded from the scarp. Based on the thickness of the colluvial wedge (units 6a and 5A), the vertical component of fault slip during the second earthquake was at least 0.9 m (table 4).

(4) During the following few hundreds of years, a long, wash-facies wedge of organic-rich A-horizon sediment (unit 5A) was gradually deposited, mostly through surface wash, over units 6a and 6b. Based on the oldest of four AMRT ages from unit 5A, the debris facies of the colluvial wedge from the second earthquake (and hence the earthquake) are older than 3.0-2.3 ka (table 1). The three other AMRT ages from unit 5A are younger, but a TL age of 4.0-2.8 ka from the upper part of unit 5A is considerably older (table 2; plate 2). Although the TL sample may have been insufficiently exposed to sunlight prior to burial, its age overlaps our best estimate of the time of earthquake A at East Ogden, which we correlate with the second earthquake below. Thus, our age range for the second earthquake at Garner Canyon is 4.0-2.3 ka (figure 8).

(5) A third surface-faulting earthquake (probably earthquake B at East Ogden site; see discussion in section V) displaced units 5A through 7d down to the west, and unit 5A was buried by a new debris wedge (units 4a, 4b, and 4c) that was longer and thinner than the previous wedge. During the third earthquake, a small antithetic fault displaced units 5A and the easternmost parts of units 6 and 7 down to the east by a few tenths of a meter. The sliver of sediment between the antithetic fault and fault F1 that was deformed during the third earthquake is mapped as unit 6b. A TL age from the debris facies (unit 4a) is many thousands of years older than other ages from the exposure, and so analyzed sediment must be reworked from much older sediment formerly exposed in the free face (McCalpin, 1998, p. 146). Based on the thickness of the colluvial wedge deposited in response to the third earthquake (units 3 and 4), vertical slip during the third earthquake was at least 0.8 m (table 4).

(6) During the following few hundreds of years, a long, cobbly, silty wedge of organic-rich A-horizon sediment (units 3aA and 3bA) was gradually deposited, mostly through surface-wash, over unit 4. A TL age from the lower part of unit 3aA is thousands of years older than stratigraphically equivalent AMRT ages of 1.5-0.7 ka, and so the dated sediment must have been insufficiently exposed to sunlight prior to burial. The stratigraphically lowest of four remarkably concordant AMRT ages from the central two-thirds of unit 3aA provides a minimum age for the third earthquake of 1.5-0.7 ka, whereas ages from unit 5A beneath the wedge (2.2-1.4 ka, 2.6-1.9 ka, and 2.8-2.1 ka) are maxima. The highest and youngest age from unit 3aA indicates that the wedge from the third earthquake accumulated until 1.0-0.3 ka, when unit 3aA was buried by deposits from the final, most recent earthquake. A TL age from a similar stratigraphic position in the uppermost part of unit 3aA gave a somewhat older age of 2.0-1.2 ka (table 2), which we infer is closer to the time of earthquake B than the age of 1.5-0.7 ka. Thus, our age range for the third earthquake at Garner Canyon is 2.8-1.2 ka (figure 8).

(7) A final fourth surface-faulting earthquake (probably earthquake C at East Ogden site; see discussion in section V) displaced units 3aA through 7d down to the west. Units 3aA and

3bA were then buried by a fourth debris wedge (unit 2) that was longer and thinner than the previous wedges. During this earthquake a sliver of alluvial-fan deposits was displaced about 0.4 m down to the west, probably further deforming unit 6b, and creating a fissure along the eastern edge of the unit-3/4 debris wedge. Probably before shaking from the earthquake had stopped, a fissure (unit 2f) filled with clasts eroded and slumped from units 9, 10, 3aA, and 4c, and then was buried by cobbly debris facies (unit 2e). Based on the thickness of the complete debris wedge (units 1 and 2), vertical slip during the fourth earthquake was at least 1.0 m (table 4).

(8) During the following few hundreds of years, a long, thin, wash-facies wedge of organic-rich A-horizon sediment (unit 1) gradually accumulated over unit 2. Although thicker where it forms the upper part of the colluvial wedge, unit 1 includes the modern soil developed on the scarp slope through surface wash and mixing of organic material and previously deposited sediment by roots and animals. Based on the youngest AMRT ages from unit 3aA and the oldest age from unit 1aA, the fourth earthquake occurred after 1.0-0.3 ka and before 0.4-0 ka (table 1; plate 2; figure 8). The three TL ages from unit 1bA are all older than stratigraphically equivalent AMRT ages from the same unit, and two are older than several TL ages from underlying units. As with several other TL ages from Garner Canyon, the older ages must be on sediment that was insufficiently exposed to sunlight prior to burial (McCalpin, 1998, p. 146; Stafford and Forman, 1993). The youngest TL age of 1.7-0.5 ka is about the same age as four of the five AMRT ages from underlying unit 3aA, and so it may be only a few hundred years older than the time its dated sediment was deposited. Another factor to consider in comparing the TL and AMRT ages from unit 1 is that the AMRT ages are so shallow that they may contain enough bomb carbon to decrease their apparent ages by several hundred years.

EARTHQUAKE HISTORY OF THE NORTHERN WEBER SEGMENT

Two ways to improve our understanding of the history of large, surface-faulting earthquakes along the northern part of the Weber segment over what we can learn through study of the East Ogden and Garner Canyon exposure sites are to (1) correlate earthquake histories at the three sites along the segment with detailed records, and (2) compare the resulting composite earthquake history with measurements of surface displacement across fault scarps on surfaces of different age along the segment. Comparison of the single-point data from exposures with much less well dated but widely distributed surface-displacement data helps evaluate conclusions about the relative size and rupture extent of earthquakes and improves the precision of the times of earthquakes and resulting recurrence and slip rates. Although surface displacement data are available from the latest Pleistocene (post-Bonneville shoreline, 17-16 ka) to present, we focus our history on the middle-Holocene-to-present interval recorded by stratigraphy at the East Ogden and Garner Canyon sites.

Below we describe the measurement of surface displacements along the Weber segment, initially outlined by Nelson and Personius (1993), and comment on what displacement data suggest about the size and length of surface ruptures along the segment. Next we compare the record of surface-faulting earthquakes at East Ogden with that from Garner Canyon, only 5 km to the north, and follow that with a comparison of the earthquake histories at both sites with McCalpin and others' (1994) revised history at Kaysville, 25 km to the south. After a summary of the post-middle-Holocene recurrence of surface-faulting earthquakes derived from the histories, we offer explanations for the inconsistencies among slip rates calculated from surface displacement data versus those from the three exposure sites. Finally, we estimate the magnitude of the four most recent, surface-faulting earthquakes from displacement data at the three exposure sites.

Measurement of Surface Displacement Along the Segment

Nelson and Personius (1993) measured topographic profiles in the field across scarps at 77 locations along the Weber segment and used air photographs and a computer–assisted photogrammetric plotter (Pillmore, 1989) to construct an additional 298 profiles at these and 223 other locations. Comparisons of surface displacements calculated from paired profiles measured in the field and constructed with the plotter at the same locations show good agreement between displacements calculated using the two methods, especially for displacements <15 m (figure 5). Displacements measure vertical separation of surfaces above and below fault scarps and so are less than cumulative dip-slip separation on normal faults since the surfaces formed. Here we include more detailed diagrams of the scarp displacement data summarized in figure 2 of Nelson and Personius (1993).

Geomorphic characteristics of scarp-profile sites indicate that most profiles provide only minimum or maximum estimates of surface displacement. Principal causes of minimum displacements (about 75% of the profiles) include: 1) burial of the base of scarps by younger colluvial or fluvial sediment, 2) rounding of surfaces above scarps through erosion of lower edges of surfaces and col-

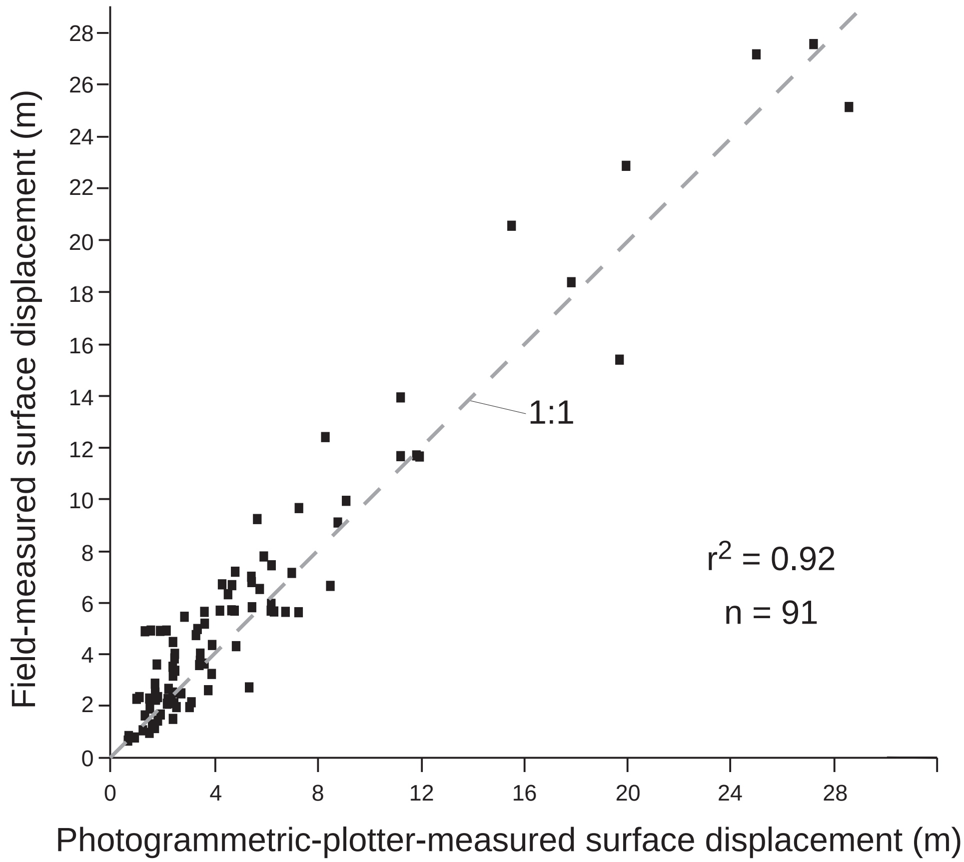

Figure 5. *Comparison of surface displacement at the same locations (75 locations along the Weber segment, 16 along the Brigham City segment of Personius, 1993) calculated from topographic profiles (method of Machette, 1989) measured across scarps in the field (methods of Bucknam and Anderson, 1979, and Pitty, 1968) and with a computer-assisted photogrammetric plotter on 1952-53 1:10,000-scale air photography (method of Pillmore, 1989). Most displacements from paired field and plotter profiles are within 10% of each other and all are within 25%. Thus, the variation between paired displacements has about the same range as the estimated errors in calculating displacements on individual profiles due to uncertainty in projecting surfaces above and below scarps (Nelson and Personius, 1993).*

luvial deposition on upper edges of surfaces, and 3) measurement of displacements across only some of a series of parallel scarps at sites where scarps have been modified or destroyed. About 10% of profiles yield maximum displacements because: 1) deposition of young, alluvial-fan sediment on upper surfaces of preexisting scarps increases the apparent height of scarps, 2) reconstruction of prefaulting topography is difficult because the scarps trend through steep shorelines or other irregular topography, and 3) stream erosion or landsliding (especially lateral spreading) has increased the height of scarps. Estimated errors in displacements—most a result of uncertainty in projecting upper and lower surfaces—for the remaining 25% of profiles ranged from 3 to 30% with a mean of 10±5%. Displacements for about 15% of the profiles are probably within 10% of the vertical displacement across the fault zone since the deposition of mapped deposits at those sites (Nelson and Personius, 1993; solid squares of figures 6 and 7).

Despite limited data in many areas, envelopes of surface displacement for scarps of different ages show rapidly decreasing displacements near segment boundaries, with the greatest displacements in the southern part of the northern half of the segment (Nelson and Personius, 1993; envelopes outlined by dashed lines on figures 6 and 7). Envelopes are interpretations of average ranges in displacements based on 1) displacements with lower-than-average (<10%) errors inferred to measure total displacement across the fault zone, and 2) the distribution of minimum and maximum displacements. Although we considered values of nearby displacements in classifying displacements at sites with inconclusive geomorphology as accurate, minimum, or maximum values, we relied primarily on site geomorphology to independently classify most displacements. For example, we interpreted latest Pleistocene displacements on either side of the Ogden River as probable minimum displacements due to landsliding near the scarps, but the distribution of the greatest displacements on figure 6B suggests that they are accurate measures of displacement for this age. Similarly, we inferred displacements in early and middle Holocene deposits near Jumpoff Canyon (at km 12 on figure 6A) to be maxima because exposures showed some deposits of this age to be draped over bedrock, and nearby displacements in older late Holocene deposits (at km 12 on figure 7B) to be minima due to lateral spreading (Nelson and Personius, 1993). In fact, the distribution of these maximum and minimum displacements suggests that they may be accurate meas-

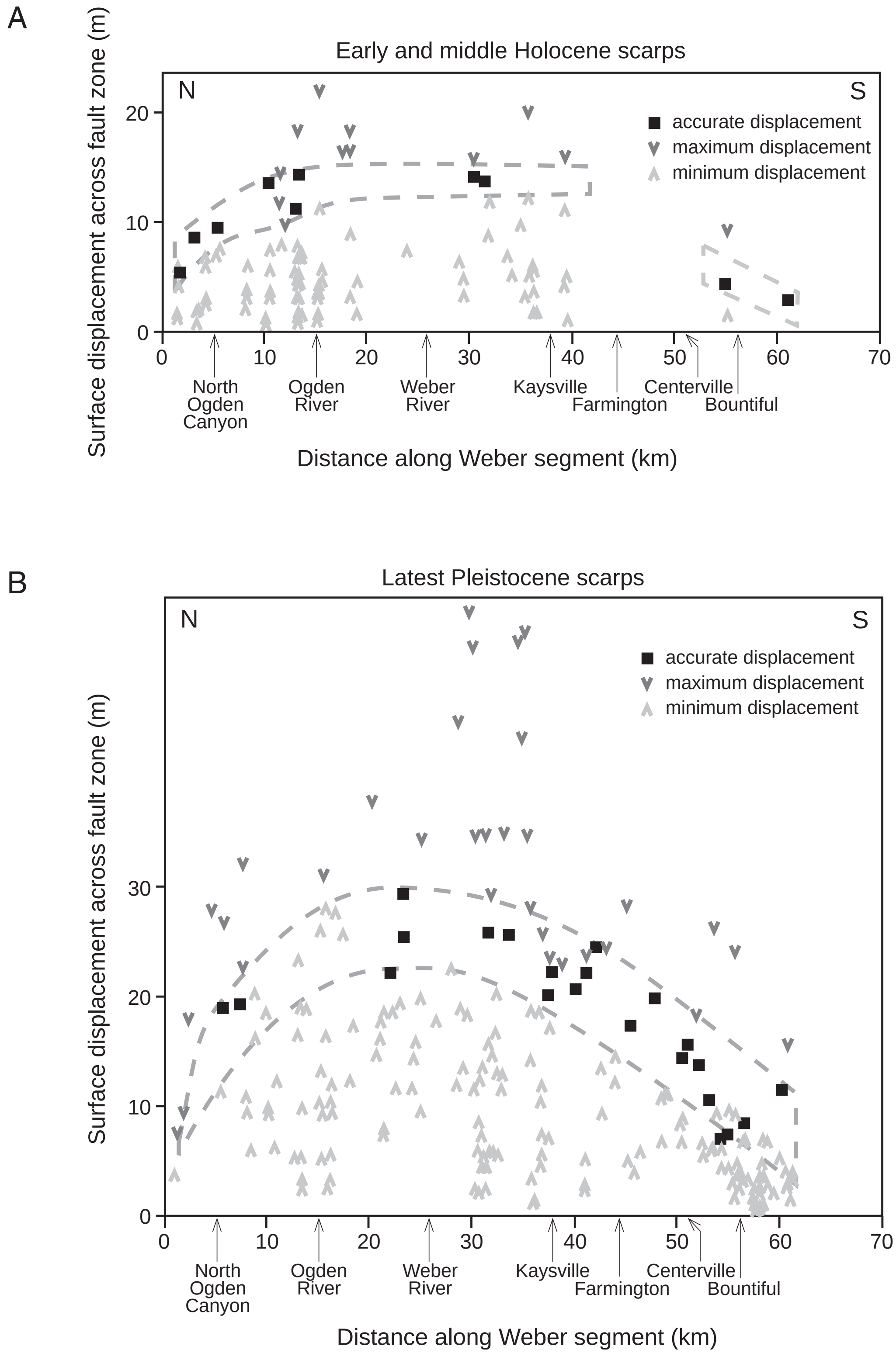

Figure 6. *Surface displacements calculated from topographic profiles across scarps on A) early and middle Holocene deposits, thought to date from about 7-4 ka, and B) latest Pleistocene deposits of the Bonneville lake cycle (17-16 ka, Oviatt and others, 1992; Lund, 2005, p. 16) along the Weber segment (modified from Nelson and Personius, 1993, figure 2). Solid squares show most accurate displacements, which probably measure total vertical displacement of early and middle Holocene or latest Pleistocene deposits at each location to within 10% (height of each symbol does not reflect estimated error). Arrowed symbols are maximum or minimum displacements as explained in text. Dashed lines outline envelopes inferred to show average range in surface displacement along the segment based on the distribution of the three types of symbols. No scarps of early and middle Holocene age were measured from north of Farmington to south of Centerville. Distance along the Weber segment is measured along 3- to 8-km-long straight-line segments parallel to the fault zone, beginning at the head of Barrett Canyon at the north end of the segment and continuing to the south end of the segment on the north flank of the Salt Lake salient (figure 1).*

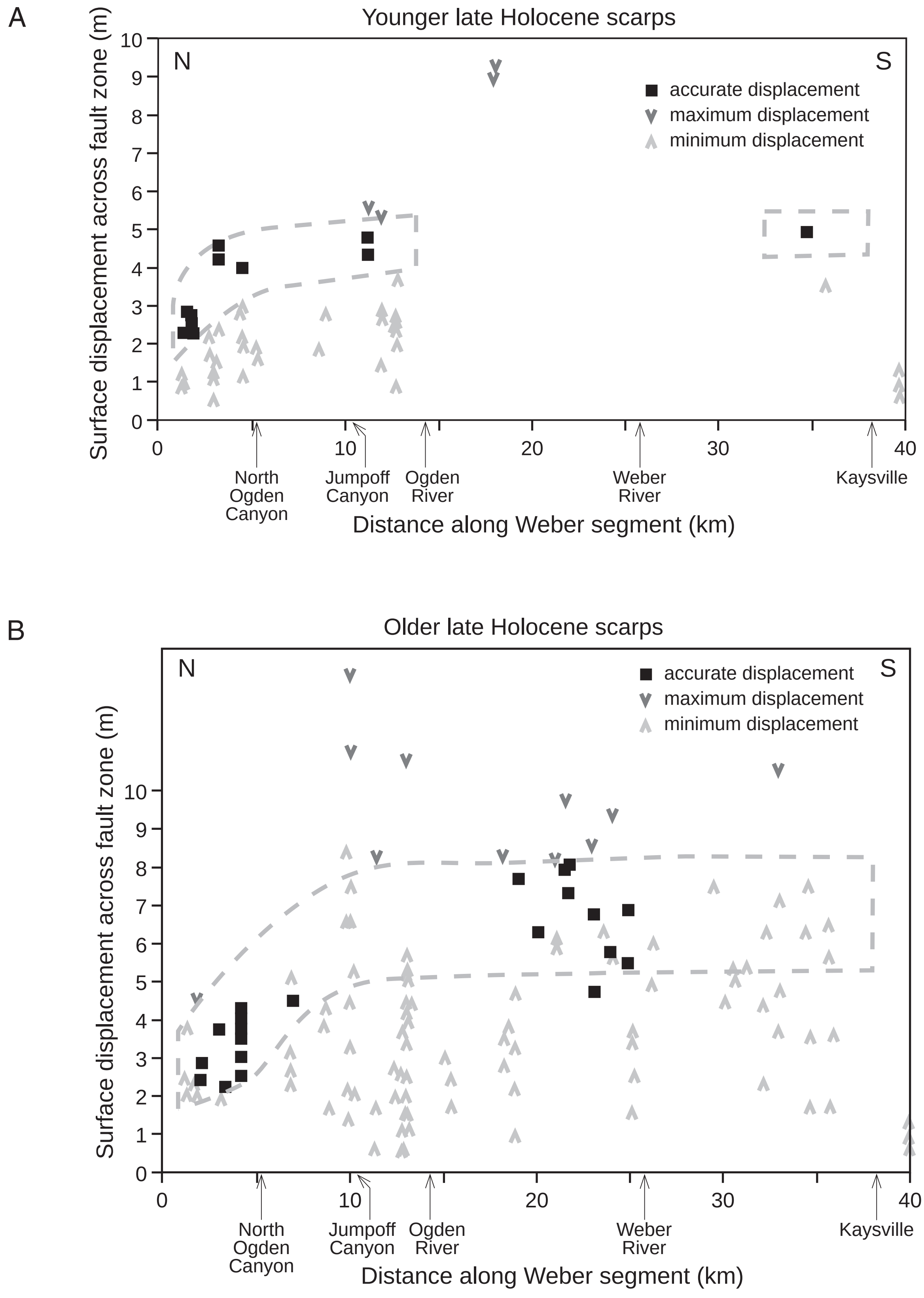

Figure 7. Surface displacements calculated from topographic profiles across scarps on younger late Holocene deposits, thought to date from <2 ka, and older late Holocene deposits, thought to date from about 4-2 ka (from data summarized by Nelson and Personius, 1993, figure 2). Solid squares show most accurate displacements, which probably measure total vertical displacement of deposits at each location to within 10% (height of each symbol does not reflect estimated error). Arrowed symbols are maximum or minimum displacements as explained in text. Dashed lines outline envelopes inferred to show average range in displacement along the segment based on the distribution of the three types of symbols. No scarps of late Holocene age were measured south of Kaysville. Distances measured as explained in figure 6.

ures of vertical fault displacement for deposits of these ages. Another reason why some of our inferred maximum and minimum displacements may be accurate (vary <10% from the true displacement across the fault zone) is that displacements recorded following historical surface faulting on normal faults commonly show greater variation than suggested by the displacement-range envelopes of figures 6 and 7 (e.g., Hemphill-Haley and Weldon, 1998, their figure 1).

Nelson and Personius (1993) draw two conclusions from the distribution of surface displacements along the Weber segment. The amount of displacement decreases dramatically within 10 km of segment boundaries—for scarps on deposits of all ages at the northern end, and for latest Pleistocene through middle Holocene deposits at the southern end (figures 6 and 7). The decrease is consistent with surface ruptures terminating near either end of the segment, and/or with a lower frequency of surface faulting near the ends of the segment. Secondly, displacements in latest Pleistocene through middle Holocene deposits are significantly smaller south of Farmington, suggesting that surface ruptures have either been smaller or less frequent along the southern third of the segment. The largest displacements in deposits of all ages are between Jumpoff Canyon and Kaysville, although the scarcity of middle and late Holocene deposits south of Farmington precludes measuring the amount of late Holocene slip along the southern part of the segment.

Correlation of Surface-Faulting Earthquakes at Garner Canyon and East Ogden

We correlate the three youngest surface-faulting earthquakes identified at Garner Canyon with the three largest of the four earthquakes at East Ogden (figure 8). In doing so, the many ages from Garner Canyon prompt us to reevaluate our estimates for the times of the East Ogden earthquakes. Because no stratigraphic contacts whose displacement could be measured across the fault zone were exposed at Garner Canyon, we estimate vertical slip during each earthquake by apportioning the surface displacement across the scarp (4.4 m) based on the relative thicknesses of colluvial wedges deposited in response to each earthquake (table 4).

We interpret four of the seven TL ages from the colluvial wedges at Garner Canyon as being much older than the time that the sampled sediment was deposited (table 2; plate 2; McCalpin, 1998, p. 146). Perhaps the present scrub oak forest vegetation at Garner Canyon is representative of vegetation over the past few thousands of years at that site, and the present grassland/sage brush vegetation at East Ogden is similarly representative of past vegetation there. If so, the difference in vegetation at the two sites may have increased the chance of the fine-grained, A-horizon sediment used for TL analyses to be exposed to sunlight at the East Odgen site relative to sediment at the Garner Canyon site. Without adequate sunlight exposure the TL signal will not be reset and sediment will yield ages older than the time of deposition (Forman and others, 1991). At Garner Canyon, the importance of root mixing, throughflow, and hillslope creep processes in the downslope transport of surface sediment would reduce the amount of time that fine-grained sediment moving downslope was exposed to sunlight. In contrast, at grassland/sagebrush settings like East Ogden, a greater proportion of near-surface, A-horizon sediment is exposed to sunlight when it is washed downslope by storms or snowmelt. The loose, gravelly sediment at Garner Canyon may have also favored the reworking of A-horizon sediment in fault free faces into new A horizons developing on colluvial wedges beneath the free face.

The most recent surface-faulting earthquake at Garner Canyon is almost certainly earthquake C at East Ogden. The size, shape, and lithology of units in the most recent colluvial wedge at Garner Canyon is similar to those of the wedges produced in response to earthquake C in trenches 2 and 3 on the 8-m scarp, and trench 5 on the 5-m scarp at East Ogden. Estimated displacement (1.3 m) during this most recent earthquake at Garner Canyon is roughly half the total displacement on both scarps during earthquake C at East Ogden.

The range of four of the five AMRT ages spanning the range of 1.5-0.6 ka from the A horizon (unit 3aA) buried by the debris wedge from the most recent earthquake fall within the range for ages on similar A horizons buried by debris wedges from earthquake C at East Ogden (table 1; plate 2; figure 4). The stratigraphically highest AMRT age from unit 3aA at Garner Canyon is somewhat younger (1.0-0.3 ka) suggesting that either the earthquake occurred a century or two after our best estimate from East Ogden, or that the youngest age from unit 3aA is contaminated with a small amount of bomb carbon. Based partly on ages from the Kaysville site (discussed below), we infer that contamination is unlikely and, therefore, that earthquake C dates from about 0.9 ka (figure 8).

The third surface-faulting earthquake at Garner Canyon probably correlates with earthquake B at East Ogden. The colluvial wedge from the third earthquake (youngest buried wedge) at Garner Canyon is similar to but smaller than the wedges deposited in response to earthquake B in trenches 1 and 2 at East Ogden. The difference in scale is reflected in the displacement estimated for earthquake B at Garner Canyon (1.0 m), which is only a quarter of the estimated site displacement at East Ogden (4.2 m, table 5).

Our age range for earthquake B at East Ogden is 3.9-2.4 ka, with a best estimate of about 3.0 ka for the time of the earthquake (figure 4). But the range at East Ogden is only directly constrained on its younger end by an age of 2.2-1.4 ka in trench 2, and, through correlation, by ages of 2.9-2.2 ka in trench 3 and by a TL age in trench 1 of 3.2-2.1 ka. At Garner Canyon, three of the four AMRT ages from the A horizon buried by the debris from the third earthquake suggest a much younger range for earthquake

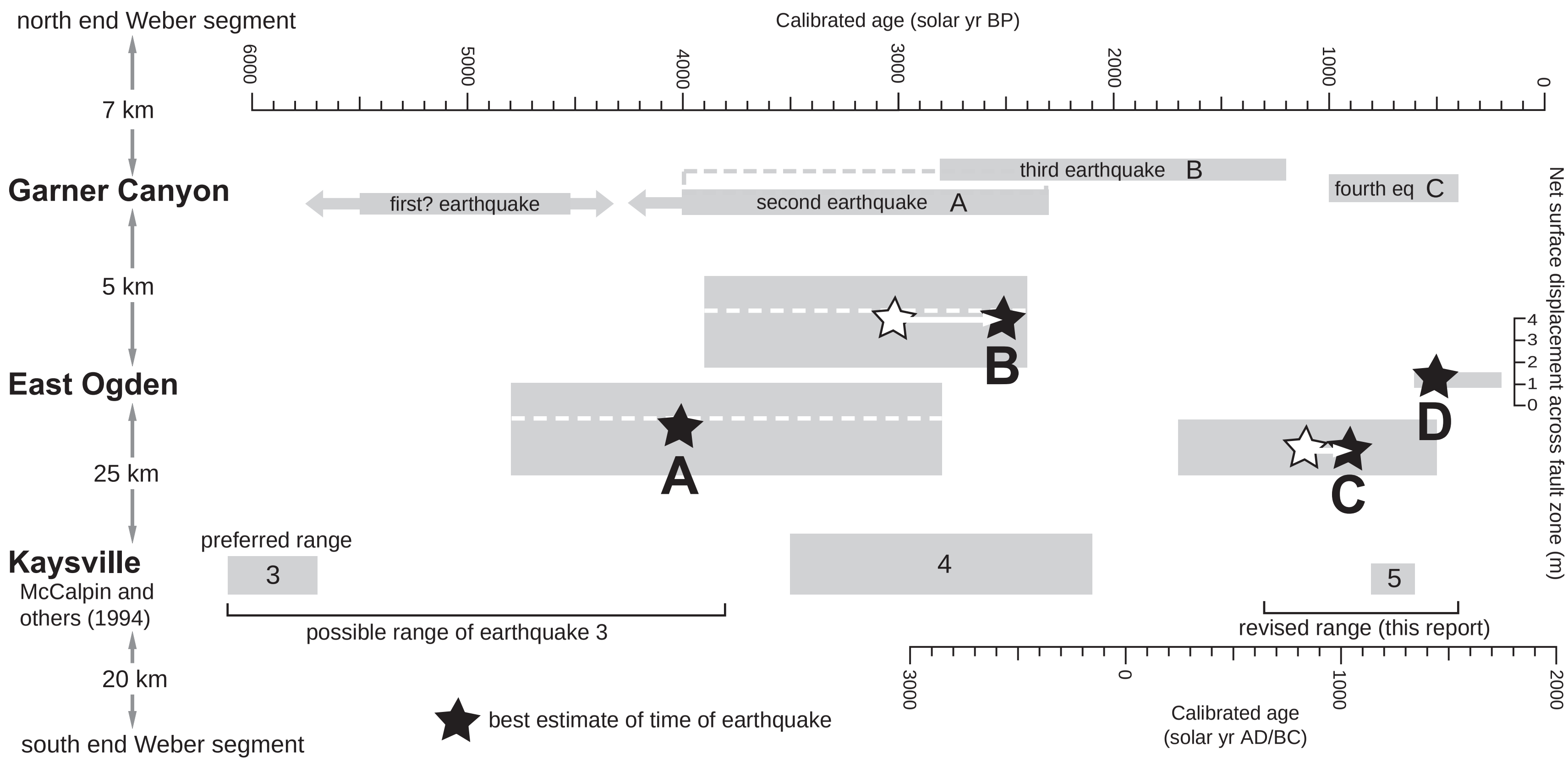

Figure 8. *Correlation of post-6-ka earthquakes at the Garner Canyon, East Ogden, and Kaysville sites along the Weber segment. Width of rectangles shows inferred age ranges for the times of earthquakes (labeled with text, letters, and numbers) based on ages discussed in text. Arrows on rectangles indicate open-ended ranges dated with only minimum or maximum ages. Rectangles for Kaysville site are preferred ranges of McCalpin and others (1994). Brackets below Kaysville rectangles show McCalpin and others' (1994) possible range for earthquake 3, and our recalculation of the range for earthquake 5 using the ages of McCalpin and others (1994). Height of rectangles shows the total displacement across the fault zone during each earthquake at each site. Dashed gray line for second earthquake at Garner Canyon shows displacement for that earthquake, if its lower debris wedge has been misinterpreted as a deposit from an earlier (first) earthquake. Dashed white lines for earthquakes A and B at East Ogden show reduced displacements, if 1.5 m of unrecognized antithetic faulting is included. Solid stars are the best estimates of the times of earthquakes A, B, C, and D along the northern Weber segment; white arrows to right of stars show how we revise two estimates from East Ogden based on ages for correlative deposits at Garner Canyon and Kaysville. Uncertainties in the best estimates for the times of earthquakes along the northern Weber segment are difficult to determine. One measure of uncertainty is the range of overlap in the age ranges for each earthquake at the Garner Canyon and East Ogden sites. Distances between sites along the Weber segment are listed in the left hand column.*

B of 2.8-1.4 ka (table 1). The TL age of 4.0-2.8 ka from a more distal, upper part of the buried debris wedge is considerably older and may include insufficiently reset sediment (McCalpin, 1998, p. 146). Assuming our correlation of earthquake B is correct, a best estimate of about 2.5 ka for earthquake B falls near the upper end of our original age range at East Ogden (figure 4) and is consistent with the ages from Garner Canyon (figure 8). Although possible, we discount an alternative interpretation—that the third earthquake at Garner Canyon is several hundred years younger than earthquake B and so is not recorded at East Ogden—as unlikely (e.g., Machette and others, 1992, their figure 1).

No maximum ages are available to help in correlating the colluvial wedges from the first (probable) and second earthquakes at Garner Canyon. On the basis of position in the stratigraphic sequence and thickness of colluvial wedges, the second earthquake correlates with earthquake A at East Ogden and the first earthquake at Garner Canyon predates earthquake A. In this case, the estimated displacement during earthquake A at Garner Canyon (1.1 m) would only be a quarter of the site displacement at East Ogden (4.2 m). Alternatively, if the deposits attributed to the first earthquake at Garner Canyon are part of a thick colluvial wedge from the second earthquake, then estimated displacement during this earthquake would be 2.1 m, or half the site displacement at East Ogden during earthquake A.

The lack of evidence for probable earthquake D at Garner Canyon is not a strong argument that this earthquake did not occur and, therefore, has been misinterpreted at East Ogden. Surface displacement data show that earthquake ruptures tend to die out near the northern boundary of the Weber segment (figures 6 and 7), and so the amount of surface rupture during earthquake D would be expected to be smaller at Garner Canyon, which is 5 km closer to the northern boundary of the Weber segment, than at East Ogden. Estimated displacements for earthquakes A, B, and C at Garner Canyon are at best half the site displacements for the same earthquakes at East Ogden. Surface faulting of less than half the inferred 0.5-0.8 m vertical displacement during earthquake D at East Ogden might be very difficult to identify in a loose, gravelly fault zone like that exposed at Garner Canyon. Alternatively, an earthquake rupture of only the central part of the Weber segment could extend to East Ogden but not as far north as Garner Canyon (table 6).

Correlation of Surface-Faulting Earthquakes Among Three Exposure Sites

Our correlation of surface-faulting earthquakes among the three sites on the Weber segment where fault-scarp stratigraphy has been studied in detail—Garner Canyon, East Ogden, and Kaysville (figure 1)—largely follows the correlations of McCalpin and others (1994) and McCalpin and Nishenko (1996). Correlations and estimates of the times of Weber segment earthquakes (figure 8) are improved over those of Nelson (1988), Forman and others (1991), and Machette and others (1992) due to many more recent ages from the Garner Canyon (McCalpin and Forman, 1989; Stafford and Forman, 1993; McCalpin, 1998, p. 145) and Kaysville (McCalpin and others, 1994) sites. The original, pioneering study of the Kaysville site by Swan and others (1980) was limited to a single ^{14}C age.

On the basis of concordant AMRT (one) and TL (three) ages from a debris-buried A horizon in the Kaysville trench, McCalpin and others (1994) concluded that the third-most recent earthquake at Kaysville (earthquake 3 on figure 8) was at least a millenium older than earthquake A at East Ogden. Using a select set of ages from Weber segment exposures, McCalpin and Nishenko (1996, their table 3) calculated an age difference between earthquakes A and 3 of 1.5-2.0 kyr. Although we concur with McCalpin and others (1994) that his preferred age for earthquake 3 at Kaysville (6.1-5.7 ka) certainly excludes a correlation with earthquake A, his *possible* range for earthquake 3 overlaps our ranges for earthquake A at East Ogden and Garner Canyon (figure 8; McCalpin and others, 1994, their figure 7). Like McCalpin and others (1994), we are confused as to why an earthquake with a site displacement across the fault zone as large as earthquake A's at East Ogden would leave no record at Kaysville, only 25 km to the south (discussed below). If McCalpin and others' (1994) preferred age for earthquake 3 at Kaysville is accurate, the undated, earliest (probable) earthquake at Garner Canyon might correlate with it (figure 8).

Correlations of earthquake B at East Ogden and Garner Canyon with earthquake 4 at Kaysville, and earthquake C at East Ogden and Garner Canyon with earthquake 5 at Kaysville, are supported by the overlapping age ranges for the earthquakes developed at each site (figure 8; McCalpin and others, 1994). Our revision of the best estimate of the age of earthquake B from 3.0 ka to 2.5 ka, based on ages at Garner Canyon, agrees well with McCalpin and others' (1994) range for earthquake 4, but is half a millennium younger than the mean age calculated from the select ages of McCalpin and Nishenko (1996, their table 3). In our correlation of earthquake C, we revised the range for McCalpin and others' (1994, their table 5) ages for earthquake 5 at Kaysville to make them comparable to the way we calculated the age ranges at East Ogden and Garner Canyon (based on the age intervals in table 1). With our less precise methods the range for earthquake 5 increases from 0.8-0.6 ka to 1.3-0.4 ka. In considering the range and quality of the ages for earthquake C from both the Garner Canyon and Kaysville sites, we revise our best estimate for the time of earthquake C at East Ogden from 1.1 ka to 0.9 ka, a value about a century younger than the mean age calculated by McCalpin and Nishenko (1996, their table 3), but well within the broad age range recommended by Lund (2005; figure 8).

Table 6. *Prehistoric earthquake magnitude from mean vertical displacement for the Weber segment.*

Earthquake[1]	Displacement (m)[2]	Rupture 15 km[3] ***M 6.4-6.6***	Rupture 30 km[4] ***M 6.7-6.9***	Rupture 45 km[5] ***M 6.9-7.1***	Rupture 61 km[6] ***M 7.0-7.2***
A (~4.0 ka)	2.7 (1.9)	—	7.0-7.5 (6.9-7.4)	—	—
			7.1-7.5 (7.0-7.3)	—	—
B (~2.5 ka)	2.7 (2.2)	—	7.0-7.5 (7.0-7.4)	7.0-7.5 (7.0-7.4)	7.1-7.7 (7.0-7.6)
		—	*7.1-7.5 (7.0-7.4)*	*7.1-7.5 (7.0-7.4)*	*7.1-7.5 (7.0-7.4)*
C (~0.9 ka)	1.9	—	6.9-7.4	6.9-7.4	7.0-7.6
		—	*7.0-7.3*	*7.0-7.3*	*7.0-7.3*
D (~0.5 ka)	0.5	—	—	—	—
		6.5-6.7	—	—	—

[1]Prehistoric earthquakes as labeled at the East Ogden site. Best age estimate for earthquake in parentheses as explained in text.

[2]Mean displacement for earthquake as averaged from one, two, or three sites along segment (calculated from site displacements for each site as explained in text). Here we assume four earthquakes are recorded at Garner Canyon; if we use a larger displacement obtained by assuming a record of only three earthquakes at Garner Canyon, calculated magnitudes increase by less than 0.1M. Values in parentheses assume 1.5 m of unrecognized antithetic faulting during earthquakes A and B at East Ogden site.

[3]Range in earthquake magnitude estimated from the inferred surface displacement for earthquake D at the East Ogden site (hypothetical surface rupture of 15 km) using methods of Wells and Coppersmith (1994, their figure 9, second line in italics). For comparison, the one-standard-error range in magnitude for a surface-rupture length of 15 km (Wells and Coppersmith, 1994) is shown in italics in the column heading. Because displacement is available from only one site, the method of Hemphill-Haley and Weldon (1998) cannot be used to estimate the magnitude of earthquake D.

[4]Range in earthquake magnitude estimated from mean surface displacement at two sites for a hypothetical surface rupture of 30 km (earthquakes B and C at East Ogden and Garner Canyon sites) using methods of Hemphill-Haley and Weldon (1998, first line) and Wells and Coppersmith (1994, their figure 9, second line in italics). For comparison, the one-standard-error range in magnitude for a surface-rupture length of 30 km (Wells and Coppersmith, 1994) is shown in italics in the column heading. Values in parentheses assume 1.5 m of unrecognized antithetic faulting during earthquakes A and B at East Ogden site.

[5]Range in earthquake magnitude estimated from mean surface displacement at three sites for a hypothetical surface rupture of 45 km (earthquakes B and C at East Ogden, Garner Canyon, and Kaysville sites) using methods of Hemphill-Haley and Weldon (1998, first line) and Wells and Coppersmith (1994, their figure 9, second line in italics). For comparison, the one-standard-error range in magnitude for a surface-rupture length of 45 km (Wells and Coppersmith, 1994) is shown in italics in the column heading. Earthquakes A and D were not identified at the Kaysville site (McCalpin and others, 1994). Values in parentheses assume 1.5 m of unrecognized antithetic faulting during earthquakes A and B at East Ogden site.

[6]Range in earthquake magnitude estimated from the surface displacement at three sites for a hypothetical surface rupture of 61 km along entire Weber segment (earthquakes A, B and C at East Ogden, Garner Canyon, and Kaysville sites) using methods of Hemphill-Haley and Weldon (1998, first line) and Wells and Coppersmith (1994, their figure 9, second line in italics). For comparison, the one-standard-error range in magnitude for a surface-rupture length of 61 km (Wells and Coppersmith, 1994) is shown in italics in the column heading. Values in parentheses assume 1.5 m of unrecognized antithetic faulting during earthquakes A and B at East Ogden site.

As correctly outlined by McCalpin and others (1994), their revision of the earthquake history at the Kaysville site casts doubt on the validity of probable earthquake D at East Ogden because the revised Kaysville history includes no evidence of surface rupture about the time of earthquake D. However, our confidence in the stratigraphic evidence for earthquake D in trench 3 at East Ogden leads us to suggest two equally plausible alternatives to a misinterpretation of the evidence for earthquake D. (1) If the total displacement across the fault zone during earthquake D at East Ogden was larger than at Garner Canyon and Kaysville—a pattern displayed by earthquakes A and B (figure 8)—then the displacement at the latter two sites would have been so small (0.2-0.4 m, or perhaps less) that it would be difficult to identify in most fault exposures. (2) Earthquake D's displacement is so small that its surface rupture probably only extended along part of the Weber segment (similar to hypothetical rupture of 15 km on table 6), and so may not have reached the Kaysville site. Both alternatives are consistent with the history of surface rupture suggested by the distribution of surface displacements along the segment (figures 6 and 7).

Recurrence of Surface-Faulting Earthquakes

Considering only the two intervals between the three large, most recent earthquakes, the recurrence of major surface-faulting earthquakes on the Weber segment is roughly 1.5-1.6 kyr (using best estimates on figure 8). The possible range for recurrence based on our full age ranges for the times of earthquakes at each site is much greater: from zero to more than 3.0 kyr. The average for the same two intervals, calculated by us from the values of Lund (2005) who used the data of McCalpin and Nishenko (1996, their table 3), is about 1.8±0.9 kyr.

In our view, including older and younger less well documented earthquakes of the Weber segment in recurrence calculations obscures the complexity of the segment's earthquake history. By including the longer interval between earthquakes 3 and 4 at Kaysville, McCalpin and Nishenko (1996, their table 3) calculated a mean interval of about 1.8 kyr, whereas Lund's (2005) average for the same three intervals was 1.6±0.6 kyr. But the two-interval averages might only apply to the northern part of the Weber segment, particularly if earthquake A's rupture never reached Kaysville, as suggested by McCalpin and others (1994). Other uncertainties are raised by the apparent interval between the youngest earthquake (D) at East Ogden and earthquake C, which is much shorter than earlier intervals—probably a few hundred years or less (figure 8). Because surface displacement during earthquake D was significantly smaller than displacements during earlier dated earthquakes, earthquake D's rupture was probably significantly shorter than the ruptures of the earlier earthquakes. For this reason, the shorter average recurrence interval (e.g., Lund, 2005's average was 1.0±1.4 kyr) obtained by averaging the earthquake C/D interval with earlier intervals gives an interval that probably does not accurately reflect the history of the entire segment. If earthquake D was so difficult to identify that evidence of it was found in only one of six exposures, might not similar small ruptures that occurred between the largest surface-faulting earthquakes along the segment have gone unidentified? Surface faulting during earthquakes of large displacement, like those at East Ogden, tends to destroy subtle evidence of earlier earthquakes of small displacement. By this reasoning, earthquakes of sufficient magnitude to rupture to the surface along the northern Weber segment might be more frequent than indicated by Lund's (2005) average of 1.0±1.4 kyr. Conversely, the average recurrence of the largest surface-faulting earthquakes, which ruptured more than half of the Weber segment, may be similar to the two-interval recurrence values of Lund (2005) and this report (1.5-1.6 kyr).

Inconsistent Fault Slip Rates

With the exception of latest Pleistocene rates derived from displacements of the well-dated Lake Bonneville shorelines, fault slip rates derived from surface displacements along the Weber segment are inconsistent with the much lower rates calculated from displacement data at exposure sites (figure 9; table 5). Slip-rate envelopes derived from surface-displacement envelopes and estimated age ranges (figures 6 and 7; Nelson and Personius, 1993) for Holocene deposits have unreasonably high upper bounds (figure 9) compared with rates in earlier publications (e.g., Machette and others, 1992; Nelson and Personius, 1993; McCalpin and others, 1994; McCalpin and Nishenko, 1996). In the same way, rates for all three exposure sites fall below the corresponding slip-rate envelope for younger late Holocene scarps, and rates derived from older late Holocene and middle Holocene deposits at Garner Canyon and Kaysville fall below those corresponding envelopes as well (figure 9).

Are Holocene slip rates derived from surface displacements along the Weber segment systematically in error? The high rates might be due to 1) shorter recurrence of large surface-faulting earthquakes in the late Holocene than in the early Holocene and latest Pleistocene, 2) earthquakes of greater magnitude with greater surface displacement in the late Holocene, 3) ages of most Holocene deposits being as old as or older than the older end of the estimated age ranges of Nelson and Personius (1993), and 4) systematic interpretation of maximum displacements in Holocene deposits (but not latest Pleistocene deposits) along the segment as accurate displacements (<10% difference from true displacement across the fault zone). Although the earthquake histories from the three exposure sites are not long enough and detailed enough to completely rule out reasons 1 and 2 as contributing factors, the lower slip rates from exposures sites, particularly from Garner Canyon and Kaysville, suggest that the high rates are primarily the result of reason 3—displacement deposits are older than inferred by Nelson and Personius (1993). Note, however, that East Ogden slip rates for older late Holocene and middle Holocene deposits are much higher than rates for the other two sites and fall within the corresponding slip-rate envelopes (figure 9).

Does this mean that the large displacements and inconsistent slip rates from East Ogden (figures 8 and 9, table 5) are based on displacement and/or age data that have been misinterpreted or incorrectly measured? The distribution of latest Pleistocene surface displacements along the segment suggest that post-Provo shoreline displacement at the East Ogden site could be as much as 20% greater than at Kaysville, but not much greater at Garner Canyon, only 5 km to the north. Apparent surface displacements in Holocene deposits do not suggest any significant difference in slip rates between the East Ogden area and other parts of the segment (figures 6 and 7). Highly variable surface displacements are typical of historical ruptures (e.g., Hemphill-Haley and Weldon, 1998, their figure 1), but if anomalously large displacements had repeatedly occurred on the fault in the Ogden area we would expect to see them reflected in the surface-displacement data. Nor are hypothetical, frequent ruptures that were short enough to break the surface at East Ogden, but not at Garner Canyon or Kaysville (<30 km), likely to have added enough displacement at the East Ogden site to account for the much greater slip rates. For these reasons, we suspect that insufficient antithetic fault displacement has been subtracted from the total displacements for earthquakes A and B on the middle Holocene fans at East Ogden and that total site displacement across the entire fault zone may be 1-1.5 m less than we estimate for the site. If an additional 1.5 m of antithetic faulting is subtracted from the site displacements for earthquakes A and B, the A-to-B-interval slip rates becomes 1.8 mm/yr, which is only a little higher than the post-Provo-shoreline rate (table 5). Perhaps northeast-facing scarps recording the additional antithetic displacement were buried or eroded during the deposition of late Holocene fan deposits.

To reconcile the high Holocene slip rate encompassed by the envelopes with the much lower Holocene displacement rates from exposure sites we make two suggestions: (1) many displaced Holocene surfaces along the Weber segment are 20-100% older than inferred by Nelson and Personius (1993), and (2) site displacements during earthquakes A and B at East Ogden were about 1.5 m less than

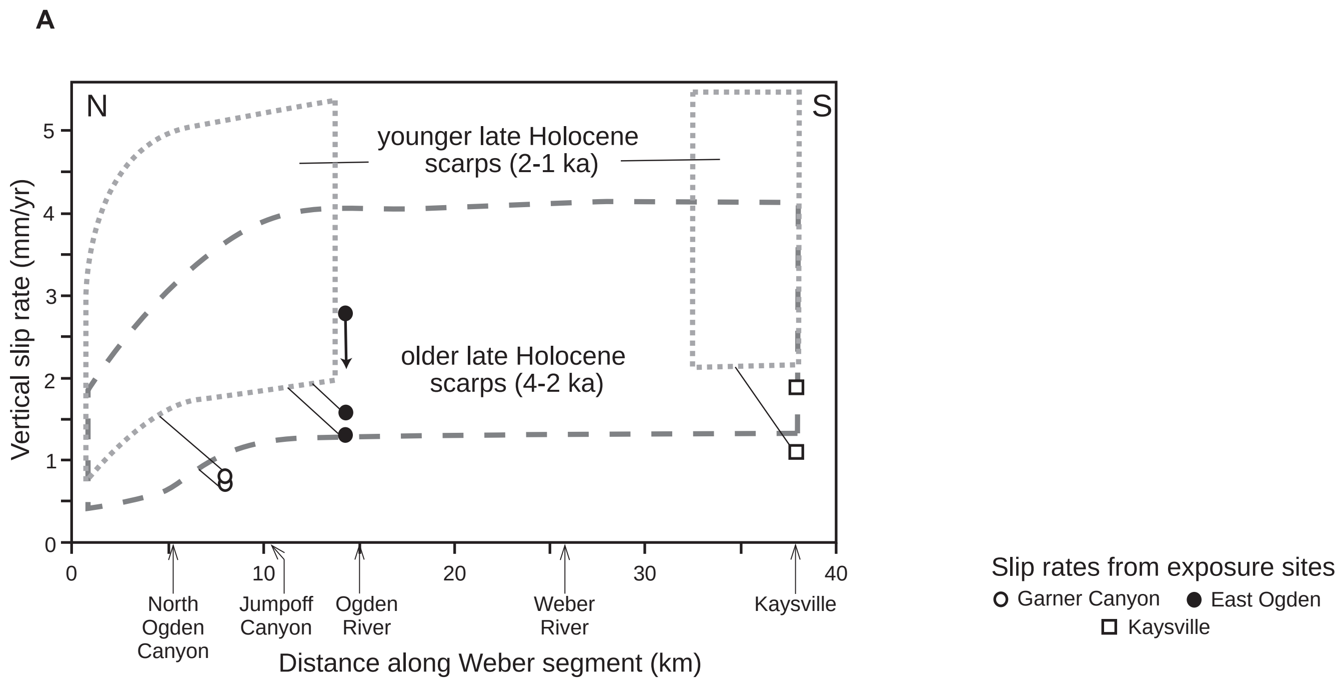

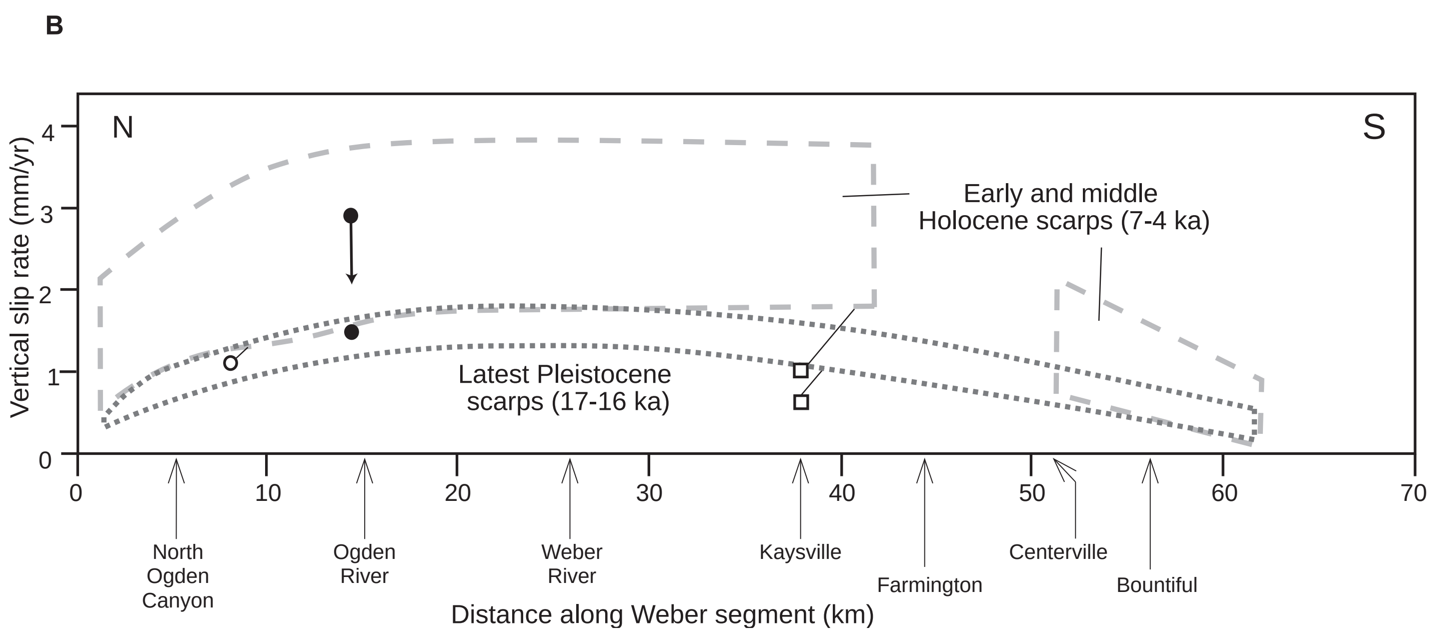

Figure 9. *Slip-rate envelopes derived from surface-displacement envelopes of figures 6 and 7 and listed age ranges for scarps in A) younger and older late Holocene deposits, and B) early and middle Holocene and latest Pleistocene deposits along the Weber segment. Age range for latest Pleistocene deposits (those related to Bonneville or Provo shorelines) is based on Oviatt and others (1992); Oviatt (1997), and Lund (2005, p. 16). Age estimates for Holocene deposits are based on a few ^{14}C ages (Swan and others, 1980; McCalpin and others, 1994; Machette and others, 1992), relative soil-profile development, and geomorphic position, as discussed by Nelson and Personius (1993). Younger late Holocene deposits are assumed to be >1 ka to eliminate impossibly high slip rates. Slip rates calculated from displacements and ages at the three exposure sites for deposits of similar age are shown by symbols. Leaders on symbols show rates that fall below the envelope for deposits of similar age. The anomalously high slip rates shown by the heights of the Holocene envelopes, especially when compared to the exposure site slip rates, suggest that most Holocene deposits along the segment are thousands of years older than inferred by Nelson and Personius (1993). Arrows on two symbols at the East Ogden site show how slip rates would decrease if we assume 1.5 m of unrecognized antithetic faulting during earthquakes A and B at that site.*

our estimates due to unrecognized antithetic faulting. The latter suggestion makes displacements—and therefore slip rates—at East Ogden comparable with those at the Garner Canyon and Kaysville sites (figure 8; table 5 footnotes).

Magnitude of Surface-Faulting Earthquakes

We estimate a magnitude range for four of the earthquakes recorded at the Garner Canyon, East Ogden, and Kaysville sites from mean total displacements for each earthquake at each site by two methods (Wells and Coppersmith, 1994; Hemphill-Haley and Weldon, 1998; table 5). Using the method of Hemphill-Haley and Weldon (1998) requires estimating the percentage of the rupture spanned by the sites with mean displacements. Because we have no information on rupture length along the Weber segment for specific earthquakes, we use four hypothetical rupture lengths that the world wide displacement-surface-rupture-length regressions of Wells and Coppersmith (1994) suggest are reasonable for our mean displacements from the three Weber segment sites. For example, in table 6 we assume that the mean total displacements for earthquakes B and C (means of total displacements from either two or three sites) could record a rupture 30 km long at only the Garner Canyon and East Ogden sites, a rupture 45 km long that includes all three sites, or a 61-km-long rupture of the entire Weber segment. We use only the method of Wells and Coppersmith (1994) for earthquake D (only East Ogden site) because the method of Hemphill-Haley and Weldon (1998) requires displacements from two or more sites. For comparison, table 6 also lists magnitude ranges (shown as a one-standard-error interval) for hypothetical ruptures of these lengths derived from the magnitude-rupture length regressions of Wells and Coppersmith (1994).

We calculate two different mean displacements for earthquakes A and B (table 6). One using our displacement values for the East Ogden site (table 5), and the other assuming displacements were 1.5 m less than those values to account for possible unrecognized antithetic faulting (shown in parentheses in table 6). The lower displacements result in magnitude ranges that are lower by only 0.1M.

The magnitude ranges for earthquake A suggest that its rupture extent was greater than the distance indicated by the correlations of figure 8. We calculate a magnitude range for earthquake A only for the 30-km rupture because this earthquake was not recorded at Kaysville (and therefore inferred not to extend south of Kaysville; figure 1). However, the mean displacement for earthquake A is the same as that for earthquake B and the magnitude range calculated for earthquake A is similar to the range calculated by either method (Hemphill-Haley and Weldon, 1998; or Wells and Coppersmith, 1994) for a rupture of 45 km, or a rupture of the entire Weber segment.

CONCLUSIONS

Analysis of stratigraphy and ages from five trenches across two parallel scarps and a small antithetic scarp, which cut middle and late Holocene alluvial fans at the base of the mountain front on the east edge of the city of Ogden, yield a history of three large surface-faulting earthquakes and a smaller, most recent, surface-faulting earthquake. Earthquakes are correlated among the five trenches based on the position of trenches on the same or different scarps, the amount of stratigraphic displacement of the same debris-flow and stream-channel deposits in adjacent trenches, the relative amount of slip during earthquakes suggested by colluvial-wedge thicknesses and scarp perpendicular topographic profiles, and TL and AMRT ^{14}C ages on buried A horizons, which place minimum- and maximum-age constraints on the times of earthquakes. We concur with Gilbert (1928) that surface rupture during the most recent earthquake broke only the higher of the two parallel scarps.

East Ogden site data yield the following best estimates of the times and total displacements across the entire fault zone for the four earthquakes: 4.2 m for earthquake A about 4.0 ka (range 4.8-2.8 ka), 4.2 m for earthquake B about 3.0 ka (range 3.9-2.4 ka), 2.6 m for earthquake C about 1.1 ka (range 1.7-0.5 ka), and 0.8 m for earthquake D about 0.5 ka (range 0.6-0.2 ka).

An artificial exposure at Garner Canyon, cut into a 4-m-displacement scarp on the main trace of the Weber segment 5 km north of the East Ogden site, shows a similar record of at least three and probably four surface-faulting earthquakes. TL and apparent mean residence ^{14}C ages from buried A horizons indicate that the three most recent earthquakes correlate with the three largest earthquakes at East Ogden, but earthquake displacements are less than half the displacements at East Ogden. Consideration of the many additional ages from Garner Canyon (McCalpin, 1998, p. 145; Stafford and Forman, 1993) leads us to revise our best estimates of the times of earthquakes B (about 2.5 ka, range 2.8-2.4 ka) and earthquake C (about 0.9 ka, range 1.0-0.5 ka).

Comparison of the earthquake history at Kaysville revised by McCalpin and others (1994), 25 km south of East Ogden, with the composite history for the East Ogden and Garner Canyon sites suggests surface-faulting earthquakes of different size rupturing different lengths of the Weber segment. Displacements and ages solidly support a correlation of earthquakes B and C among all three sites yielding a rupture extent of at least 35 km, and probably at least three-fourths of the 61-km-long segment. Earthquake A is unrecorded at Kaysville, unless an earthquake there thought to date about 5.9 ka is much younger (McCalpin and others, 1994). Because earthquake A's displacements at the northern sites equal or exceed those for earthquakes B and C, earthquake A's displacements are inconsistent with a rupture extent confined to the northern half of the segment north of Kaysville. Earthquake D is not recorded at Garner Canyon or Kaysville and so its surface rupture was probably small (<0.5 m), of limited extent (perhaps <15 km), and may not have reached either site.

Earthquakes of differing magnitude, implied by ruptures of different size and length, also complicate recurrence interval calculations. The two intervals between earthquakes A, B, and C at East Ogden and Garner Canyon give an average recurrence of about 1.5 kyr, similar to Lund's (2005) value of 1.6±0.6 kyr for three intervals between middle to late Holocene earthquakes calculated from the data of McCalpin and Nishenko (1996). Our two-interval average may only apply to the northern Weber segment. An additional complication is the much shorter interval between earthquakes C and D at East Ogden. Because earthquake D records an earthquake significantly smaller than the earlier dated earthquakes, averaging the earthquake C/D interval with earlier intervals gives a shorter average recurrence interval (e.g., Lund's, 2005, average is 1.0±1.4 kyr) that may not accurately reflect the history of the Weber segment.

The distribution of surface displacements measured across scarps along the Weber segment and summarized here in more detail than in Nelson and Personius (1993) also points to differences in rupture extent, and hence earthquake magnitude, along the segment. Displacements decrease dramatically within 10 km of segment boundaries—for scarps on deposits of all ages at the northern end, and for latest Pleistocene through middle Holocene deposits at the southern end. The decrease is consistent with surface ruptures terminating near either end of the segment, and/or with a lower frequency of rupture near the ends of the segment. Displacements in latest Pleistocene through middle Holocene deposits are significantly smaller south of Farmington, suggesting that ruptures have either been smaller or less frequent along the southern third of the segment. The largest displacements in deposits of all ages occur between Jumpoff Canyon and Kaysville suggesting larger displacements or more frequent ruptures along the northern half of the segment.

With the exception of latest Pleistocene fault slip rates derived from displacements of well dated Lake Bonneville shorelines, slip rates derived from surface displacements along the Weber segment are inconsistent with the much lower rates calculated from displacement data at two of the three exposure sites. To reconcile both types of rates we suggest that many displaced Holocene surfaces along the Weber segment are 20-100% older than inferred by Nelson and Personius (1993), and that our estimated displacements during earthquakes A and B at East Ogden are about 1.5 m too high due to unrecognized antithetic faulting. These age and displacement adjustments yield rates along much of the segment of about 1-2 mm/yr, with the highest rates between Kaysville and Ogden. The adjusted rates are comparable to those for other central segments of the Wasatch fault zone (Machette and others, 1992; McCalpin and Nishenko, 1996; Chang and Smith, 2002; Lund, 2005).

Estimates of the magnitudes of the four most recent surface-faulting earthquakes along the Weber segment, derived from displacement data at the three exposure sites, are: earthquake A, 7.0-7.5M; earthquake B, 7.0-7.5M; earthquake C, 6.9-7.4M; and earthquake D, 6.5-6.7M. Assuming 1.5 m of unrecognized antithetic faulting at East Ogden reduces the magnitudes of earthquakes A and B by about 0.1M.

ACKNOWLEDGMENTS

This work was supported by the Earthquake Hazards Program of the U.S. Geological Survey and the Utah Geological Survey. We thank Mike Machette, Bill Lund, Jim McCalpin, Ernie Anderson, and many Utah geologists for their continuing guidance and interest in our exposure site studies. The City of Ogden gave permission for trench excavation. Bill Lund, Bill Black, and other Utah Geological Survey personnel provided logistical support for the East Ogden investigation. The U.S. Bureau of Reclamation loaned us hydraulic shoring. Primary trench loggers were Nelson, Lowe, and Garr. Jim McCalpin collected TL samples in the East Ogden trenches, and he and Steve Forman and Tom Stafford sampled the Garner Canyon exposure. Forman did TL analyses and Stafford did ^{14}C analyses from Garner Canyon. Kathy Haller did the initial ink drafting of trench logs, which were reformatted by Lee-Ann Bradley. Bradley helped with other graphics as well. We thank Tom Stafford for use of ^{14}C ages published in McCalpin (1998, p. 145). Comments by Bill Lund, Gary Christenson, and Chris DuRoss strengthened the report.

REFERENCES

Birkeland, P.W., 1984, Soils and geomorphology: New York, Oxford University Press, 372 p.

—1999, Soils and geomorphology: New York, Oxford University Press, 430 p.

Black, B.D., Giraud, R.E., and Mayes, B.H., 2000, Paleoseismic investigation of the Clarkston, Junction Hills, and Wellsville faults, West Cache fault zone, Cache County, Utah: Utah Geological Survey Special Study 98, 23 p.

Black, B.D., Lund, W.R., Schwartz, D.P., Gill, H.E., and Mayes, B.H., 1996, Paleoseismology of Utah, volume 7 - Paleoseismic investigation on the Salt Lake City segment of the Wasatch fault zone at the South Fork Dry Creek and Dry Gulch sites, Salt Lake County, Utah: Utah Geological Survey Special Study 92, 22 p.

Bronk Ramsey, C., 1995, Radiocarbon calibration and analysis of stratigraphy: The OxCal program: Radiocarbon, v. 37, p. 425-430.

—2001, Development of the radiocarbon program OxCal: Radiocarbon, v. 43, p. 355-363.

Bucknam, R.C., and Anderson, R.E., 1979, Estimation of fault-scarp ages from a scarp-height-slope-angle relationship: Geology, v. 7, p. 11-14.

Chang, W.L., and Smith, R.B., 2002, Integrated seismic-hazard analysis of the Wasatch Front, Utah: Bulletin of the Seismological Society of America, v. 92, p. 1904-1922.

Dreimanis, Aleksis, 1962, Quantitative gasometric determination of calcite and dolomite by using Chittick apparatus: Journal Sedimentary Petrology, v. 32, p. 520-529.

Foley, L.L., Martin, R.A., Jr., and Sullivan, J.T., 1986, Seismotectonic study for Joes Valley, Scofield and Huntington North Dams, Emery County and Scofield Projects, Utah: U.S. Bureau of Reclamation Seismotectonic Report 86-7, 132 p., 3 pls.

Forman, S.L., Jackson, M.E., McCalpin, J.P., and Maat, P., 1989a, The potential of using thermoluminescence to date buried soils developed on colluvial and fluvial sediments from Utah and Colorado, U.S.A.: preliminary results: Quaternary Science Reviews, v. 7, p. 287-293.

Forman, S.L., Machette, M.N., Jackson, M.E., and Maat, Paula, 1989b, An evaluation of thermoluminescence dating of paleoearthquakes on the American Fork segment, Wasatch fault zone, Utah: Journal of Geophysical Research, v. 94, no. B2, p. 1622-1630.

Forman, S.L., Nelson, A.R., and McCalpin, J.P., 1991, Thermoluminescence dating of fault-scarp-derived colluvium—Deciphering the timing of paleoearthquakes on the Weber segment of the Wasatch fault zone, north central Utah: Journal of Geophysical Research, v. 96, no. B1, p. 595-605.

Forman, S.L., Pierson, J., and Lepper, K., 2000, Luminescence geochronology *in* Noller, J.S., Sowers, J.M., and Lettis, W.R, eds., Quaternary geochronology; methods and applications: American Geophysical Union Reference Shelf, v. 4, p.157-176.

Gile, L.H., Peterson, F.F., and Grossman, R.B., 1966, Morphological and genetic sequences of carbonate accumulation in desert soils: Soil Science, v. 101, p. 347-360.

Gilbert, G.K., 1928, Studies of Basin-Range structure: U.S. Geological Survey Professional Paper 153, 92 p.

Hemphill-Haley, M.A., and Weldon, R.J.I., 1999, Estimating prehistoric earthquake magnitude from point measurements of surface rupture: Bulletin of the Seismological Society of America, v. 89, p. 1264-1279.

Jackson, M.E., 1991, Paleoseismology of Utah, volume 3 - The number and timing of Holocene paleoseismic events on the Nephi and Levan segments, Wasatch fault zone, Utah: Utah Geological Survey Special Studies 78, 23 p.

Jackson, M.L., 1956, Soil chemical analysis—advanced course [unpublished laboratory manual]: Madison, Wisconsin, University of Wisconsin, Department of Soil Science, 656 p.

Kihl, Rolf, 1975, Physical preparation of organic matter samples for ^{14}C dating, appendix in Andrews, J.T., Radiocarbon date list II from Cumberland Peninsula, Baffin Island, N.W.T., Canada: Arctic and Alpine Research, v. 7, p. 90-91.

Kristiansen, S.M., Dalsgaard, K., Holst, M.K., Aaby, B., and Heinemeier, J., 2003, Dating of prehistoric burial mounds by ^{14}C analysis of soil organic matter fractions: Radiocarbon, v. 45, p. 2003.

Lund, W.R., 2005, Consensus preferred recurrence interval and vertical slip-rate estimates—Review of Utah paleoseismic-trenching data by the Utah Quaternary Fault Parameters Working Group: Utah Geological Survey Bulletin 134, 109 p., 5 appendices.

Lund, W.R., and Black, B.D., 1998, Paleoseismology of Utah, volume 8 - Paleoseismic investigation at Rock Canyon, Provo segment, Wasatch fault zone, Utah County, Utah: Utah Geological Survey Special Study 93, 21 p.

Lund, W.R., Schwartz, D.P., Mulvey, W.E., Budding, K.E., and Black, B.D., 1991, Paleoseismology of Utah, volume 1 - Fault behavior and earthquake recurrence on the Provo segment of the Wasatch fault zone at Mapleton, Utah County, Utah: Utah Geological and Mineral Survey Special Studies 75, 41 p.

Machette, M.M., 1989, Slope-morphometric methods, *in* Forman, S.L., ed., Dating methods applicable to Quaternary geologic studies in the western United States, Utah Geological and Mineral Survey Miscellaneous Publication 89-7, p. 30-42.

Machette, M.N., Personius, S.F., and Nelson, A.R., 1987, Quaternary geology along the Wasatch fault zone—Segmentation, recent investigations, and preliminary conclusions, *in* Gori, P.L., and Hayes, W.W., eds., Assessment of regional earthquake hazards and risk along the Wasatch Front, Utah: U.S. Geological Survey Open-File Report 87-585, v. 1, p. A1-A72.

—1992, Paleoseismology of the Wasatch fault zone—A summary of recent investigations, conclusions, and interpretations, *in* Gori, P.L., and Hayes, W.W., eds., Assessing regional earthquake hazards and risk along the Wasatch Front, Utah: U.S. Geological Survey Professional Paper 1500-A, p. A1-A71.

Matthews, J.A., 1980, Some problems and implications of ^{14}C dates from a podzol buried beneath an end moraine at Haugabreen, southern Norway: Geografiska Annaler, v. 62A, p. 185-208.

—1985, Radiocarbon dating of surface and buried soils: principles, problems, and prospects, *in* Richards, K.S., Arnett, R.R., and Ellis, S., Geomorphology and soils: London, Allen and Unwin, p. 269-288.

McCalpin, J.P., editor, 1998, Paleoseismology: Orlando, Florida, Academic Press, 608 p.

McCalpin, J.P., and Berry, M.E., 1996, Soil catenas to estimate ages of movements on normal fault scarps, with an example from the Wasatch fault zone, Utah, USA: Catena, v. 27, p. 256-286.

McCalpin, J.P., and Forman, S.L., 1989, Refinement of thermoluminescence (TL) dating for the Wasatch fault, Utah: Final Technical Report, U.S. Geological Survey Contract 14-08-0001-G1396, 49 p.

—2002, Paleoseismology of Utah, volume 11 - Post-Provo paleoearthquake chronology of the Brigham City segment, Wasatch fault zone, Utah: Utah Geological Survey Miscellaneous Publication 02-9, 46 p.

McCalpin, J.P., and Nelson, A.R., 1998, Introduction to paleoseismology, *in* McCalpin, J.P., ed., Paleoseismology: Orlando, Florida, Academic Press, p. 1-32.

McCalpin, J.P., Forman, S.L., and Lowe, M., 1994, Reevaluation of Holocene faulting at the Kaysville site, Weber segment of the Wasatch fault zone, Utah: Tectonics, v. 13, no. 1, p. 1-16.

McCalpin, J.P., and Nishenko, S.P., 1996, Holocene probability, temporal clustering, and probabilities of future large (M>7) earthquakes on the Wasatch fault zone, Utah: Journal of Geophysical Research, v. 101, no. B3, p. 6233-6253.

Nelson, A.R., 1988, The northern part of the Weber segment of the Wasatch fault zone near Ogden, Utah, *in* Machette, M.N., ed., In the footsteps of G.K. Gilbert – Lake Bonneville and neotectonics of the eastern Basin and Range Province, Guidebook for Field Trip Twelve: Utah Geological and Mineral Survey Miscellaneous Publication 88-1, p. 33-37.

—1992, Lithofacies analysis of colluvial sediments–an aid in interpreting the recent history of Quaternary normal faults in the Basin and Range Province, western United States: Journal of Sedimentary Petrology, v. 62, p. 607-621.

Nelson, A.R., Johnson, S.Y., Kelsey, H.M., Wells, R.E., Sherrod, B.L., Pezzopane, S.K., Bradley, L.A., Koehler, R.D., and Bucknam, R.C., 2003, Late Holocene earthquakes on the Toe Jam Hill fault, Seattle fault zone, Bainbridge Island, Washington: Geological Society of America Bulletin, v. 115, p. 1388-1403.

Nelson, A.R., Klauk, R.H., Lowe, Michael, and Garr, J.D., 1987, Holocene history of displacement on the Weber segment of the Wasatch fault zone at Ogden, northern Utah [abs.]: Geological Society of America Abstracts with Programs, v. 19, no. 5, p. 322.

Nelson, A.R., and Personius, S.F., 1993, Surficial geologic map of the Weber segment, Wasatch fault zone, Weber and Davis Counties, Utah: U.S. Geological Survey Miscellaneous Investigations Map I-2199, 22 p. pamphlet, 1 sheet, scale 1:50,000.

Nelson, A.R., and VanArsdale, R.B., 1986, Recurrent late Quaternary movement on the Strawberry normal fault, Basin and Range—Colorado plateau transition zone, Utah: Neotectonics, v. 1, p. 7-37.

Ostenaa, D. A., 1984, Relationships affecting estimates of surface fault displacements based on scarp-derived colluvial deposits: Geological Society of America, Abstracts with Programs, v. 16, no. 5, p. 327.

Oviatt, C.G., 1997, Lake Bonneville fluctuations and global climate change: Geology, v. 25, p. 155-158.

Oviatt, C.G., Currey, D.R., and Sack, Dorothy, 1992, Radiocarbon chronology of Lake Bonneville, eastern Great Basin, USA: Palaeogeography, Palaeoclimatology, Palaeoecology, v. 99, p. 225-241.

Oyama, M., and Takehara, H., 1970, Revised standard soil color charts: Ministry of Agriculture and Forestry, Japan, 40 p.

Paul, E.A., Follett, R.F., Leavitt, S.W., Halvorson, A., Peterson, G.A., and Lyon, D.J., 1997, Radiocarbon dating for determination of soil organic matter pool sizes and dynamics: Soil Science Society of America Journal, v. 61, p. 1058-1067.

Personius, S.F., 1991, Paleoseismology of Utah, volume 2 - Paleoseismic analysis of the Wasatch fault zone at the Brigham City trench site, Brigham City, Utah, and Pole Patch trench site, Pleasant View, Utah: Utah Geological and Mineral Survey Special Studies 76, 39 p.

—1993, Surficial geologic map of the Brigham City segment and adjacent parts of the Weber and Collinston segments, Wasatch fault zone, Box Elder and Weber Counties, Utah: U.S. Geological Survey Miscellaneous Investigations Series Map I-1979, scale 1:50,000.

Pessenda, L.C.R., Gouveia, S.E.M., and Aravena, R., 2001, Radiocarbon dating of total soil organic matter and humin fraction and its comparison with ^{14}C ages of fossil charcoal: Radiocarbon, v. 43, p. 595-601.

Pillmore, C.L., 1989, Geologic photogrammetry in the U.S. Geological Survey: Photogrammetric Engineering and Remote Sensing, v. 55, p. 1185-1189.

Pitty, A.F., 1968, A simple device for the field measurement of hillslopes: Journal of Geology, v. 76, p. 717-720.

Rumpel, C., Balesdent, J., Grootes, P., Weber, E., Koegel-Knabner, I., 2003, Quantification of lignite- and vegetation-derived soil carbon using ^{14}C activity measurements in a forested chronosequence: Geoderma, v. 112, p. 155-166.

Scharpenseel, H.W., and Becker-Heidmann, P., 1992, Twenty-five years of radiocarbon dating soils: paradigm of erring and learning: Radiocarbon, v. 34, p. 541-549.

Scharpenseel, H.W., Pietig, F., Schiffman, H., and Becker-Heidmann, P., 1996, Radiocarbon dating of soils: database contribution by Bonn and Hamburg: Radiocarbon, v. 38, p. 277-294.

Scharpenseel, H.W., and Schiffman, H., 1977, Radiocarbon dating of soils: a review: Zeitschrift fur Pflanzenernahrung Dungung und Bodenkunke, v. 140, p. 159-174.

Schwartz, D.P., and Coppersmith, K.J., 1984, Fault behavior and characteristic earthquakes—Examples from the Wasatch and San Andreas fault zones: Journal of Geophysical Research, v. 89, no. B7, p. 5681-5698.

Scott, E.M., Aitchison, T.C., Harkness, D.D., Cook, G.T., and Baxter, M.S., 1990, An overview of all three stages of the International Radiocarbon Intercomparison: Radiocarbon, v. 32, p. 309-320.

Scott, E.M., Harkness, D.D., and Cook, G.T., 1998, Interlaboratory comparisons: lessons learned: Radiocarbon, v. 40, p. 331-340.

Singer, M.J., and Janitzky, P., eds., 1986, Field and laboratory procedures used in a soil chronosequence study: U.S. Geological Survey Bulletin 1648, 45 p.

Soil Survey Staff, 1975, Soil Taxonomy: Agriculture Handbook No. 436, Soil Conservation Service, U.S. Department of Agriculture, 754 p.

Stafford, T.W., Jr., and Forman, S.L., 1993, Radiocarbon and thermoluminescence dating of Wasatch faulting events, Garner Canyon, Utah: Utah Geological Survey Contract Report 93-4, 15 p.

Storer, D.A., 1984, A simple high sample volume ashing procedure for determination of soil organic matter: Communications in Soil Science and Plant Analysis, v. 15, p. 759-772.

Stuckenrath, R., Miller, G.H., and Andrews, J.T., 1979, Problems of radiocarbon dating Holocene organic-bearing sediments, Cumberland Peninsula, Baffin Island, N.W.T., Canada: Arctic and Alpine Research, v. 11, p. 109-120.

Stuiver, M., and Kra, R., eds., 1986, Calibration issue—Proceedings of the 12th International Radiocarbon Conference, Trondheim, Norway: Radiocarbon, v. 28, no. 2B, 225 p.

Stuiver, M., Reimer, P.J., Bard, E., Beck, J.W., Burr, G.S., Hughen, K.A., Kromer, B., McCormac, G., Plicht, J.v.d., and Spurk, M., 1998, INTCAL98 radiocarbon age calibration, 24,000-0 cal BP: Radiocarbon, v. 40, p. 1041-1084.

Sullivan, J.T., Nelson, A.R., LaForge, R.C., Wood, C.K., and Hansen, R.A., 1988, Central Utah regional seismotectonic study for USBR dams in the Wasatch Mountains: Seismotectonic Report 88-5, Engineering and Research Center, U. S. Bureau of Reclamation, Denver, Colorado, 338 p.

Swan, F.H., III, Schwartz, D.P., and Cluff, L.S., 1980, Recurrence of moderate to large magnitude earthquakes produced by surface faulting on the Wasatch fault zone, Utah: Bulletin of the Seismological Society of America, v. 70, no. 5, p. 1431-1462.

Taylor, R.E., 1987, Radiocarbon dating—an archaeological perspective: Orlando, Florida, Academic Press, 212 p.

Taylor, R.E., Stuiver, M., and Reimer, P.J., 1996, Development and extension of the calibration of the radiocarbon time scale: archaeological applications: Quaternary Science Reviews, v. 15, p. 655-668.

Trumbore, S., and Zheng, S., 1996, Comparison of fractionation methods for soil organic matter ^{14}C analysis: Radiocarbon, v. 38, p. 219-230.

Tsao, C.W., and Bartha, R., 1999, Differential extraction of radiocarbon associated with soil biomass and humus: Soil Science, v. 164, p. 235-241.

Walkley, A., and Black, I.A., 1934, An examination of the Degtjareff method for determining soil organic matter and a proposed modification of the chromic acid titration method: Soil Science, v. 34, p. 29-38.

Wang, Y., Amundson, R., and Trumbore, S., 1996, Radiocarbon dating of soil organic matter: Quaternary Research, v. 45, p. 282-288.

Waterbolk, H.T., 1983, Ten guidelines for the archaeological interpretation of radiocarbon dates, *in* Mook, W.G., and Waterbolk, H.T., eds., Proceedings of the First International Symposium, ^{14}C and Archaeology: PACT Journal of the European Study Group on Physical, Chemical, and Mathematical Techniques Applied to Archaeology, v. 8, p. 57-70.

Wells, D., and Coppersmith, K. J., 1994, New empirical relationships among magnitude, rupture length, rupture width, rupture area, and surface displacement: Bulletin Seismological Society of America, v. 84, p. 974-1002.

West, M.W., 1989, Neotectonics of the Darby-Hogsback and Absaroka thrust plates, Uinta County, Wyoming and Summit County, Utah with applications to earthquake hazard assessment: Golden, Colorado School of Mines, unpublished Ph.D. dissertation, 450 p., 17 pls.

—1994, Paleoseismology of Utah, volume 4 - Seismotectonics of north-central Utah and southwestern Wyoming: Utah Geological Survey Special Study 82, 93 p., 5 pls.

UTAH GEOLOGICAL SURVEY
a division of
Utah Department of Natural Resources

U.S. DEPARTMENT OF THE INTERIOR
U.S. GEOLOGICAL SURVEY

Plate 1. Trench logs, lithologic data, scarp profiles, and a map for the East Ogden site

UTAH GEOLOGICAL SURVEY
Miscellaneous Publication 05-8
2006

LITHOLOGIC DATA FOR STRATIGRAPHIC UNITS IN TRENCH 1

Stratigraphic unit[1]	Trench station (m)[2]	Genesis[3]	Earth-quake[4]	Lithology[5]	Color[6]	Matrix texture[7]	Sand sizes[8]	Soil structure[9]	Percent by volume[10] Pebbles	Cobbles	Boulders	Other features[11]
COLLUVIUM OF HANGING-WALL BLOCK												
1aA		S		si-s	10YR 4/3	ls+	f-co	wm pl	15	0	0	
1bA		S		si-s	7.5YR 5/3	ls	f-co	vw sb	15	0	0	
1cA	13-20	S		g si-s	7.5YR 4/3	sl	f-co	vw pl	15	5	0	
1cA	20-26	S		g si-s	7.5YR 3/3	ls+	f-co	w pl	15	8	0	
1cA	26-31	S		g si-s	7.5YR 4/3	ls+	f-co	vw pl	15	0	0	
1dAE		W		g si-s	7.5YR 5/3	ls	f-vco	—	15	8	2	Eluvial horizon of surface-wash sediments.
1eA	19-21	W	C	g k si-s	7.5YR 5/3	ls	f-vco	—	25	15	1	Diffuse upper contact.
2		D	C	si-s k g	7.5YR 6/5	s+	f-vco	—	30	20	1	Scarp-derived colluvial wedges from small, most recent surface-faulting earthquake.
3aA	26-30	W		g si-s	7.5YR 4/3	ls	f-co	—	15	0	0	Finest grained, most distal part of unit 1 wash facies with diffuse lower and lateral contacts.
3bA	22-26	W	B	g si-s	7.5YR 5/3	ls-	f-vco	—	20	0	0	Sandy surface-wash facies.
3bA	26-30	W	B	g si-s	7.5YR 5/3	ls-	f-vco	—	25	0	0	Coarse, sandy surface-wash facies.
3cA	19-21	W	B	g k si-s	7.5YR 4/3	sl-	f-co	—	20	15	0	Wash facies with darker color and more organic material near fault.
3cA	21-24	W&S	B	g k si-s	7.5YR 5/3	ls	f-vco	—	15	15	15	Mixture of debris and wash facies.
3d	19-21	W&S	B	g k si-s	7.5YR 5/3	ls	f-vco	—	20	25	5	
4	21-24	W&S	B	g k si-s	7.5YR 5/3	ls	f-vco	—	20	25	15	Burrowed, deformed mixture of wash facies.
5a		D&S	B	g k s	7.5YR 5/5	s+	f-vco	—	30	15	10	Unit deformed, upper contact eroded. Blocks of Bw horizon at m 21.
5b		D	B	k s g	7.5YR 5/5	s	m-cvo	—	40	20	10	Unit deformed.
6a		D	A	b k s g	7.5YR 6/3	s	f-vco	—	15	20	15	Unit deformed, upper contact deeply eroded.
6b		D	A	b k g	7.5YR 6/3	s	m-vco	—	20	25	30	Partially sorted wedge of debris facies.
6c		G	AB	k g s	7.5YR 6/3	s	f-vco	—	20	25	10	Parts of unit have clast-supported openwork structure.
6d		G	B	k s g	7.5YR 6/3	s	f-vco	—	25	25	10	
6e		D	A	s k g	7.5YR 6/3	s	f-vco	—	30	20	5	Wedge of debris facies derived from unit 12.
6f		W&S	A	g k b si-s	7.5YR 5/4	ls+	f-vco	vw sb	20	20	20	Common clay films on clasts and bridging grains.
FAN ALLUVIUM OF FOOTWALL BLOCK												
7aA	6-11	S		k si-s	7.5YR 5/3	ls+	f-co	vw sb	15	15	3	Common silt coatings on grains.
7aA	24-30	S		k si-s	7.5YR 5/4	ls+	f-vco	vw pl	15	25	10	
7bE		S		g k si-s	7.5YR 6/3	ls-	f-vco	—	15	20	2	Eluvial horizon.
7cBt		F		k si-s g	7.5YR 6/5	ls+	f-vco	m ab	25	20	5	Very few clay films lining pores, common films bridging grains.
7d		F		k s g	7.5YR 6/5	s+	m-vco	—	40	15	5	Indistinct, discontinuous, nonparallel bedding.
8a		F		b si-s g	7.5YR 6/5	ls	f-co	—	30	15	25	Some 0.1-m-thick fine-gravel lenses.
8b		C		s k g	7.5YR 5/5	s	m-vco	—	50	20	2	Parts of unit have clast-supported structure.
9a		C&F		s k g	7.5YR 6/5	s	m-vco	—	45	15	8	Some 0.1-m-thick, fine-gravel lenses.
9b		F		b si-s g	7.5YR 5/4	s+	f-vco	—	30	20	15	
10a		C		s g	7.5YR 6/5	s	m-vco	—	50	10	0	
10b		C&F		k si-s g	7.5YR 6/5	ls	f-vco	—	30	20	10	
10c		C		g	7.5YR 6/5	s+	m-vco	—	50	5	2	Common coarse gravel lenses.
10d		C		s g	7.5YR 6/5	s	m-vco	—	60	0	0	
11a		C		b si-s g	7.5YR 6/5	s+	m-vco	—	25	5	30	
11b		C		b s g	7.5YR 6/5	s	m-vco	—	50	10	30	
SHOREFACE DEPOSITS OF LAKE BONNEVILLE												
12a		L		g s	7.5YR 6/3	s	m-vco	—	30	5	0	Parallel bedded.
12b		L		s g	7.5YR 6/3	s	m-vco	—	70	0	0	Parallel bedded.
12c		L		k s g	7.5YR 6/3	s	m-vco	—	50	15	0	Parallel bedded.

[1]Major units (numbers) mapped on the basis of size, distinctness, and inferred genesis; units numbered from youngest to oldest. Subunits labeled with lowercase letters. Uppercase letters (and following lowercase letter for a few units) indicate soil horizons of Soil Survey Staff (1975) and Birkeland (1984; 1999). Color shows inferred genesis of unit (explanation in lower right corner of plate).
[2]Numbers show location along trench log where listed data apply to unit. If no numbers are shown, data apply to entire unit.
[3]C, stream (channel) deposit; F, debris-flow deposit; D, debris facies (debris element of Nelson, 1992), dominantly gravity-deposited scarp-derived colluvium; W, wash facies (wash element of Nelson, 1992), dominantly surface-wash-deposited colluvium on colluvial wedge; S, surface wash colluvium with minor amounts of loess; G, colluvial debris deposited in graben; L, lacustrine shoreface deposit; two letters indicate two genetic components.
[4]Unit inferred to have been deposited in response to listed earthquake (uppercase letters in red), as explained in text.
[5]g, gravel or gravelly; k, cobbly; b, bouldery; s, sand or sandy; si-s, silty sand.
[6]Dominant dry color of unit; Munsell color of Oyama and Takehara (1967).
[7]Methods and terminology of Soil Survey staff (1975) and Birkeland (1984; 1999); s, sand; s+, sand to loamy sand; ls, loamy sand; ls-, loamy sand to sand; ls+, loamy sand to sandy loam; sl, sandy loam; sl-, sandy loam to loamy sand.
[8]Grain sizes of sand fraction of matrix sediment; terminology of Soil Survey staff (1975); vco, very coarse; co, coarse; m, medium; f, fine; - (dash), indicates range of sizes.
[9]Methods and terminology of Soil Survey Staff (1975); maximum soil structure in unit, vw, very weak; w, weak; wm, weak to moderate; m, moderate; pl, platy; ab, angular blocky; sb, subangular blocky; dash indiates single grain structure.
[10]Visually estimated with graphic percentage chart. Most clasts are angular to subangular; rare rounded clasts are reworked from higher Lake Bonneville shorelines.
[11]Other features are discussed in text. Lithofacies terminology of Nelson (1992).

SOUTH WALL OF TRENCH 1 AT THE EAST OGDEN SITE

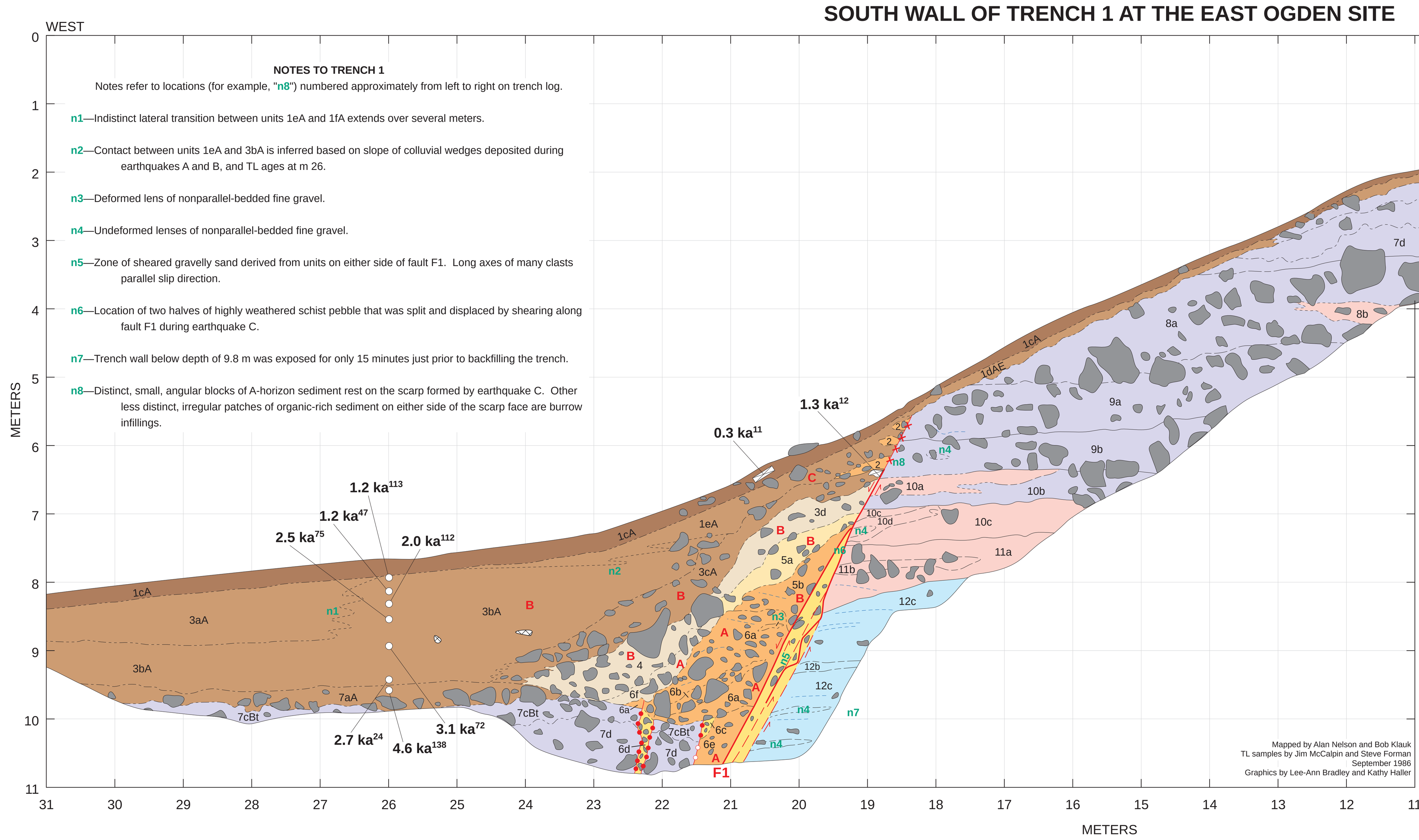

NOTES TO TRENCH 1

Notes refer to locations (for example, "n8") numbered approximately from left to right on trench log.

n1—Indistinct lateral transition between units 1eA and 1fA extends over several meters.

n2—Contact between units 1eA and 3bA is inferred based on slope of colluvial wedges deposited during earthquakes A and B, and TL ages at m 26.

n3—Deformed lens of nonparallel-bedded fine gravel.

n4—Undeformed lenses of nonparallel-bedded fine gravel.

n5—Zone of sheared gravelly sand derived from units on either side of fault F1. Long axes of many clasts parallel slip direction.

n6—Location of two halves of highly weathered schist pebble that was split and displaced by shearing along fault F1 during earthquake C.

n7—Trench wall below depth of 9.8 m was exposed for only 15 minutes just prior to backfilling the trench.

n8—Distinct, small, angular blocks of A-horizon sediment rest on the scarp formed by earthquake C. Other less distinct, irregular patches of organic-rich sediment on either side of the scarp face are burrow infillings.

MAP OF THE EAST OGDEN SITE

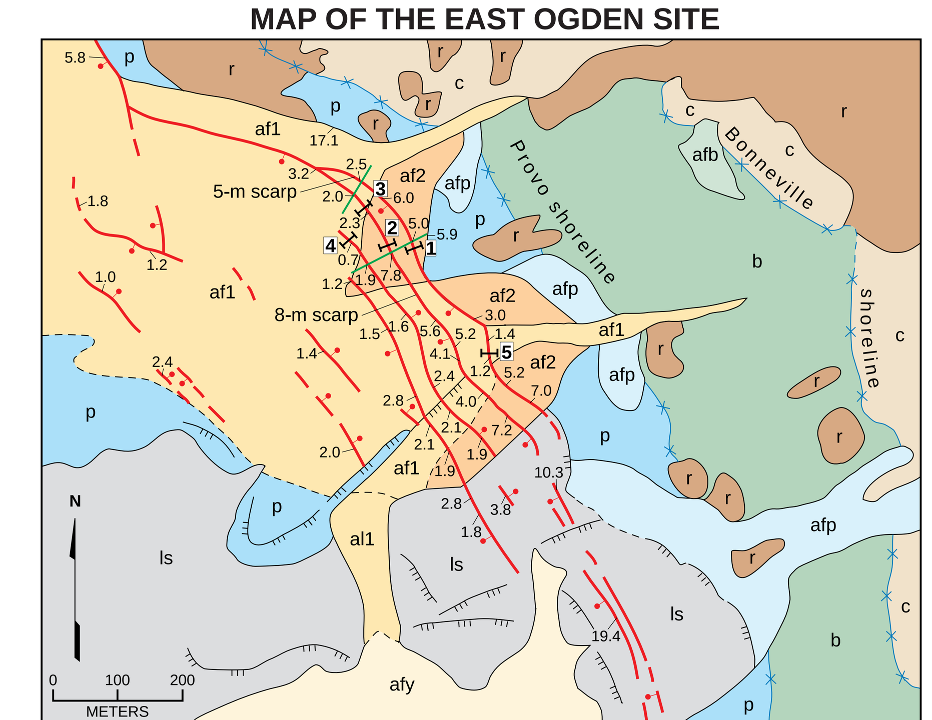

EXPLANATION OF MAP UNITS AND SYMBOLS ON THE EAST OGDEN SITE MAP

MAP UNITS

Alluvial-fan deposits
- af1 — Late Holocene (includes stream alluvium; al1)
- af2 — Middle Holocene
- afy — Holocene, undifferentiated
- afp — Provo phase (17-16 ka)
- afb — Bonneville phase (22-17 ka)

Lacustrine deposits
- p — Provo phase (17-16 ka)
- b — Bonneville phase (22-17 ka)

Colluvial deposits
- c — Talus and hillslope (Holocene)
- ls — Landslide (Holocene and late Pleistocene)

Bedrock (Paleozoic)
- r

SYMBOLS
- Fault, ball on downthrown side, dashed where approximately located
- Contact, dashed where uncertain
- Landslide scarp
- Shorelines
- 2 Trench location
- Scarp profile location
- 4.0 Measured vertical displacement across fault scarp

Mapped by Alan Nelson, 1985

PROFILE ACROSS SCARPS AT TRENCHES 1 AND 2

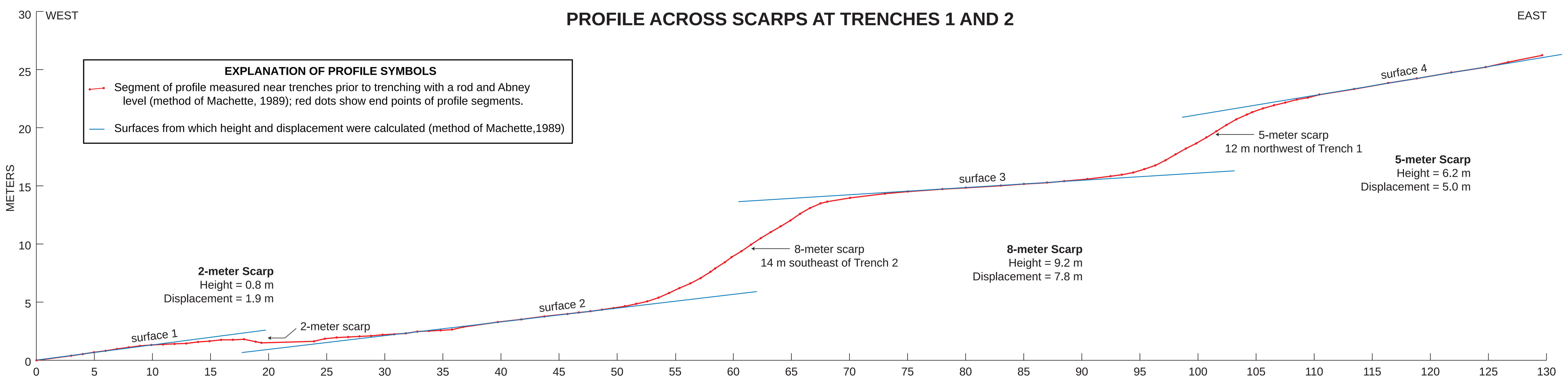

EXPLANATION OF PROFILE SYMBOLS
- Segment of profile measured near trenches prior to trenching with a rod and Abney level (method of Machette, 1989); red dots show end points of profile segments.
- Surfaces from which height and displacement were calculated (method of Machette,1989)

EXPLANATION OF SYMBOLS IN TRENCHES

Faults
- F2 Primary (distinct) —numbered in red
- Secondary —long dashes where indistinct
- Buried fault scarp
- Uneroded free face of a fault or edge of a large fracture
- Inferred free face or edge of fracture

Units deposited in response to:
- D earthquake D
- C earthquake C
- B earthquake B
- A earthquake A

Intra-unit bedding or structures
- Sharp or distinct

Contacts
- Sharp and distinct
- Gradual but distinct

Contacts (continued)
- Gradual and indistinct
- Faint
- Inferred
- Inferred lateral changes in lithofacies

Symbols
- Infilled animal burrows
- Selected cobbles and boulders
- 1.1ka[53] Mode or midpoint of radiocarbon or thermoluminescence age interval, rounded to nearest 100 yr (ka is 1000 cal yr BP); superscript is sample number on table 1)
- ^{14}C age on detrital charcoal
- Area of A horizon sampled for AMRT ^{14}C age
- Thermoluminescence age on fine-grained sediment

LITHOLOGIC DATA FOR STRATIGRAPHIC UNITS IN TRENCH 2

Stratigraphic unit[1]	Trench station (m)[2]	Genesis[3]	Earth-quake[4]	Lithology[5]	Color[6]	Matrix texture[7]	Sand sizes[8]	Soil structure[9]	Percent by volume[10] Pebbles	Cobbles	Boulders	Other features[11]
COLLUVIUM OF HANGING-WALL BLOCK												
1aA	0-9	S		si-s	10YR 4/3	sl+	f-co	wm pl	10	5	0	
1aA	23-31	S		si-s	10YR 4/2	sl+	f-vco	w pl	10	10	0	
1bA		S		si-s	10YR 4/2	sl	f-co	w pl	10	5	0	
1cA	10-17	S		g si-s	10YR 4/3	ls	f-vco	vw pl	10	5	1	
1cA	17-20	S		g si-s	10YR 5/3	ls-	f-vco	—	20	10	2	
1dA		S	C	g si-s	7.5YR 5/3	ls	f-co	—	35	20	1	Small clast-supported gravel lenses near west end.
1eA		D	D?	k g	7.5YR 6/3	s+	m-vco	—	60	35	0	Entirely clast supported.
1fA		W	C	g s	7.5YR 5/3	s	m-vco	—	20	10	0	Partially clast supported.
1gA		W	C	s k g	7.5YR 5/3	s	m-vco	—	70	20	0	Entirely clast supported.
1hA	21-31	S&W	C	g k s	7.5YR 5/3	sl-	f-vco	—	10	0	0	Very uniform, massive unit.
1hA	18-21	W	C	g k s	7.5YR 5/3	s+	m-vco	—	40	40	10	
1iA		S		g k si-s	10YR 4/2	ls	f-co	vw ab	10	10	5	
2a	15-17	D&W	C	g k s	7.5YR 7/4	s	m-vco	—	30	25	5	Angular clasts of A-horizon sediment in upper half.
2a	17-19	D&W	C	g k s	7.5YR 6/4	s	m-vco	—	30	20	5	
2b		D	C	g s	7.5YR 7/3	s	m-vco	vw sb	30	2	50	
2d		D	C	g k si-s	7.5YR 5/3	ls	f-co	—	20	20	20	Small lower debris-facies wedge.
2e		D	C	g k s	7.5YR 5/4	s	f-co	—	20	20	5	Sheared sediment along fault.
3aA	17-19	S	B	g k si-s	7.5YR 4/2	ls+	f-co	vw ab	15	20	10	
3aA	19-23	S	B	g k si-s	7.5YR 5/3	ls	f-co	vw ab	20	5	10	Lateral contact with unit 1hA very diffuse.
3bEj		S	B	g k si-s	7.5YR 5/3	ls-	f-vco	—	20	20	15	Upper half of unit is a weakly developed eluvial horizon.
3cBw		S&W	B	g k si-s	7.5YR 5/4	ls-	m-vco	—	25	20	5	Lenses are clast supported.
4a		D	B	ksg	7.5YR 5/4	s+	m-vco	—	20	10	5	
4bA		W&G	B	g k s	7.5YR 5/3	s+	m-vco	—	25	20	20	Jumbled mixture of blocks of adjacent units.
4c		W&G	B	g k s	7.5YR 6/4	s	m-vco	—	30	25	30	Jumbled mixture of blocks of adjacent units.
5aA	19-20	S	A	g si-s	7.5YR 6/3	ls	f-vco	—	20	10	0	
5aA	21-23	S	A	g si-s	7.5YR 5/3	ls+	vf-co	—	15	15	0	
5b		D	A	g s	7.5YR 6/4	s	m-vco	—	25	20	2	
6a		D&G	A	b g s	7.5YR 6/3	s+	f-vco	—	20	25	25	Unit exposed for 15 minutes.
6b		D	A	g s	7.5YR 6/3	s	m-vco	—	20	10	0	Unit exposed for 15 minutes.
FAN ALLUVIUM OF FOOTWALL BLOCK												
7A		S		g k si-s	7.5YR 5/3	ls+	vf-co	—	15	15	2	Upper and lateral contacts extremely diffuse.
8aE		F		g k s	7.5YR 5/3	s+	f-vco	—	25	20	2	Weakly developed eluvial horizon in parts of unit.
8bBt		F		k si-s	7.5YR 6/4	ls	f-vco	w ab	35	20	8	Common 10-cm-thick gravel lenses.
8c		F		k s g	7.5YR 6/3	s	m-vco	—	50	10	5	Faint, discontinuous, parallel bedding.
8d		F&C		s g	7.5YR 6/4	s	m-co	—	40	20	0	Common 10-cm-thick gravel lenses.
9a		F&C		s g	7.5YR 6/4	s	m-vco	—	40	10	0	Faint, discontinuous, parallel bedding.
9b		C		s g	7.5YR 6/3	s	co-vco	—	70	15	0	Faint, discontinuous, parallel bedding.
10a		F		g b s	7.5YR 6/4	s+	m-vco	—	10	10	20	Nonparallel sand lenses in lower half.
10b		C		k s g	7.5YR 6/4	s	f-co	—	60	15	5	
11a		F		g k s	7.5YR 6/4	s	f-co	—	15	15	0	
11b		F		g k s	7.5YR 6/4	s	m-vco	—	20	10	2	Few, 5-cm-thick gravel lenses.
11c		F		g k s	7.5YR 6/4	s	f-vco	—	20	20	5	Few, 5-cm-thick gravel lenses.
11d		C		g s	7.5YR 6/3	s	co-vco	—	10	5	0	
12a		F		g s	7.5YR 6/3	s	co-vco	—	20	0	0	Faint, discontinuous wavy bedding.
12b		F		g k s	7.5YR 6/4	s	m-co	—	20	5	0	
12c		F		g s	7.5YR 6/4	s	m-vco	—	35	2	0	
12d		C		s g	7.5YR 6/4	s	co-vco	—	60	5	0	Deformed parallel beds.
SHOREFACE DEPOSITS OF LAKE BONNEVILLE												
13		L		g s	7.5YR 7/3	s	m-vco	—	20	0	0	Distinct, continuous, parallel bedding.

[1]Major units (numbers) mapped on the basis of size, distinctness, and inferred genesis; units numbered from youngest to oldest. Subunits labeled with lowercase letters. Uppercase letters (and following lowercase letter for a few units) indicate soil horizons of Soil Survey Staff (1975) and Birkeland (1984; 1999). Color shows inferred genesis of unit (explanation in lower right corner of plate).
[2]Numbers show location along trench log where listed data apply to unit. If no numbers are shown, data apply to entire unit.
[3]C, stream (channel) deposit; F, debris-flow deposit; D, debris facies (debris element of Nelson, 1992), dominantly gravity-deposited scarp-derived colluvium; W, wash facies; dominantly surface-wash-deposited colluvium on colluvial wedge; S, surface wash colluvium with minor amounts of loess; G, colluvial debris deposited in graben; L, lacustrine shoreface deposit; two letters indicate two genetic components.
[4]Unit inferred to have been deposited in response to listed earthquake (uppercase letters in red), as explained in text.
[5]g, gravel or gravelly; k, cobbly; b, bouldery; s, sand or sandy; si-s, silty sand.
[6]Dominant dry color of unit; Munsell color of Oyama and Takehara (1967).
[7]Methods and terminology of Soil Survey staff (1975) and Birkeland (1984; 1999); s, sand; s+, sand to loamy sand; ls, loamy sand; ls-, loamy sand to sand; ls+, loamy sand to sandy loam; sl, sandy loam; sl-, sandy loam to loamy sand.
[8]Grain sizes of sand fraction of matrix sediment; terminology of Soil Survey staff (1975); vco, very coarse; co, coarse; m, medium; f, fine; - (dash), indicates range of sizes.
[9]Methods and terminology of Soil Survey Staff (1975); maximum soil structure in unit, vw, very weak; w, weak; wm, weak to moderate; m, moderate; pl, platy; ab, angular blocky; sb, subangular blocky; dash indiates single grain structure.
[10]Visually estimated with graphic percentage chart. Most clasts are angular to subangular; rare rounded clasts are reworked from higher Lake Bonneville shorelines.
[11]Other features are discussed in text.

NORTH WALL OF TRENCH 2 AT THE EAST OGDEN SITE

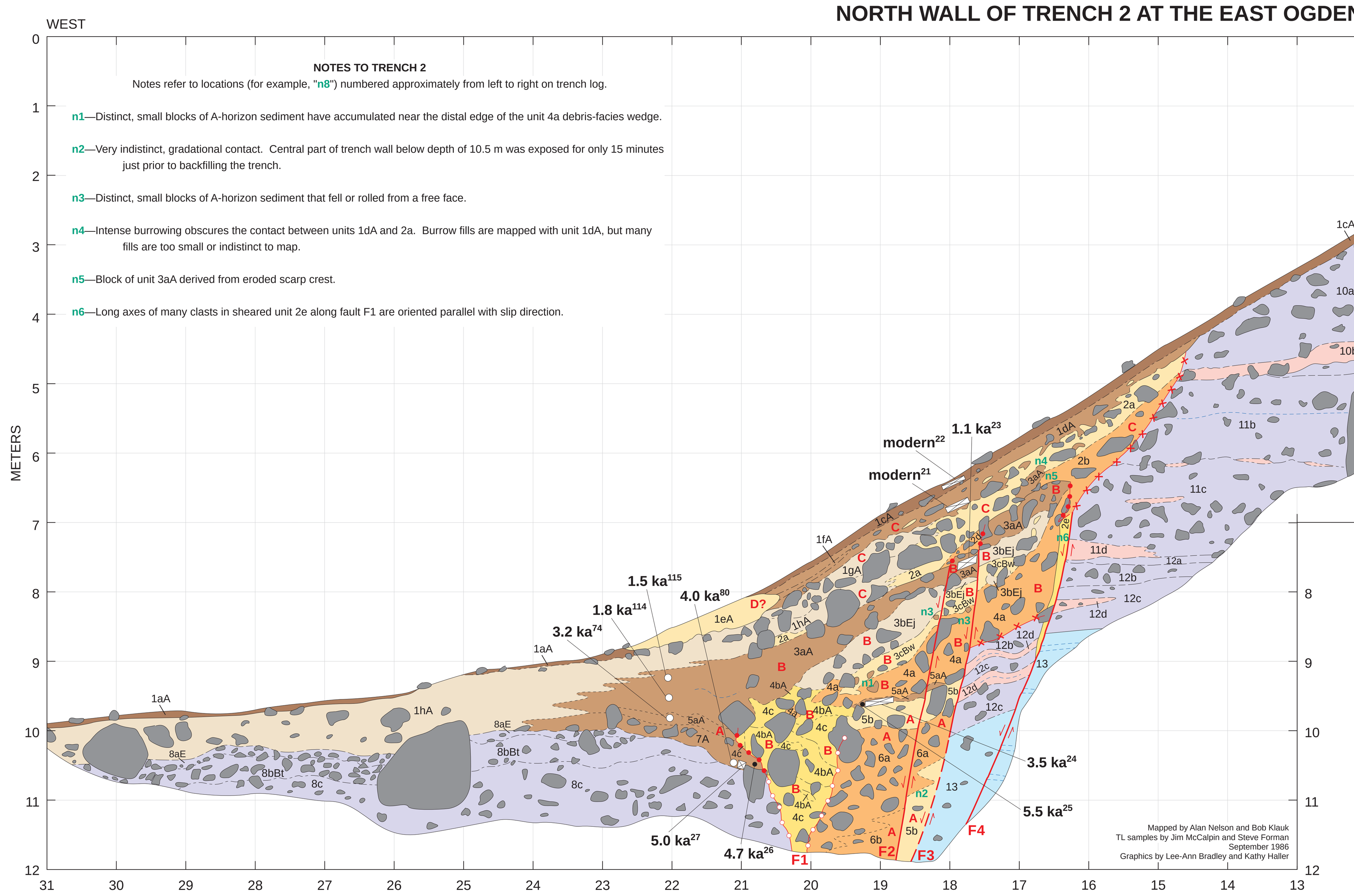

NOTES TO TRENCH 2

Notes refer to locations (for example, "n8") numbered approximately from left to right on trench log.

n1—Distinct, small blocks of A-horizon sediment have accumulated near the distal edge of the unit 4a debris-facies wedge.

n2—Very indistinct, gradational contact. Central part of trench wall below depth of 10.5 m was exposed for only 15 minutes just prior to backfilling the trench.

n3—Distinct, small blocks of A-horizon sediment that fell or rolled from a free face.

n4—Intense burrowing obscures the contact between units 1dA and 2a. Burrow fills are mapped with unit 1dA, but many fills are too small or indistinct to map.

n5—Block of unit 3aA derived from eroded scarp crest.

n6—Long axes of many clasts in sheared unit 2e along fault F1 are oriented parallel with slip direction.

EXPLANATION OF COLORS USED TO SHOW GENESIS OF TRENCH LOG UNITS

Lacustrine
- Shoreface deposits

Fluvial
- Stream-channel deposits
- Debris-flow deposits

Colluvial (facies terminology of Nelson, 1992)

Debris facies
- Lower
- Upper
- Fissure fill and sheared sediment

Wash facies
- Lower
- Upper (buried A horizon)
- Upper (modern A horizon)